

UNCLASSIFIED

AD NUMBER

AD864884

LIMITATION CHANGES

TO:

Approved for public release; distribution is unlimited.

FROM:

Distribution authorized to U.S. Gov't. agencies and their contractors;  
Administrative/Operational Use; OCT 1969. Other requests shall be referred to Army Aviation Materiel Labs., Fort Eustis, VA.

AUTHORITY

USAAMRDL ltr 10 Sep 1971

THIS PAGE IS UNCLASSIFIED

AD 864884

1

AD

## USAAVLABS TECHNICAL REPORT 69-67

### GRAPHITE FIBER-RESIN COMPOSITE STRUCTURE STUDY

By

Robert G. Shaver



October 1969

U. S. ARMY AVIATION MATERIEL LABORATORIES  
FORT EUSTIS, VIRGINIA

CONTRACT DAAJ02-68-C-0062  
GENERAL TECHNOLOGIES CORPORATION  
RESTON, VIRGINIA

This document is subject to special  
export controls, and each trans-  
mittal to foreign governments or  
foreign nationals may be made only  
with prior approval of US Army  
Aviation Materiel Laboratories,  
Fort Eustis, Virginia 23604.



Reproduced by the  
CLEARINGHOUSE  
for Federal Scientific & Technical  
Information Springfield Va. 22151

122

DISCLAIMER

The findings in this report are not to be construed as an official Department of the Army position unless so designated by other authorized documents.

When Government drawings, specifications, or other data are used for any purpose other than in connection with a definitely related Government procurement operation, the United States Government thereby incurs no responsibility nor any obligation whatsoever; and the fact that the Government may have formulated, furnished, or in any way supplied the said drawings, specifications, or other data is not to be regarded by implication or otherwise as in any manner licensing the holder or any other person or corporation, or conveying any rights or permission, to manufacture, use, or sell any patented invention that may in any way be related thereto.

Trade names cited in this report do not constitute an official endorsement or approval of the use of such commercial hardware or software.

DISPOSITION INSTRUCTIONS

Destroy this report when no longer needed. Do not return it to the originator.

21



DEPARTMENT OF THE ARMY  
HEADQUARTERS US ARMY AVIATION MATERIEL LABORATORIES  
FORT EUSTIS, VIRGINIA 23604

This program was performed under Contract DAAJ02-68-C-0062 with General Technologies Corporation, Reston, Virginia.

The data contained in this report are the result of research concerned with the development of techniques to fabricate and test filament-wound tube structures of whiskerized graphite fiber in epoxy resin.

The report has been reviewed by the U. S. Army Aviation Materiel Laboratories and is considered to be technically sound. It is published for the exchange of information and the stimulation of future research.

Task IF162204A17001  
Contract DAAJ02-68-C-0062  
USAAVLABS Technical Report 69-67  
October 1969

GRAPHITE FIBER-RESIN COMPOSITE  
STRUCTURE STUDY

Final Report

By

Robert G. Shaver

Prepared by

General Technologies Corporation  
Reston, Virginia

for

U. S. ARMY AVIATION MATERIEL LABORATORIES  
FORT EUSTIS, VIRGINIA

This document is subject to special export controls, and  
each transmittal to foreign governments or foreign nationals  
may be made only with prior approval of US Army Aviation  
Materiel Laboratories, Fort Eustis, Virginia 23604.

## SUMMARY

This program has been concerned with the development of techniques to fabricate filament-wound tube structures of whiskerized graphite fiber in epoxy resin. The first efforts on the program were devoted to the selection of an optimized whiskerizing level on PAN-precursor graphite fiber of 60 million psi modulus through evaluation of flat laminates in two phases:

1. Static Evaluations—tensile and compressive testing of honeycomb sandwich beam configurations of unidirectional and cross-ply laminates, short beam shear testing, torsion rod testing, and plate saddle shear testing.
2. Fatigue Evaluations—tensile-zero-tensile fatigue testing of unidirectional laminates to  $10^7$  cycles.

From these flat laminate phases, an optimum 3% whiskerizing level was selected and applied to continuous tow for development of filament-winding techniques in two further phases:

1. NOL Ring Configuration—filament-winding techniques were evolved to attain a nominal 50 volume %, low void content, hoop-wound cylinder from which NOL rings were cut and evaluated.
2. Torsion Tube Configuration—the winding techniques were applied to form 1-inch ID, thin-walled cylinders for torsion shear testing in unidirectional (hoop), two orthotropic cross-ply and one isotropic cross-ply configuration.

The 3% whiskerized fiber was found to filament wind to the desired composite under nearly the same conditions of impregnation and tension as the same type of fiber received with the manufacturer's surface treatment. The most significant difference in filament-winding characteristics was found to be between the high-modulus and intermediate-modulus types of PAN-precursor graphite fibers. Interlaminar and unidirectional in-plane shear strengths for the 3% whiskerized material were measured as equal to or greater than those of the surface-treated fiber. The shear strength and modulus in the unidirectional configurations increased directly with whiskerizing content. The shear properties of  $\pm 45^\circ$  orthotropic and the isotropic tube configurations were found to be relatively independent of fiber surface treatments but highly dependent on fiber strength, modulus, and volume content. The fatigue strength (at  $10^7$  cycles) of the whiskerized fiber laminates was found to be essentially equal to that of laminates of the virgin fiber from which the whiskerized fiber was produced, even though a significant reduction in static tensile strength was found. All configurations in which shear between the fiber and matrix played a decisive role in determining the properties were improved by the presence of whiskerizing; for

example, the shear beams, torsion rods, and saddle shear plates, the  $\pm 45^\circ$  laminates in tension and compression, and the unidirectional torsion tubes. The presence of whiskerizing did not appreciably affect such properties as tensile and compressive moduli of  $0^\circ$  and  $0^\circ$ - $90^\circ$  laminates, laminate Poisson's ratios, NOL ring moduli, and shear properties of torsion tubes having fibers in or near the  $45^\circ$  and  $135^\circ$  helices of maximum tensile and compressive stress under torsion.

## FOREWORD

This work was accomplished under Contract No. DAAJ02-68-C-0062 for the U.S. Army Aviation Materiel Laboratories, Fort Eustis, Virginia. The technical direction for the Army was provided by Mr. A. J. Gustafson of the Physical Sciences Division. The work at General Technologies Corporation was performed under the direction of Dr. R. G. Shaver with the assistance of Mr. O. L. Ferguson in composite specimen fabrication and analysis, Mr. E. F. Abrams in equipment design and construction, and Mr. L. G. Davies in testing. Whiskerizing services were performed by the Thermokinetic Fibers Division of GTC by Mr. N. H. Chavasse.

## TABLE OF CONTENTS

	<u>Page</u>
SUMMARY . . . . .	iii
FOREWORD . . . . .	v
LIST OF ILLUSTRATIONS. . . . .	ix
LIST OF TABLES . . . . .	xii
INTRODUCTION . . . . .	1
DEVELOPMENT OF PROCESSING . . . . .	6
Lamination . . . . .	6
Development of Filament Winding . . . . .	6
RESULTS OF LAMINATE PROPERTIES EVALUATIONS. . . . .	15
Honeycomb Sandwich Beams. . . . .	15
Shear Modulus Plates . . . . .	15
Shear Beams and Torsion Rods . . . . .	22
Tensile Fatigue Specimens . . . . .	22
Composite Analysis and Microstructure. . . . .	30
RESULTS OF FILAMENT-WOUND STRUCTURE PROPERTIES EVALUATIONS . . . . .	41
DISCUSSION OF RESULTS . . . . .	46
Tensile and Compressive Strength . . . . .	46
Tensile and Compressive Modulus . . . . .	51
Ultimate Elongation . . . . .	51
Poisson's Ratio . . . . .	56
Plate Shear Modulus . . . . .	59
Beam and Rod Shear Strength . . . . .	59
Tensile Fatigue . . . . .	64
Filament Winding of NOL Rings . . . . .	70
NOL Ring Properties . . . . .	70
Torsion Tubes . . . . .	73

TABLE OF CONTENTS (continued)

	<u>Page</u>
CONCLUSIONS AND RECOMMENDATIONS . . . . .	78
Laminates . . . . .	78
Filament-Wound NOL Rings and Tubes . . . . .	79
LITERATURE CITED. . . . .	80
APPENDIX	
Experimental Techniques . . . . .	83
DISTRIBUTION . . . . .	108

## LIST OF ILLUSTRATIONS

<u>Figure</u>		<u>Page</u>
1	Whisker Growth on PAN-Precursor, High-Modulus Graphite Fibrils, 400X . . . . .	2
2	Appearance of Whisker Growth on PAN-Precursor, High-Modulus Graphite Fiber, 4400X . . . . .	3
3	Whisker Growths and Nuclei on Pan-Precursor, High-Modulus Graphite Fiber, 23,000X . . . . .	4
4	Filament-Wound Graphite-Epoxy Ring and NOL Rings Machined From It . . . . .	7
5	NOL Ring Winder . . . . .	8
6	Typical Distribution of Fiber and Voids in Filament-Wound NOL Rings of Continuous Graphite Tow, 80X . . . . .	12
7	Typical Distribution of Fiber and Whiskers in NOL Rings of 3% Whiskerized Continuous Graphite Fiber, 800X . . . . .	13
8	Fatigue Tester With Direct Stress Attachment and GTC-Designed Grips . . . . .	24
9	Appearance of Fatigue-Tested Specimens . . . . .	29
10	Section of 0°-90°/90°-0° Cross-Ply Laminate, No. 224 (100X) . . . . .	36
11	Section of 45°-135°/45°-135° Cross-Ply Laminate, No. 150 (100X) . . . . .	36
12	Cross Section of Void-Free Composite, No. 230 (100X) . . . . .	37
13	Cross Section of Composite Showing Voids, No. 232 (100X) . . . . .	37
14	High Interlaminar Whisker Concentration, No. 234 (100X, dark field) . . . . .	38
15	Maldistributions of Graphite Fiber, No. 167 (100X, dark field) . . . . .	38

## LIST OF ILLUSTRATIONS (continued)

<u>Figure</u>		<u>Page</u>
16	Un-Whiskerized Composite, No. 227 (1500X) . . . . .	40
17	Whiskerized Composite, No. 152 (1500X) . . . . .	40
18	Typical Fracture of Graphite Fiber NOL Rings . . . . .	43
19	Typical Modes of Failure of Torsion Tubes . . . . .	45
20	Strength of 0° Composites . . . . .	47
21	Strength of 0°-90°/90°-0° Composites . . . . .	48
22	Strength of 45°-135°/45°-135° Composites . . . . .	49
23	Strength of 90° Composites . . . . .	50
24	Tensile and Compressive Moduli . . . . .	52
25	Effect of Whiskerizing on Ultimate Strain of 0° and 0°-90°/90°-0° Composites . . . . .	53
26	Effect of Whiskerizing in Ultimate Strain of 45°-135°/45°-135° Composites . . . . .	54
27	Effect of Whiskerizing on Ultimate Strain, 90° . . . . .	55
28	Stress-Strain Curves of 45°-135°/45°-135° Composites . . . . .	57
29	Poisson's Ratio vs. Percentage of Whiskerizing . . . . .	58
30	Effect of Whiskerizing on Shear Modulus . . . . .	60
31	Effect of Whiskerizing on Shear Strength . . . . .	61
32	Effect of Fiber Content on Shear Strength . . . . .	63
33	S-N Diagram for 0° Composites of 5% Whiskerized Graphite Fiber (Laminates 258, 261) . . . . .	65

LIST OF ILLUSTRATIONS (continued)

<u>Figure</u>		<u>Page</u>
34	S-N Diagram for 0° Composite of 3% Whiskerized Graphite Fiber (Laminate 255) . . . . .	66
35	S-N Diagram for 0° Composite of Surface-Treated Graphite Fiber (Laminate 237) . . . . .	67
36	S-N Diagram for 0° Composite of Virgin Graphite Fiber (Laminate 238) . . . . .	68
37	Effect of Void Content on Shear Strength of NOL Rings . . . . .	72
38	Graphite-Epoxy Composite Specimens . . . . .	85
39	Composite Specimen Density Measurement Apparatus . . . . .	87
40	Honeycomb Sandwich Beams, 13-Inch and 24-Inch Lengths . . . . .	90
41	Torsion Rod Fixture and Machined Specimens . . . . .	96
42	Tinius Olsen Testing Machine With Split-Disc Grip . . . . .	100

## LIST OF TABLES

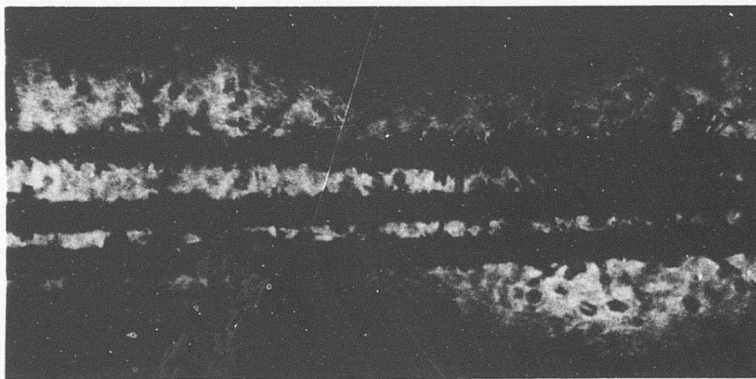
<u>Table</u>		<u>Page</u>
I	NOL Ring and Torsion Tube Filament-Winding Data . . . . .	9
II	Honeycomb Sandwich Beam Testing: 0° Composites . . . . .	16
III	Honeycomb Sandwich Beam Testing: 0°-90°/90°-0° Composites . . . . .	18
IV	Honeycomb Sandwich Beam Testing: 45°-135°/45°-135° Composites . . . . .	19
V	Honeycomb Sandwich Beam Testing: 90° Composites . . . . .	20
VI	Plate Shear Modulus Testing . . . . .	21
VII	Short-Beam and Torsion Shear Testing . . . . .	23
VIII	Laminate Properties . . . . .	25
IX	Static Tensile Testing Data . . . . .	25
X	Residual Strength After Stress Cycling . . . . .	26
XI	Fatigue Test Results . . . . .	27
XII	Results of Composite Fiber Content Analysis . . . . .	31
XIII	Results of Whiskerizing Analysis . . . . .	33
XIV	NOL Ring Test Results . . . . .	42
XV	Results of Tube Torsion Testing . . . . .	44
XVI	Comparison of Fatigue Limits of Composites . . . . .	69
XVII	Comparison of Strengths of Composites by Several Tests . . . . .	73
XVIII	Comparison of Composite Torsion Tube Data . . . . .	75

## INTRODUCTION

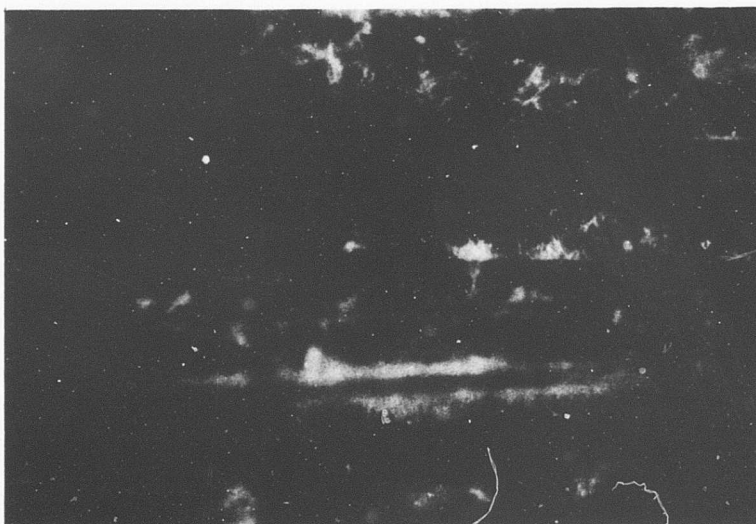
The objective of this program was to develop techniques necessary to fabricate graphite fiber-resin tubular composites with integral interlaminar reinforcement based on the use of silicon carbide whiskers grown from the graphite fiber surface to achieve interstitial reinforcement. The course of development to achieve this objective proceeded from the use of flat laminate construction to obtain optimum whisker content based on tensile, shear, and fatigue properties, to the development of filament-winding techniques using NOL ring configuration at the optimum whisker content, followed by fabrication of torsion tube test sections in various fiber orientations.

The process of growing the silicon carbide whiskers on the graphite fibers is called "whiskerizing"; it was originated and developed by the Thermokinetic Fibers Division of General Technologies Corporation. The process is a high-temperature vapor phase transport and crystal growth utilizing the graphite fiber as growth substrate. Figure 1 shows the actual whisker growth resulting from the process on the high-modulus PAN-precursor graphite fiber used in this program at the optimum treatment level selected in this effort. Very little detail of the whisker morphology can be seen in optical microscopy. However, in the scanning electron photomicrograph of Figure 2, whiskers can be seen to be of relatively uniform diameter, approximately 0.3 to 0.5 micron, and are attached to the substrate fibrils at random points distributed along the substrate. Their orientation is more or less perpendicular to the substrate surface, and the whisker growth morphology occasionally displays the abrupt change in growth direction that is often found in whisker synthesis of many diverse materials<sup>(1,2)</sup>. The whiskerizing process is similar in growth mechanism to the process used to grow long staple length wools of beta silicon carbide commercially. The deposition process in this case takes place by means of a vapor-liquid-solid mechanism employing a molten droplet of iron-silicon eutectic alloy at the growth tip of the whiskers<sup>(3)</sup>. Constituent species from the vapor phase condense into the molten droplet and deposit upon the underlying crystal tip, causing it to elongate. The droplet growth nuclei upon the surface of the graphite fibers can be seen in Figure 2 and are very evident at the higher magnification in Figure 3.

In the case of beta silicon carbide whisker wool manufacture, these growth droplets are deliberately seeded through the application of an iron alloy powder to the growth substrate. In the case of the whiskerizing process, these V-L-S growth droplets form spontaneously from the iron and silicon present in the vapor phase due to the high-temperature hydrogen reduction of the impure silicate raw material. Strong attachment of the whiskers to the graphite substrate is probably due to the gradual merging of the two materials through carbon-rich intergrades of silicon-carbide at the point of juncture.



a. Transmitted Light.



b. Reflected Light.

**Figure 1. Whisker Growth on PAN-Precursor, High-Modulus Graphite Fibrils, 400X.**

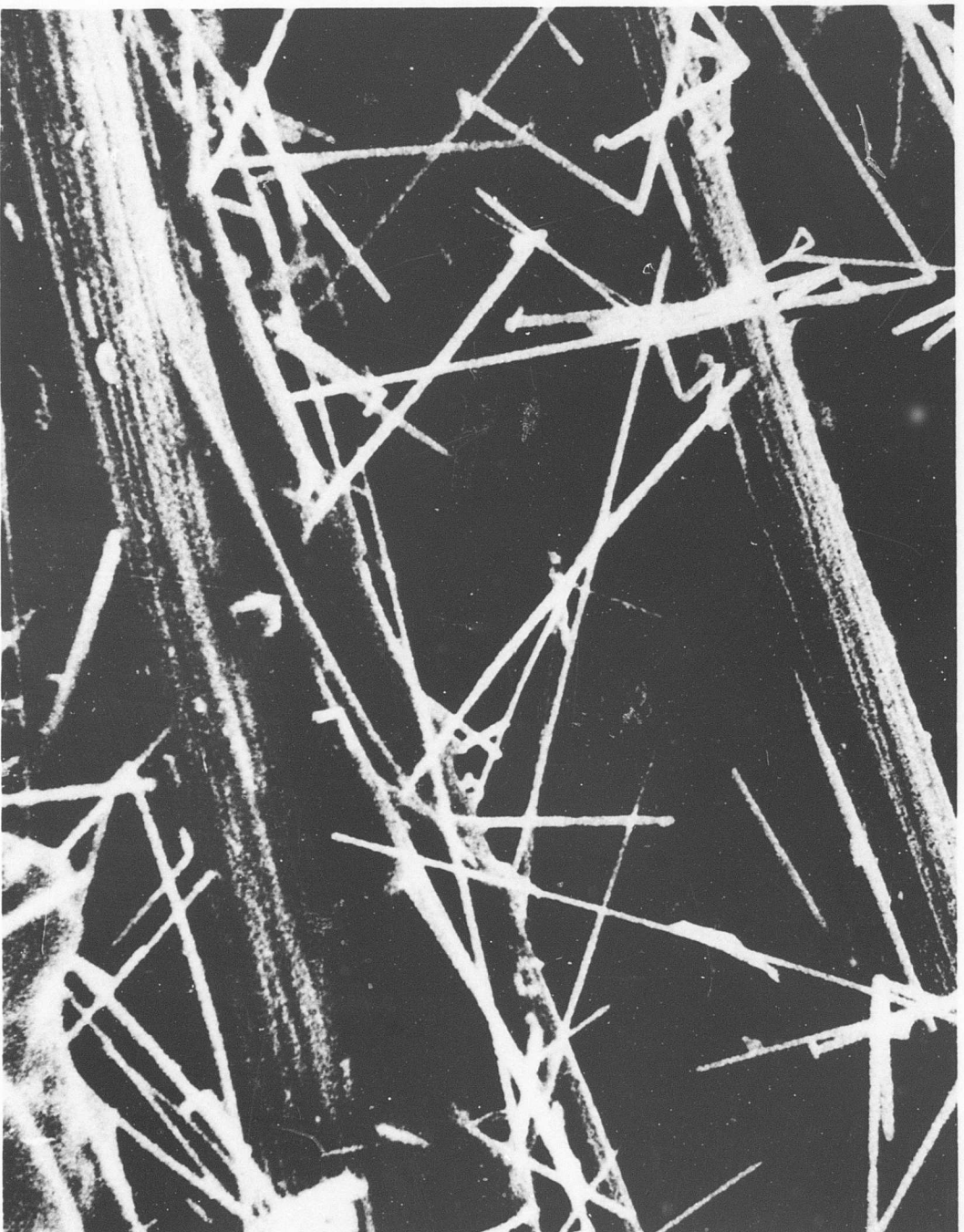
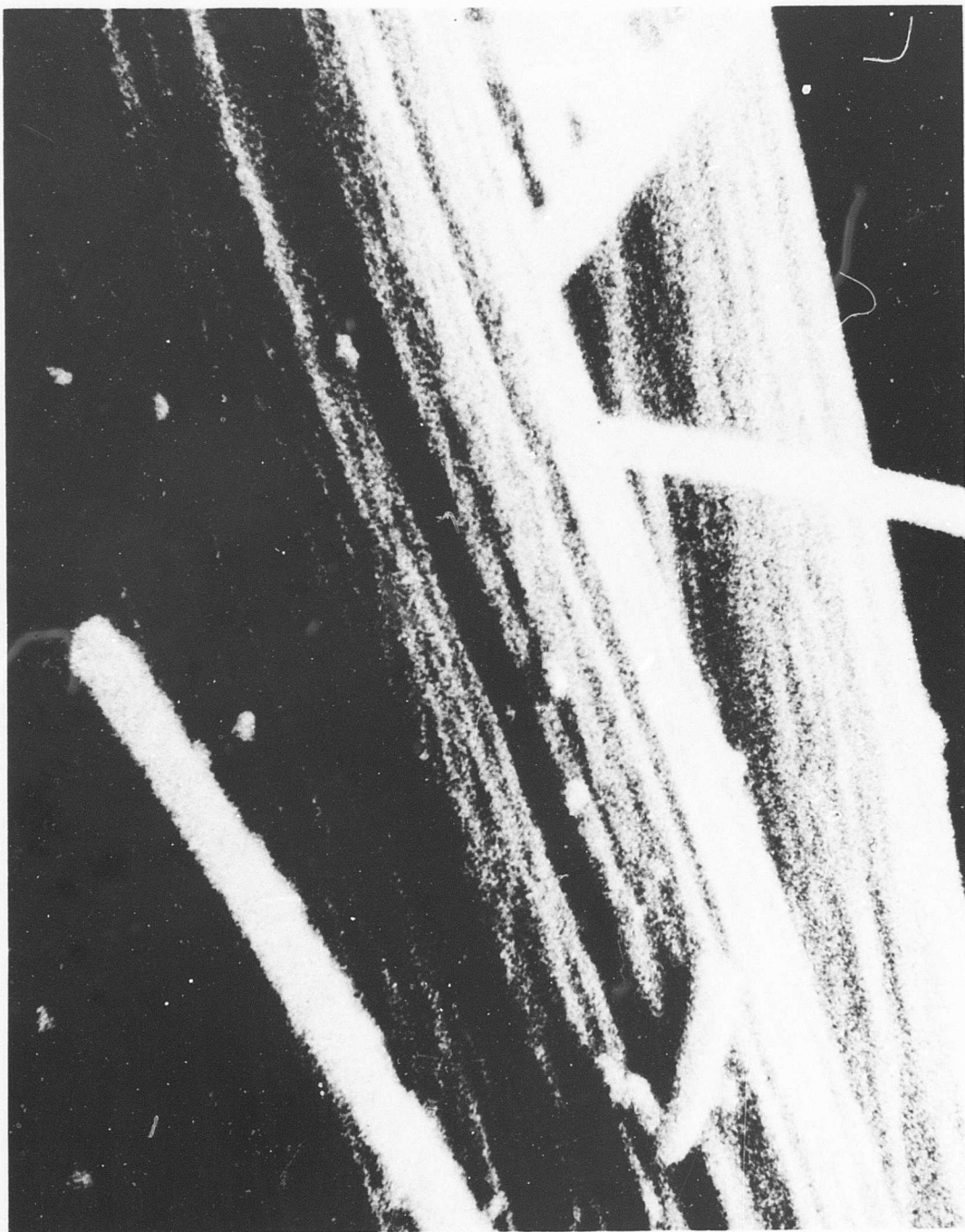


Figure 2. Appearance of Whisker Growth on PAN-Precursor, High-Modulus Graphite Fiber, 4400X,  $\downarrow$  1 micron.



**Figure 3. Whisker Growths and Nuclei on PAN-Precursor, High-Modulus Graphite Fiber, 23,000X,  $\rightarrow$  1 micron.**

The differing proportions of whiskers relative to graphite fiber that are produced by the different levels of treatment such as those used in the early phases of this program are obtained by two simultaneously occurring phenomena: the extension of existing whiskers to greater lengths and the start of new whisker growth from nuclei formed in the space between existing whiskers, thus increasing the population density as well as whisker length of the higher treatment levels.

Prior art in compositing whiskerized graphite fiber began with the studies at the Naval Ordnance Laboratory(4,5,6) showing that the poor interlaminar shear resistance of many high-modulus graphite fiber composites can be overcome by whiskerizing. The prior efforts at GTC have consisted of the process developmental studies carried out in part under contract to the Naval Ordnance Laboratory together with in-house efforts to develop composite fabrication techniques applicable to the treated fiber to extract maximum properties(7,8). These studies found several effects of significance to the formation of composites. The location, orientation, and properties of the whiskers attached to the graphite fibrils are responsible for marked changes in the processing characteristics of the fiber. The most pronounced changes are with regard to resin impregnation and ease of compaction. It can be readily visualized that the addition of these large populations of small-diameter fibers to the graphite fiber bundles causes a drastic change in the interstitial properties both before and after compositing. Most immediately noticeable is the greater apparent stiffness of the whiskerized graphite fiber bundles before any impregnation. This effect is due to the mechanical interlocking of the fibrils within the graphite bundles by means of the whisker-to-whisker contacts. This effect is progressive with degree of whiskerizing and varies from a scarcely noticeable yarn stiffness to a very stiff bundle at the extremes of treatment. This yarn stiffness carries over into the impregnated form and has an obvious interaction with filament winding.

Also very significant is the progressively high fluid retentiveness of the whiskerized fibers as the degree of treatment increases. This greatly affects the resin impregnation step since the whiskerized fiber may be able to absorb severalfold more liquid resin than the untreated fiber without draining away.

Finally, among the major effects upon composite processing is the resistance of the interstitial fiber growths to the sidewise compaction required in lamination and filament winding. This, too, is an effect that is directly related to the amount of whiskerizing growth, and all of these factors must be balanced and compromised with respect to the desired composite composition and final properties, while retaining the ease of fabrication that is characteristic of resin-matrix composites.

## DEVELOPMENT OF PROCESSING

### LAMINATION

The lamination technique used in this program had been developed essentially in previous work<sup>(7,8)</sup>. It involved the impregnation of unidirectional laminas with acetone-diluted resin in a fixed excess, evaporation of the solvent, vacuum-treating and B-staging, layup, compaction to precalculated dimensions, and cure in matched metal molds. The details are given in the Experimental Techniques section. The cross-ply laminates ( $\pm 45^\circ$ ,  $0^\circ$ - $90^\circ$ ) were similarly formed by cutting the unidirectional layups at the appropriate angle. The standard laminate from which all sandwich beams and tensile fatigue specimens were cut was 3 inches by 13 inches by 0.08 inch. Shear plates (4 inches by 4 inches) were formed in an oversized mold and trimmed. Short beam shear specimens were molded in a 0.5-inch by 0.2-inch by 4.5-inch mold.

### DEVELOPMENT OF FILAMENT WINDING

The final phases of the program required the development of filament winding to allow the testing of NOL rings and torsion tubes. The goal of the filament-winding development was to achieve void-free composite NOL rings at 50 volume % fiber, in order to be as comparable as possible to the laminates used earlier.

NOL ring winding was used to develop the winding technique and was carried out in this program on a mandrel having the standard 5.75-inch diameter but a 1-inch width. It had been found earlier that the large graphite fiber tow cannot be effectively wound into a 1/4-inch-wide mandrel space, as is normally done, because the tows do not pack properly. To achieve good fiber content, a wide ring is therefore wound, and the standard 1/4-inch widths are cut off on a lathe. This is illustrated in Figure 4. The winding apparatus is shown in Figure 5.

The results of the filament-winding development sequence using the graphite continuous tow are shown in Table I. At first, impregnation was accomplished with solvent-diluted resin, a technique developed earlier and reported in a recent SPI paper<sup>(8)</sup>. Windings 160709 - 160712 were made by this technique. It was obvious that control of voids was difficult, so the decision was made to switch to impregnation by passing through a heated bath of the undiluted resin. Another effect found in this initial sequence was that the void content and ring density did not respond significantly to winding tension increases. This was also believed to be due to difficulties with solvent removal.

The sequence 160713 to 160718 shows the development of the hot resin technique using un-whiskerized high-modulus graphite fiber. In general, it was found that very low void contents (about 1% by inspection) could be achieved routinely and

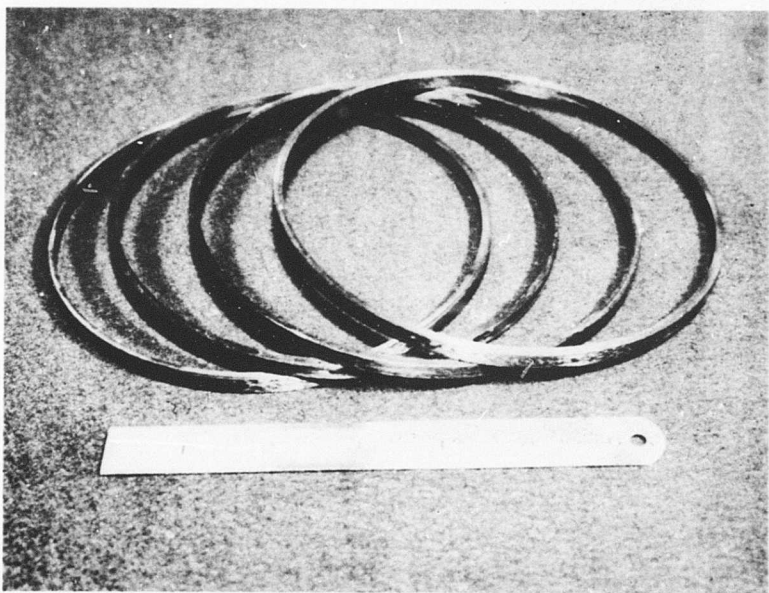
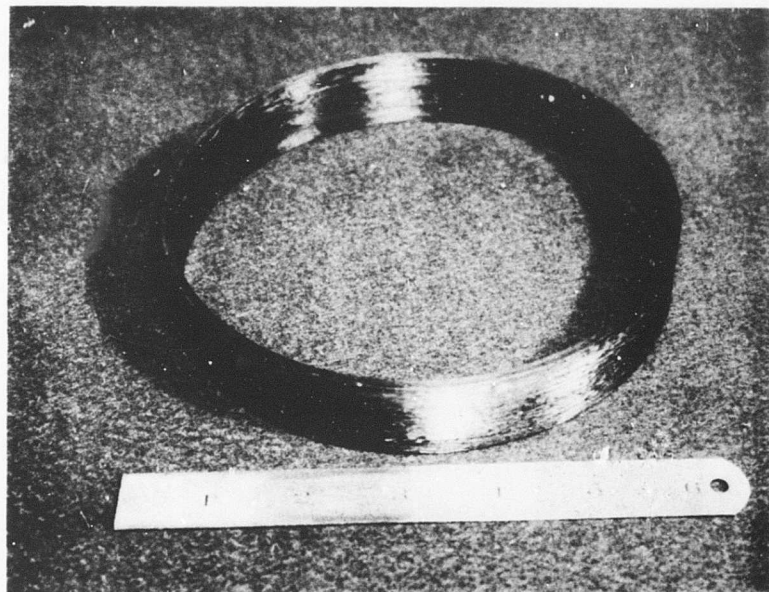


Figure 4. Filament-Wound Graphite-Epoxy Ring and NOL Rings Machined From It.

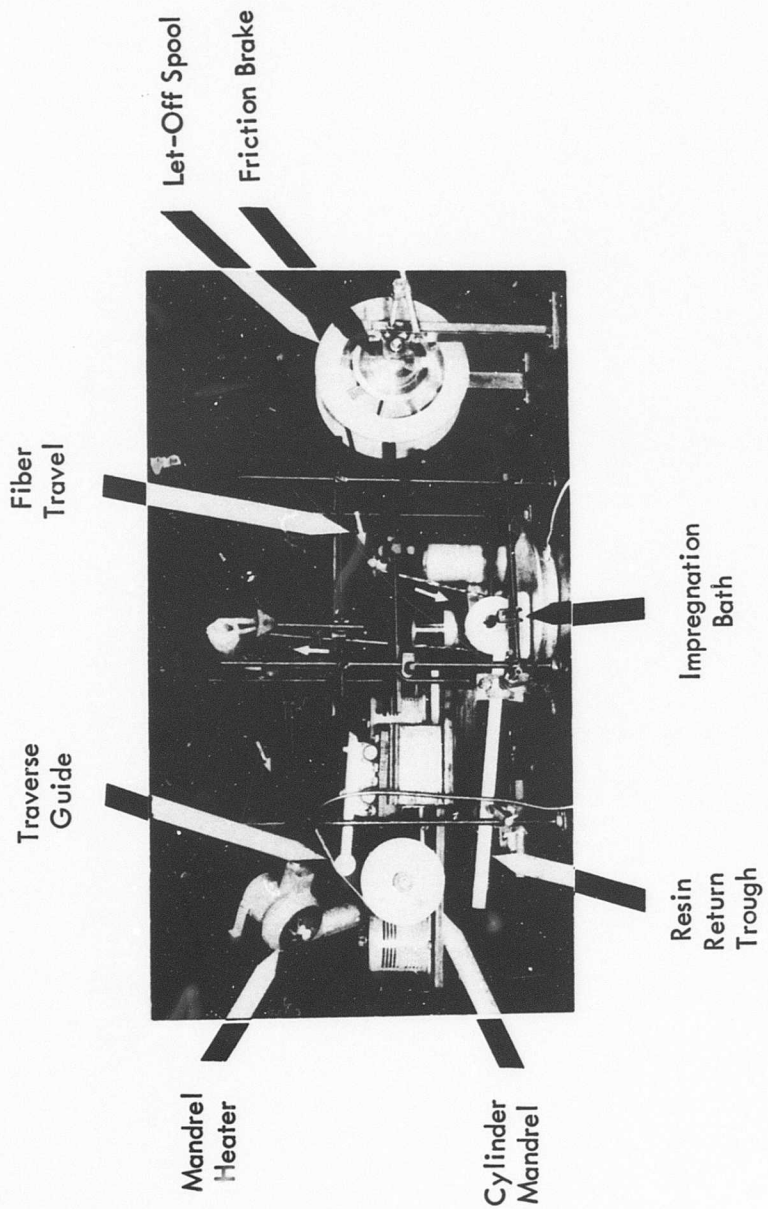


Figure 5. NOL Ring Winder.

TABLE I. NOL RING AND TORSION TUBE FILAMENT-WINDING DATA

Winding Number	Fiber Treatment	Impregnation Method	Winding Tension (grams)	Ring Density (g./cc)	Fiber Content (weight %)	Void Content (%)
<u>NOL Rings:</u>						
160709	treated	solvent	1400	1.30	51.8	14.3
160710	"	"	2500	1.40	63.5	12.7
160711	"	"	3400	1.33	51.3	11.8
160712	"	"	5500	1.38	57.0	10.2
160713	"	hot resin	1500	1.48	51.7	3.7
160714	"	"	4700	1.48	51.2	3.1
160715	"	"	6600	1.50	56.2	4.4
160716	"	"	2500	1.54	60.2	2.5
160717	"	"	2500	1.56	62.0	0.1
160718	"	"	3500	1.57	61.4	1.4
160720	3% whiskerized	"	1000	1.49	52.0	3.0
160721	"	"	350	1.43	38.2	1.0
160722	"	"	1950	1.53	55.4	2.2
160723	"	"	350	1.41	38.8	2.4
160724	"	"	1950	1.53	50.5	- 0.1
160726	"	"	2500	1.57	45.6	0.2
160727	"	"	2500	1.54	52.5	0.3
160728	"	"	3000	1.62	61.0	- 0.7

TABLE I - Continued

Winding Number	Fiber Treatment	Impregnation Method	Winding Tension (grams)	Ring Density (g/cc)	Fiber Content (weight %)	Void Content (%)
<b>Torsion Tubes:</b>						
160730	treated	hot resin	3000	1.57	62.0	1.9
160731	"	"	3000	1.57	62.4	2.4
160732	"	"	3000	1.52	56.3	2.7
160435	intermediate modulus fiber, treated	"	3000	1.49	65.0	2.1
160736	treated	"	3000	1.55	56.4	0.5
160739	3% whiskerized	"	3000	1.55	56.3	1.1
160741	"	"	3000	1.53	52.2	1.9
160743	"	"	3000	1.42	41.3	3.1
160744	"	"	3000	1.53	56.1	2.5

that somewhat higher winding tensions were necessary than with the solvent technique. This is presumably due to the need for massive resin flow at the winding mandrel with the hot resin technique.

The decrease in winding tension and improvement in ring density achieved between 160715 and 160716 was due to the use of a hot mandrel (ca. 110°C) in the latter winding. Previously, the mandrel was warmed only by resin carry-over. This was a very significant development and allowed the excellent subsequent rings to be fabricated. The results in terms of tensile strength, modulus, and shear strength that were obtained with 160717 and 160718 were fully equivalent to those of the control specimens of Phase I laminates, so the winding development was halted with the control fiber. The microstructure of these rings is shown in Figure 6. The filament-winding effort was then directed at employing the 3% whiskerized continuous tow using the hot resin technique. Sequence 160720 - 160728 was the outcome of this development. Considerable difficulty was experienced with sequence 160720 - 160723 due to fiber breakage and tow raveling. The 350-gram tensions in windings 160721 and 160723 were due to the extreme tendency to ravel and break. This difficulty was finally traced to a particular spool of fiber tow, designated L143, which had been used starting with 160720. This particular spool contained fiber that was markedly more raveled before unspooling than any other used in this program. It had the following virgin strength, as determined by the wet strand technique, compared to that used in sequence 160709 - 160718, spool L166:

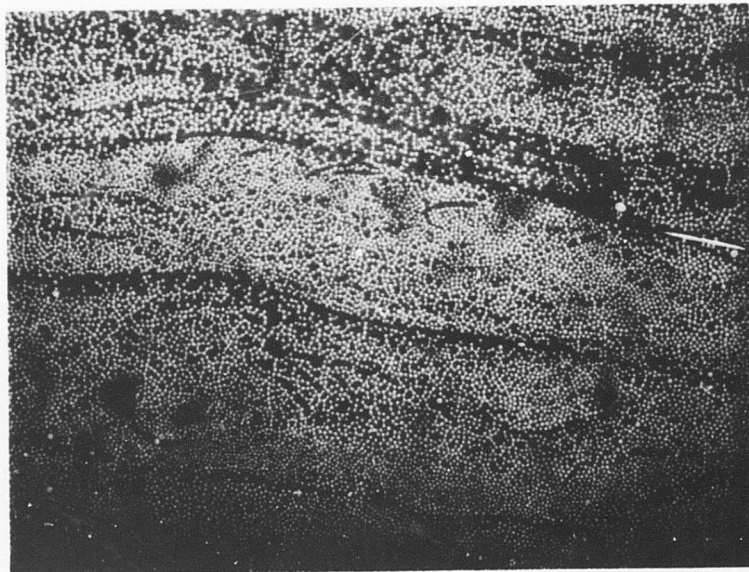
spool L143 - - 232,000  $\pm$  26,000 psi  
spool L166 - - 275,000  $\pm$  31,000 psi

Because of the apparent poor quality of L143, use of it was discontinued and a new spool, L168, was whiskerized. The virgin strength of this spool was 256,000 psi by wet strand.

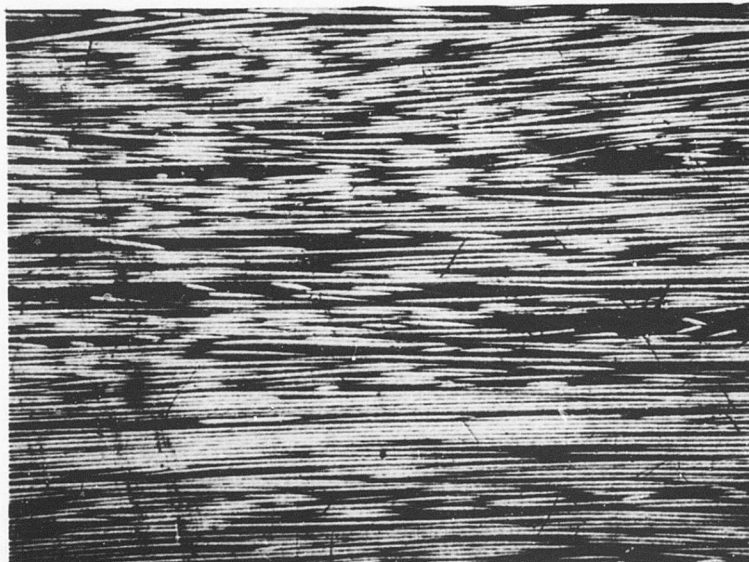
No further difficulty was experienced with fiber breakage and raveling under high tensions with this new fiber. Windings 160724 - 160728 were carried out with no complications. It was found that fiber contents above 60 weight % could be obtained with the whiskerized fiber using a winding tension of 3000 grams, whereas 2500 grams was required with the un-whiskerized fiber. The rings of over 60 weight % fiber meet the goal of 50 volume % fiber. Void contents in the latter runs were all very low - less than 1%. The need for high-quality fiber for filament winding is obvious.

Figure 7 shows the microstructure of the 3% whiskerized rings cut from winding 160728. There is no appreciable difference, except for the presence of whiskers, between this and that seen earlier in Figure 6.

In the torsion tube fabrication phase of the program, the filament-winding technique

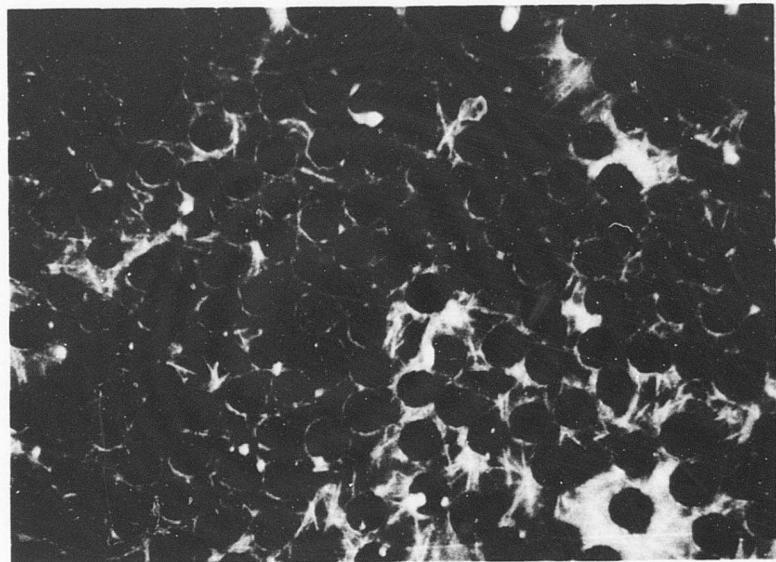


a. Transverse.

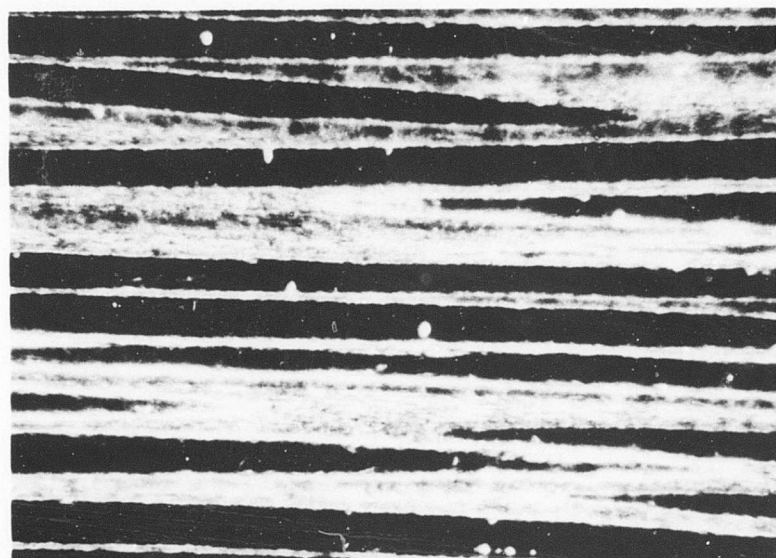


b. Axial.

Figure 6. Typical Distribution of Fiber and Voids in  
Filament-Wound NOL Rings of Continuous  
Graphite Tow, 80X.



a. Transverse Section.



b. Longitudinal Section.

Figure 7. Typical Distribution of Fiber and Whiskers in NOL Rings of 3% Whiskerized Continuous Graphite Fiber, 800X.

developed with the NOL rings was directly adapted to applying the hoop-wound layers. The unidirectional tubes ( $90^\circ$ ) were completely fabricated by this technique. The tubes were 1.0 inch ID by 3.0 inches by 0.05-0.10 inch thick in nominal dimensions. In Table I, the results of this can be seen in windings 160730, 160735 and 160739, which are the  $90^\circ$  torsion tubes of treated high-modulus graphite, treated intermediate-modulus graphite, and whiskerized high-modulus graphite fibers, respectively. The fiber contents and void contents achieved were quite similar to those of the NOL rings at similar winding tensions. The intermediate-modulus fiber actually gave a markedly higher fiber content than is apparent on the weight percent basis. The 65 weight % is 56 volume % fiber. Thus, the same winding conditions gave greater compaction (45 volume % vs. 51 volume %) with intermediate-modulus fiber than with high-modulus fiber. This effect has been found by others<sup>(9)</sup> and is apparently due to the modulus difference, since the morphologies of the two types are nearly identical.

The hoop-winding technique was also used as the finishing layers on the  $90^\circ$ - $0^\circ$ / $0^\circ$ - $90^\circ$  orthotropic tubes and the  $\pm 30^\circ$ ,  $90^\circ$  isotropic tubes, which provided the compaction to the underlying laid-up cross-ply layers at angles other than  $90^\circ$ . These tubes are numbers 160731, 160732, 160736, 160741, 160743, and 160744. Generally, the densities, fiber contents, and void contents obtained in these angle-ply filament-wound tubes are the same as the hoop-wound tubes. The notable exception is 160743, whose low density and fiber content are not due to any obvious cause. Despite this exception, the filament-winding technique as developed was found to be reproducibly capable of making well-compacted composites in both 1-inch- and 5.75-inch-diameter cylinders with both treated tow and whiskerized tow. A perhaps serious limitation on the direct use of the graphite tow is the relatively thick resulting laminas, about 15-20 mils each. A flattened tape formed from the tow would allow more laminas in a given composite thickness.

## RESULTS OF LAMINATE PROPERTIES EVALUATIONS

The data obtained from the testing of the laminates made from batch-whiskerized, high-modulus, PAN-precursor graphite fiber in epoxy resin, Epon 828/Epon 1031/-NMA/BDMA, are given in the tables of this section together with those obtained on a similar series of laminates made with un-whiskerized but manufacturer surface-treated fiber. Shear strength data on completely untreated fiber are also given. The composites were fabricated to a target of 55 volume % total fiber and no voids, with the exception of some shear specimens that were deliberately fabricated at significantly higher and lower fiber contents.

### HONEYCOMB SANDWICH BEAMS

Three- by thirteen-inch molded laminate panels were fabricated with fiber of various percentages of whiskerizing and with manufacturer-treated un-whiskerized fiber in four fiber configurations:

- a. 2-layer,  $0^\circ$  orientation
- b. 3-layer,  $90^\circ$  orientation
- c.  $45^\circ$ - $135^\circ$ / $45^\circ$ - $135^\circ$  orientation
- d.  $0^\circ$ - $90^\circ$ / $90^\circ$ - $0^\circ$  orientation

In all cases in this program, the fiber that was subjected to whiskerizing treatment had not been surface-treated by the manufacturer. These laminate panels were cut lengthwise into 1- by 13-inch face plates for sandwich beam construction. The gage sections of the composite face plates were instrumented with strain gages in the longitudinal and transverse orientations. Beams having face plates from each laminate panel were tested in either the tensile or the compressive mode, depending on the position in the beam flexure. The results of these tests are given in Tables II through V for the four fiber layup configurations. The details of the beam fabrication and testing methods are given in later sections.

### SHEAR MODULUS PLATES

Five 4- by 4-inch laminate plates were fabricated with whiskerizing contents from 0% to 9% and tested in diagonal loading for shear modulus. These laminates all had unidirectional graphite tow fibers. An additional plate laminate (number 230) was deemed unsuitable for shear modulus testing because of a poorly compacted area, but it was utilized for shear testing by cutting into beams and a torsion rod. The results of this are cited in a later section. The results of the five diagonal-loading shear modulus tests from the good specimens are given in Table VI. The as-calculated values are given as well as the values corrected for the effect of loading slightly inboard of the extreme corners of the samples.

TABLE II. HONEYCOMB SANDWICH BEAM TESTING: 0° COMPOSITES

Specimen Number	Percent Whiskerizing	Type of Load	Fiber Content (v/o)	Void Content (v/o)	Composite Density (g/cc)	Strength (10 <sup>3</sup> psi)	Young's Modulus (10 <sup>6</sup> psi)	Ultimate Elongation (%)	Poisson's Ratio
168-1	0 (treated)	tensile	53	0	1.63	107.4	33.9	0.30	0.55
168-2	"	compression	"	"	>54.0	S	33.3	>0.16	0.66
168-3	"	compression	"	"	>68.3	S	34.0	>0.20	0.63
171-2	0 (treated)	tensile	52	0.6	1.61	>25.6	F	>0.08	0.51
171-1	"	tensile	"	"	>36.6	S	31.7	>0.11	0.65
171-3	"	compression	"	"	>27.0	S	32.5	>0.11	0.65
155-1	2.2	tensile	55	1.5	1.64	86.1	33.4	0.26	0.63
155-2	"	compression	"	"	>84.0	S	36.1	>0.26	0.58
155-3	"	compression	"	"	>95.1	S	35.0	>0.27	0.62
148-1	3.6	tensile	54	-0.6	1.66	69.9	39.9	0.17	0.64
148-2	"	compression	"	"	>51.0	S	31.9	>0.15	0.58
148-3	"	compression	"	"	85.9	S	33.3	0.25	0.68
208-1	4.0	tensile	54	-0.5	1.67	51.4	34.0	0.15	0.51
208-2	"	compression	"	"	>49.5	S	32.5	>0.15	0.70
208-3	"	compression	"	"	63.2	S	33.1	0.18	0.67
158-1	4.6	tensile	54	0.5	1.65	51.1	34.9	0.15	0.60
158-2	"	compression	"	"	60.8	S	36.0	0.17	0.59
161-1	5.3	tensile	57	-1.8	1.70	63.0	38.8	0.16	0.58
161-2	"	compression	"	"	>54.5	S	40.9	>0.14	0.71
161-3	"	compression	"	"	80.1	S	38.5	0.22	0.69

F = Failure of bond between steel backing plate and core in moment-arm area.

S = Shear failure between laminate and core in moment-arm area.

TABLE II - Continued

Specimen Number	Percent Whiskerizing	Type of Load	Fiber Content (v/o)	Void Content (v/o)	Composite Density (g/cc)	Strength (10 <sup>3</sup> psi)	Young's Modulus (10 <sup>6</sup> psi)	Ultimate Elongation (%)	Poisson's Ratio
159-1	7.5	tensile	55	1.1	1.66	>46.6 <sup>F</sup>	37.4 (29.5) <sup>A</sup>	>0.12 (>0.12) <sup>FA</sup>	0.44
159-2	"	tensile	"	"	"	>47.2 (27.7) <sup>A</sup>	(0.17) <sup>S</sup>	-	(0.36) <sup>A</sup>
159-3	"	compression	"	"	"	>29.9 <sup>S</sup> 64.6	30.5 30.4	>0.09 <sup>S</sup> 0.2 <sup>A</sup>	0.57 0.63

F = Failure of bond between steel bucking plate and core in moment-arm area.

A = Longitudinal strain gage data in doubt.

S = Shear failure between laminate and core in moment-arm area.

TABLE III. HONEYCOMB SANDWICH BEAM TESTING: 0°-90°/90°-0° COMPOSITES

Specimen Number	Percent Whiskerizing	Type of Load	Fiber Content (v/o)	Void Content (v/o)	Composite Density (g/cc)	Strength (10 <sup>3</sup> psi)	Young's Modulus (10 <sup>6</sup> psi)	Ultimate Elongation (%)	Poisson's Ratio
169-3	0 (treated)	tensile	57	1.3	1.65	>50.8D	17.2	>0.27D	0.037
169-2	"	compression	"	"	"	54.4	17.4	0.29	—
169-1	"	compression	"	"	"	>23.1S	17.3	>0.13S	0.010
154-1	1.2	tensile	55	1.0	1.64	>48.3S	17.5	>0.27S	0.25
154-2	"	compression	"	"	"	>28.6S	17.7	>0.17S	0.027
154-3	"	compression	"	"	"	73.6	17.8	0.42	0.021
149-1	3.8	tensile	57	-0.8	1.69	32.6	19.4	0.16	0.043
149-2	"	compression	"	"	"	35.6	17.0	0.22	0.032
160-1	6.5	tensile	56	-0.7	1.69	>33.3S	21.5	>0.15S	0.044
160-2	"	tensile	"	"	"	24.7	18.5	0.13	0.035
160-3	"	compression	"	"	"	38.9	19.9	0.20	0.035
224-1	11.2	tensile	54	0.9	1.68	12.1	16.6	0.07	0.039
224-2	"	compression	"	"	"	>29.4S	21.6	>0.14S	0.008
224-3	"	compression	"	"	"	>58.7S	18.3	>0.33S	0.020

D = Failure of bond in shear doubler splice.

S = Shear failure between laminate and core in moment-arm area.

TABLE IV. HONEYCOMB SANDWICH BEAM TESTING: 45°-135°/45°-135° COMPOSITES

Specimen Number	Percent Whiskerizing	Type of Load	Fiber Content (v/o)	Void Content (v/o)	Composite Density (g/cc)	Strength (10 <sup>3</sup> psi)	Young's Modulus (10 <sup>6</sup> psi)	Ultimate Elongation (%)	Poisson's Ratio
170-2	0 (treated)	tensile	57	-1.6	1.68	9.44	2.71	0.40	0.93
170-1	"	compression	"	"	"	11.01	2.97	0.76	0.86
214-2	2.0	tensile	55	1.9	1.63	11.25	2.55	1.20	0.95
214-1	"	compression	"	"	"	12.32	2.81	3.08	1.05
150-1	2.3	tensile	60	0.5	1.69	9.53	2.18	0.75	0.68
150-2	"	compression	"	"	"	10.49	2.88	2.62	0.81
165-1	6.2	tensile	54	-0.3	1.66	17.30	3.98	0.74	0.59
165-2	"	compression	"	"	"	17.70	4.08	2.70	0.89
226-1	14.9	tensile	52	7.4	1.59	7.02	3.22	0.22	1.00
226-2	"	compression	"	"	"	9.16	3.97	0.36	1.09

TABLE V. HONEYCOMB SANDWICH BEAM TESTING: 90° COMPOSITES

Specimen Number	Percent Whiskerizing	Type of Load	Fiber Content (v/o)	Void Content (v/o)	Composite Density (g/cc)	Strength (10 <sup>3</sup> psi)	Young's Modulus (10 <sup>6</sup> psi)	Ultimate Elongation (%)	Poisson's Ratio
172-2	0 (treated)	tensile	51	-0.5	1.62	4.08	1.66	0.27	0.009
172-1	"	compression	"	"	13.77	1.77	0.87	0.011	
225-2	1.4	tensile	55	1.7	1.63	3.43	1.47	0.25	0.008
225-1	"	compression	"	"	14.14	1.44	0.69	0.010	
156-1	1.6	tensile	58	0.3	1.67	3.43	1.60	0.22	0.007
156-2	"	compression	"	"	13.94	1.61	0.95	0.009	
235	6.5	tensile	63	0.3	1.74	3.64	2.07	0.18	0.005
213-2	6.7	tensile	54	1.2	1.65	3.28	1.57	0.20	0.009
213-1	"	compression	"	"	10.77	1.53	0.81	0.006	
234-1	8.3	compression	54	0	1.68	9.24	1.67	0.53	0.006
234-2	"	tensile	"	"	4.29	1.70	0.25	0.006	

TABLE VI. PLATE SHEAR MODULUS TESTING

Laminate Number	Percent Whiskerizing	Fiber Content (v/o)	Void Content (v/o)	Composite Density (g/cc)	Measured* Shear Modulus (10 <sup>6</sup> psi)	Corrected** Shear Modulus (10 <sup>6</sup> psi)
176	0 (treated)	57	0	1.66	0.88 ± 0.02	0.75 ± 0.02
180	1.8	52	0	1.63	0.84 ± 0.02	0.70 ± 0.02
217	4.2	52	2.6	1.61	0.94 ± 0.02	0.78 ± 0.02
233	6.7	58	1.3	1.68	1.21 ± 0.10	0.99 ± 0.08
209	9.1	59	0	1.72	1.56 ± 0.06	1.30 ± 0.05

\* Average of 8 values.

\*\* Corrected for amount of specimen diagonals overhanging the loading points.

## SHEAR BEAMS AND TORSION RODS

A series of short beams was fabricated over the range of whiskerizing and subjected to the horizontal 3-point flexure loading for shear testing. Reliable shear failures could not be obtained with this method at whiskerizings higher than about 2.5% because of the high shear strength/composite fiber strength ratio, which led to tensile failures, even at very low span/depth ratios. Two alternative methods—I-beams and torsion rods—were used to obtain shear failures and therefore shear strength values. The I-beams were cut from shear beam laminates by narrowing the beams in the middle to form narrow webs resembling an I-beam configuration. These cuts were made by longitudinal passes with an abrasive high-speed cut-off wheel. The torsion rods were cylindrical specimens with longitudinal fiber orientation. These rods were made two ways: machining on a lathe from laminate stock, and molding in a cylindrical matched-metal mold. All tests with the I-beam and torsion rod configurations yielded shear failures, although there was some indication in a few of the torsion-rod tests that the failure was grip-initiated. The results of all shear testing are given in Table VII.

Some of the specimens machined into torsion rods were from laminates fabricated earlier than this program (laminates 60, 130, 131, and 133). These tests are from remnant pieces of these laminates and were made for early verification of the suitability of the torsion test before a rod-molding die was available.

## TENSILE FATIGUE SPECIMENS

Flat laminates of batch-whiskerized high-modulus PAN-precursor fiber, manufacturer-surface-treated un-whiskerized fiber, and untreated un-whiskerized fiber of the same manufacturer's batch as the whiskerized fiber were fabricated for this phase of the program by the same technique used to form the 0° sandwich beam face plates. All three types of laminates were evaluated in static tensile tests with glass fiber composite tabs applied and were subjected to fatigue testing.

The fatigue testing consisted of tension-zero-tension cycling at constant stress until failure (load release) or until runout defined as  $10^7$  cycles was obtained. The direct stress apparatus used in this testing is shown in Figure 8. Specimens carried to runout were then subjected to one or the other of the following:

- a. Cycles at high stress level until failure or past  $10^6$  cycles.
- b. Tensile test for residual static strength.

The results of the evaluations and tests are given in Tables VIII-XI. The appearance of the specimens that had undergone the fatigue cycling is shown in Figure 9. A

TABLE VI. SHORT-BEAM AND TORSION SHEAR TESTING

Laminate Number	Percent Whiskerizing	Fiber Content (v/o)	Composite Density (g/cc)	Void Content (v/o)	Short-Beam Shear Strength ( $10^3$ psi)			Torsion Shear Modulus ( $10^8$ psi)
					5.2/1	4.3/1	3.1/1	
60	0 (no treatment)	63	1.68	1.1	-	2.54 ± 0.06	-	-
236	0 (no treatment)	55	1.64	0.3	-	-	-	2.81 <sup>(a)</sup>
166	0 (treated)	55	1.65	0	6.06 ± 0.20	6.74 ± 0.20	-	3.23 <sup>(b)</sup>
205	0 (treated)	57	1.67	-0.6	6.23 ± 0.16	6.10 ± 0.14	7.17 ± 0.14	-
188	0 (treated)	49	1.59	0.9	4.58 ± 0.33	4.58 ± 0.54	-	-
227	0 (treated)	55	1.65	0	-	-	-	5.87 <sup>(b)</sup>
228	0 (treated)	52	1.63	0.3	-	-	-	0.55 <sup>(b)</sup>
157	1.9	57	1.67	-0.2	2.91 ± 0.09	3.17 ± 0.73	-	-
182	1.8	58	1.67	0	-	-	-	5.92 <sup>(b)</sup>
152	2.6	55	1.65	1.7	4.38 ± 0.05	4.71 ± 0.10	-	-
162	2.7	60	1.69	0.8	(5.84 ± 0.31) <sup>T</sup>	(6.24 ± 0.11) <sup>T</sup>	(6.96 ± 0.43) <sup>T</sup>	(8.22 ± 0.54) <sup>T</sup>
167	2.9	56	1.66	0.8	4.95 ± 0.10	5.09 ± 0.20	-	-
230	4.4	54	1.63	0.5	(6.31 ± 0.38) <sup>T</sup>	(6.92 ± 0.41) <sup>T</sup>	-	8.95 <sup>(a)</sup>
133	5.3	58	1.70	-0.4	(6.38 ± 0.30) <sup>T</sup>	(7.65 ± 0.32) <sup>T</sup>	-	11.27 ± 0.30 <sup>T</sup>
231	5.4	53	1.63	1.1	-	-	-	10.3 <sup>(a)</sup>
131	6.0	64	1.74	0.2	(6.02 ± 0.41) <sup>T</sup>	(6.31 ± 0.40) <sup>T</sup>	-	4.25 <sup>(b)</sup>
130	7.1	59	1.70	1.0	(5.20 ± 0.41) <sup>T</sup>	-	-	9.0 <sup>(b)</sup>
232	7.3	59	1.68	1.0	-	-	-	0.82 <sup>(a)</sup>
							-	5.87 <sup>(b)</sup>

(a) Machined rod from flat laminate.

(b) Molded rod.

(c) I-beam configuration of short beam at 5/1.

T = Failed in tension.

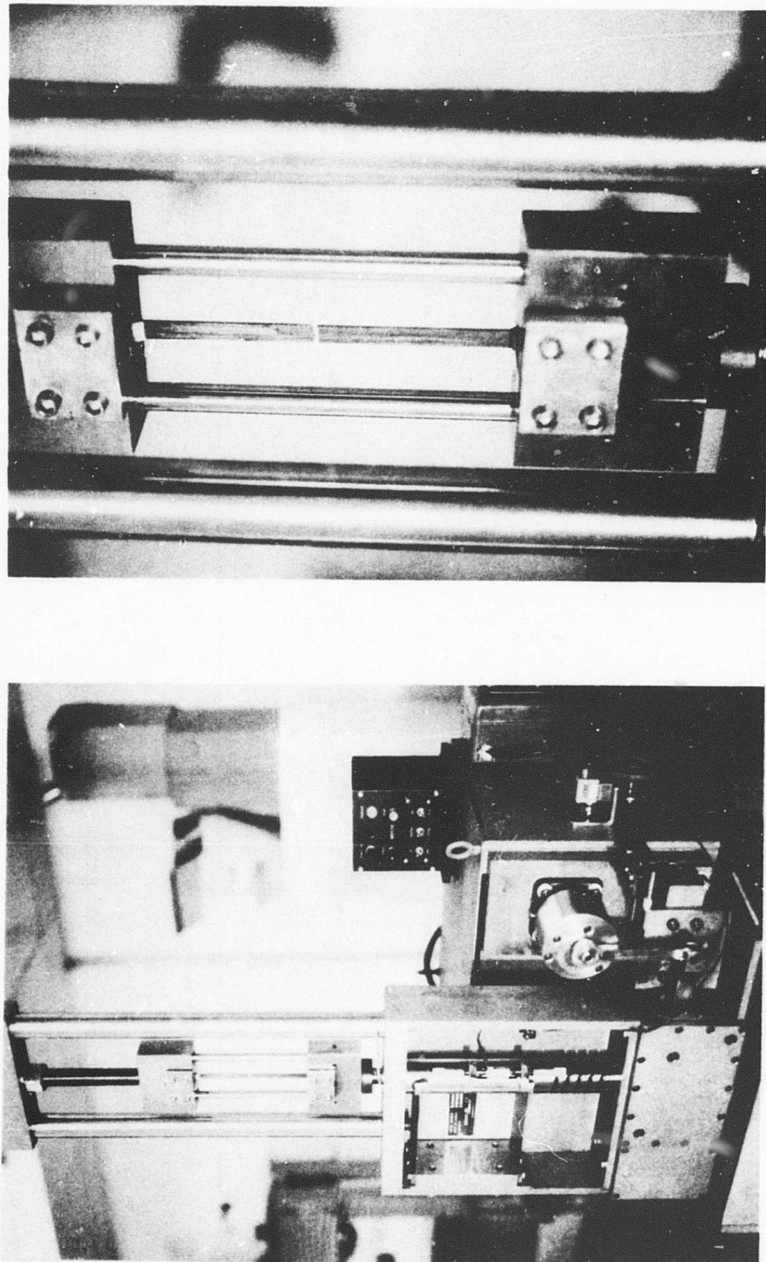


Figure 8. Fatigue Tester With Direct Stress Attachment and GTC-Designed Grips.

TABLE VIII. LAMINATE PROPERTIES

	Laminate Number				
	258	261	265	237	238
% Whiskerizing <sup>(a)</sup>	5.0	5.1	2.9	0 <sup>(d)</sup>	0 <sup>(e)</sup>
v/o Total Fiber <sup>(b)</sup>	53	56	55	52	52
v/o Void <sup>(c)</sup>	-0.4	-1.0	1.5	1.1	2.0
Composite Density (g/cc)	1.65	1.69	1.64	1.61	1.60

(a) By ignition of composite samples.  
 (b) By acid analysis of composite samples.  
 (c) Calculated from specimen density, fiber content.  
 (d) Manufacturer surface-treated.  
 (e) Untreated, un-whiskerized fiber from same batch as in laminates 258, 261, and 265.

TABLE IX. STATIC TENSILE TESTING DATA

	Laminate Number				
	258	261	265	237	238
Strength ( $10^3$ psi):	51.0	63.0	93.9	107.6	(96.8) SH
	74.9	(39.8) TT	(71.8) TT	122.2	(88.9) SH
	61.7	40.9	(63.7) TT	(116.6) SH	102.7
	49.8	68.8	62.0	144.5	82.6
	50.3	53.9	88.0	120.6	(83.1) SH
		67.2	(86.0)	(102.2) TT	94.8
			70.0	111.6	(96.4) SH
				(74.6) TT	(81.0) SH
					(99.0) SH
					105.3
					97.2
Average of					
Gage Section Breaks:	57.5	58.8	79.2	121.3	96.5
Standard Deviation:	10.9	11.5	13.0	14.3	8.9
Average Young's					
Modulus ( $10^6$ psi):	35.7	36.9	36.7	31.8	34.0

TT = Tensile failure at tab end.  
 SH = Shear failure in tab end.

TABLE X. RESIDUAL STRENGTH AFTER STRESS CYCLING

Specimen Number	Cyclic Stress Level ( $10^3$ psi)	Percent of Static	Cycles of Stress	Residual Strength ( $10^3$ psi)	Percent of Original Static
258-2	42.3, 44.6	74, 78	11,100,000 2,300,900	58.3	101
261-2	42.0, 45.1	71, 77	4,806,100 2,110,000	68.1	116
265-7	59.5	75	8,875,000	100.1	126
265-8	60.0	76	9,012,000	77.2	97
265-12	54.7	69	10,195,000	73.0	92
237-11	80.0	66	10,100,000	130.8	108
238-7	60.2	62	9,404,000	87.8	91
238-8	62.5	65	3,210,000	90.8	94
238-9	62.5	65	5,490,000	111.4	115

TABLE XI. FATIGUE TEST RESULTS

Specimen Number	Percent of Static	Maximum Stress ( $10^3$ psi)	Cycles to Failure	Cycles to Runout	Remarks
258-1	76	43.6	30,300	-	
258-2	74	42.3	-	11,100,000	
"	78	44.6	-	2,300,900	to residual testing
258-4	80	46.0	8,500	-	
261-1	78	46.1	150	-	
261-2	71	42.0	-	4,806,100	
"	77	45.1	-	2,110,000	to residual testing
261-4	78	46.0	78,200	-	
265-1	76	60.0	-	10,195,000	
"	82	65.0	4,300	-	
265-3	82	64.9	93,300	-	
265-4	79	62.4	26,100	-	
265-6	63	50.1	-	10,018,000	
"	72	56.7	2,900	-	
265-7	75	59.5	-	8,875,000	to residual testing
265-8	76	60.0	-	9,012,000	to residual testing
265-10	89	70.1	100	-	
265-11	77	61.0	141,500	-	
265-12	69	54.7	-	10,195,000	to residual testing
265-15	76	60.0	-	11,120,000	
"	88	70.0	2,140	-	
237-1	64	78.2	-	500,700	grip mechanism failure
237-2	69	83.5	150	-	
237-4	60	72.6	-	8,300	grip mechanism failure
237-5	58	70.0	-	7,590,000	splits
"	74	90.1	150	-	
237-6	59	72.0	831,400	-	split at 60,000 cycles
237-9	54	65.9	-	3,800	split along edge no load release
237-10	70	84.7	700	-	
237-11	66	80.0	-	10,100,000	to residual testing

TABLE XI - Continued

Specimen Number	Percent of Static	Maximum Stress ( $10^3$ psi)	Cycles to Failure	Cycles to Runout	Remarks
238-1	67	65.0	3,900	-	split at 3400 cycles
238-2	64	62.1	13,600	-	split at 12,000 cycles
238-3	74	71.0	163,700	-	
238-4	64	62.0	1,196,500	-	
238-5	74	71.0	100	-	
238-6	63	61.5	-	6,030,000	
"	84	81.1	50	-	
238-7	62	60.2	-	9,404,000	to residual testing
238-8	65	62.5	-	3,210,000	to residual testing
238-9	65	62.5	-	5,490,000	to residual testing

Specimen No.
237-10
237-2
237-9
237-6
237-5
237-4
237-11
237-1
261-1
261-2
261-4
258-1
258-2
258-4
265-1
265-3
265-4
265-6
265-7
265-8
265-10
265-11
265-12
265-15

Figure 9. Appearance of Fatigue-Tested Specimens.

few of the specimens broke at several places at fatigue failure, resulting in loss of fragments in the middle. The whiskerized specimens generally exhibited cleaner, more brittle appearing breaks than the un-whiskerized specimens, which tended to break with a good deal of axial splitting and fraying. Some of these latter specimens were noted to have split longitudinally at a number of cycles far short of load release. These are noted in the results. No whiskerized specimen exhibited this low-cycle splitting.

#### COMPOSITE ANALYSIS AND MICROSTRUCTURE

The composite laminates used in the physical properties testing of this program were sampled for analysis of composition. With the honeycomb beam plates, samples of about one square inch were taken within the gage sections. Pieces were cut from the shear beams, torsion rods, shear modulus plates, or fatigue specimen laminates. The details of the analytical technique are given later in the Experimental Techniques section, but they consisted of digestion of the resin matrix with hot nitric acid to determine total fiber content, ignition of the residue of acid digestion to determine percentage of whiskerizing, and ignition of undigested composite samples to verify percentage of whiskerizing. The results of these analyses are given in Tables XII and XIII, together with the values estimated from the amounts of material used in the lamination process that were used for initial evaluation of the suitability of the laminates.

The fiber contents derived from these analyses helped in general to resolve some of the apparently anomalous properties, such as calculated void contents significantly less than 0%, which is of course impossible. Most of these instances were resolved by use of the analytical data to determine the calculated values of fiber volume % (v/o) and void content. Five of the instances of fiber v/o calculated to be over 60 v/o by means of the material balance data were found to be in the range of 55-59 v/o, thus reducing the apparent scatter of compositions. The nominal value of 55 v/o fiber aimed for on this program is equivalent to 57 weight % in a void-free composite. The extent to which this was adhered to can be seen in Table XII. The laminates with numbers in the range of 60-133 were not fabricated during this program, so they are not to be compared for v/o consistency. They were fabricated to be 60 v/o composites. The average analytical fiber content of the laminations made in this program was 66.6 weight %, which is very close to the target value. The differences found in Table XII between the material balance and the analytical values are probably due to both difficulty in keeping a material balance and difference between overall laminate composition and the sample composition. However, on an average, the 48 laminations Nos. 148-265 were 66.8 weight % by material balance, which is extremely close to the 66.6-weight-% average analytical value.

An unexpected result was found in the analysis for percentage of whiskerizing, in that

TABLE XII. RESULTS OF COMPOSITE FIBER CONTENT ANALYSIS

Laminate Number	Specimen Type (a)	Total Fiber Content (Weight %) by Material Balance on Lamination (b)	Total Fiber Content (Weight %) by Nitric Acid Analysis (c)
60	SBS, TR	74.0	75.9
130	SBS, TR	69.8	72.1
131	SBS, TR	74.9	74.9, 73.8
133	SBS, TR	69.5	72.3, 66.1
148	HBP	65.3	70.7
149	HBP	66.7	67.9
150	HBP	68.6	73.0, 71.7
152	SBS	74.6	66.4
154	HBP	65.9	66.8
155	HBP	68.9	67.2
156	HBP	68.6	69.1
157	SBS	68.6	69.5
158	HBP	64.5	66.1
159	HBP	68.9	67.2
160	HBP	72.9	67.3
161	HBP	67.3	65.5
162	SBS	72.3	70.9
165	HBP	65.2	65.8
166	SBS	71.5	62.2
167	SBS	69.3	67.9
168	HBP	64.2	63.6
169	HBP	65.0	68.5
170	HBP	66.9	66.7
171	HBP	61.2	63.5
172	HBP	62.0	58.2
176	SMP	62.8	65.0
180	SMP	63.1	61.1
182	TR	62.1	68.3
188	SBS	61.7	62.3, 61.2

(a) SBS = Short beam shear specimen.  
TR = Torsion rod.  
HBP = Honeycomb sandwich beam plate.  
SMP = Shear modulus plate.

(b) Fiber weight in layup  $\div$  laminate weight.

(c) Digestion of resin matrix in nitric acid: weight fiber residue  $\div$  weight specimen.

TABLE XII - Continued

Laminate Number	Specimen Type (a)	Total Fiber Content (Weight %) by Material Balance on Lamination (b)	Total Fiber Content (Weight %) by Nitric Acid Analysis (c)
205	SBS	67.5	64.5
208	HBP	66.0	61.9
209	SMP	68.8	72.8
213	HBP	71.7	66.4
214	HBP	49.9	67.5
217	SMP	67.5	65.1
224	HBP	69.2	67.2
225	HBP	69.0	68.7
226	HBP	65.0	68.9
227	TR	63.0	59.5
228	TR	65.4	64.1
230	SMP	70.7	75.2
231	TR	68.1	65.3
232	TR	67.2	70.6
233	SMP	70.4	70.4
234	HBP	66.0	59.2
235	HBP	74.9	73.8
236	TR	66.7	66.0
237	FS	64.8	64.1
238	FS	65.5	64.5
258	FS	64.7	65.1
261	FS	66.5	67.3
265	FS	67.9	67.1

(a) SBS = Short beam shear specimen.  
TR = Torsion rod.  
HBP = Honeycomb sandwich beam plate.  
SMP = Shear modulus plate.  
FS = Fatigue specimen laminate.  
(b) Fiber weight in layup  $\div$  laminate weight.  
(c) Digestion of resin matrix in nitric acid: weight fiber residue  $\div$  weight specimen.

TABLE XIII. RESULTS OF WHISKERIZING ANALYSIS

Laminate Number	Specimen Type <sup>(a)</sup>	Percent Whiskerizing of Component Fiber Batch <sup>(b)</sup>	Percent Whiskerizing of Acid Analysis Residue <sup>(c)</sup>	Percent Whiskerizing by Composite Ignition <sup>(d)</sup>
130	SBS, TR	5.7	4.4	7.1
131	SBS, TR	4.6	3.8, 4.2	5.5, 6.5
133	SBS, TR	3.8	5.0, 2.4	5.7, 4.9
148	HBP	2.4	2.5	3.6
149	HBP	2.6	2.1	3.8
150	HBP	2.3	1.6, 1.6	2.2, 2.4
152	SBS	10.6	1.7	2.6, 2.9
154	HBP	1.6	1.0	1.2
155	HBP	1.4	2.7	2.2
156	HBP	1.2	0.9	1.6
157	SBS	1.4	0.9	1.9
158	HBP	3.4	2.9	4.6
159	HBP	9.9	2.6	7.5
160	HBP	3.4	6.5	5.8
161	HBP	3.6	3.8	5.3
162	SBS	2.3	2.4	2.7, 4.3
165	HBP	6.2	5.2	6.2
167	SBS	3.3	2.0	2.9, 2.9
180	SMP	1.8	2.3	1.8
182	TR	1.8	1.4	1.8
208	HBP	4.1	2.5	4.0
209	SMP	7.4	7.3	9.1
213	HBP	2.4	4.0	6.7
214	HBP	1.6	1.5	2.0
217	SMP	2.4	4.3	4.2
224	HBP	9.3	8.1	11.2

(a) SBS = Short beam shear specimen.  
TR = Torsion rod.  
HBP = Honeycomb sandwich beam plate.  
SMP = Shear modulus plate.

(b) Weight % of whiskers in as-received fiber batch.

(c) Weight % of ignition residue of the fiber left after nitric acid analysis.

(d) Weight % of ignition residue of composite sample divided by weight % of total fiber in composite sample (times 100).

TABLE XIII - Continued

Laminate Number	Specimen Type(a)	Percent Whiskerizing of Component Fiber Batch(b)	Percent Whiskerizing of Acid Analysis Residue(c)	Percent Whiskerizing by Composite Ignition(d)
225	HBP	8.3	2.0	1.4
226	HBP	11.8	6.1	10.9
230	SMP	4.0	3.4	4.4
231	TR	4.0	3.6	5.4
232	TR	10.9	7.3	7.3
233	SMP	4.8	4.2	6.7
234	HBP	9.3	10.0	8.3
235	HBP	4.6	4.2	6.5
258	FS	4.7	5.1	5.0
261	FS	4.9	5.3	5.1
265	FS	2.7	2.7	2.9

(a) TR = Torsion rod.  
 HBP = Honeycomb sandwich beam plate.  
 SMP = Shear modulus plate.  
 FS = Fatigue specimen laminate.  
 (b) Weight % of whiskers in as-received fiber batch.  
 (c) Weight % of ignition residue of the fiber left after nitric acid analysis.  
 (d) Weight % of ignition residue of composite sample divided by weight % of total fiber in composite sample (times 100).

the values obtained by ignition of the fiber residue left after acid analysis were, in general, significantly lower than those obtained in the quality control analyses of the fiber batches used to make up the laminates. It was decided that there was the possibility of significant whisker loss in transferring the fiber residue from the fritted disc crucible to the ignition crucible, so a parallel set of analyses was carried out using ignition of the composite itself. The residue of the analyses was related to percentage of whiskerizing (fiber basis) by using the value of total fiber content obtained from the acid digestion analysis. These values were generally more consistent with the fiber batch QC analyses and were higher, in general, than the earlier test of fiber residue ignition.

This latter test for percentage of whiskerizing is judged to give the most accurate values; hence, these values are cited throughout this report for correlation purposes.

Samples of all laminates evaluated during this program for mechanical properties were subjected to microscopic examination of structure. The samples were mounted and examined petrographically; i.e., embedded in a hard potting compound, polished through 0.3 micron alumina grit on a vibratory polisher, and examined by reflected light. The various types of layups were sectioned as follows:

- a. 0° and 90° beam plates, shear beams, shear modulus plates, torsion rods, and fatigue specimens—perpendicular to the graphite tow fibers
- b. 90°/90°-0° beam plates—perpendicular to the 0° lamina
- c. 45°-135°/45°-135° beam plates—perpendicular to the beam plate axis (all fibers sectioned at 45° therefore)

The typical microscopic appearance of the cross-ply laminates is shown in Figures 10 and 11. The microscopic observation of these sections verified in general the results of the composition analyses with regard to fiber content, apparent whisker content, and void content. For example, no significant void content could be found in those specimens having calculated void contents below 1%. The few specimens with void contents above 2% had obvious void content under microscopic examination, and these voids tended to be concentrated in the interlaminar regions. Figures 12 and 13 provide comparisons of typical examples.

Two types of nonuniformity could be found in a few laminates: regions of much higher than average whisker content and regions of grossly maldistributed graphite fiber. Figures 14 and 15 show these anomalies in typical views. The very high whisker concentration anomaly tended to be in the interlaminar regions of the relatively highly whiskerized laminates. This appears to be due to overgrowth of whiskers on the monolayer layup. The gross variations in fiber distribution within a laminate are probably due to differences in resin advancement (viscosity) from

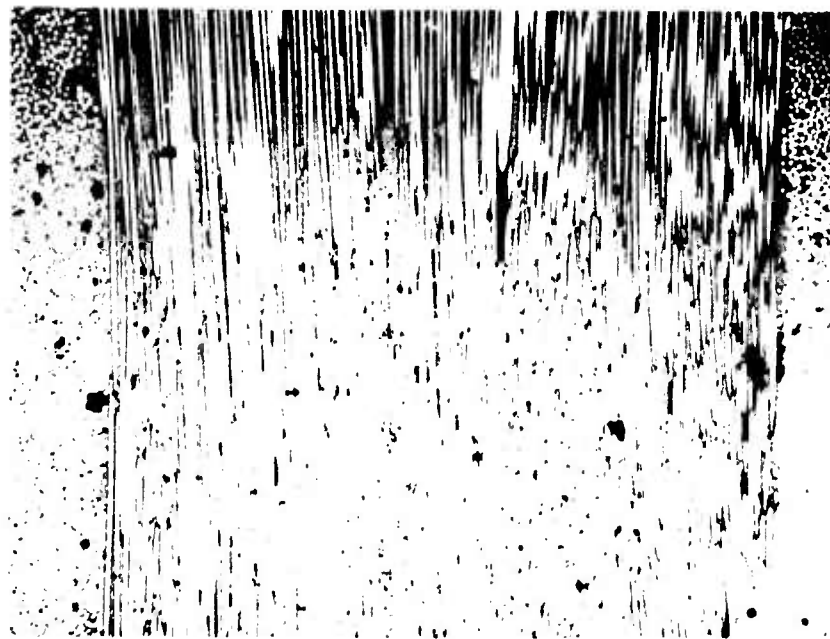


Figure 10. Section of  $0^\circ$ - $90^\circ$ / $90^\circ$ - $0^\circ$  Cross-Ply Laminate,  
No. 224 (100X).

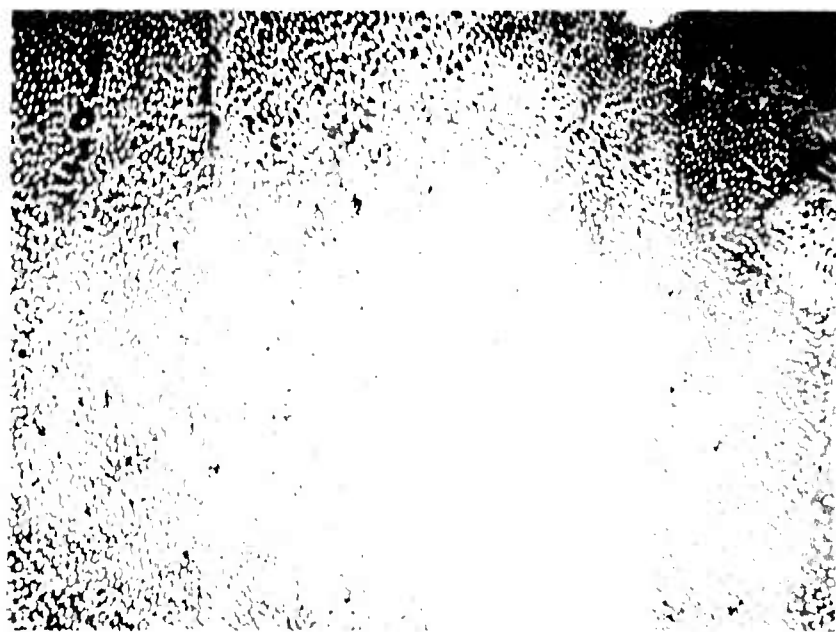


Figure 11. Section of  $45^\circ$ - $135^\circ$ / $45^\circ$ - $135^\circ$  Cross-Ply  
Laminate, No. 150 (100X).

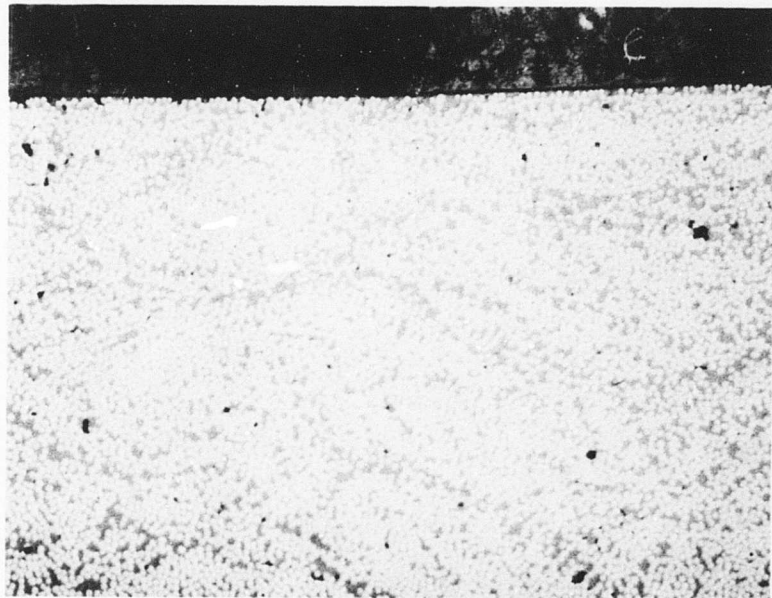


Figure 12. Cross Section of Void-Free Composite,  
No. 230 (100X).

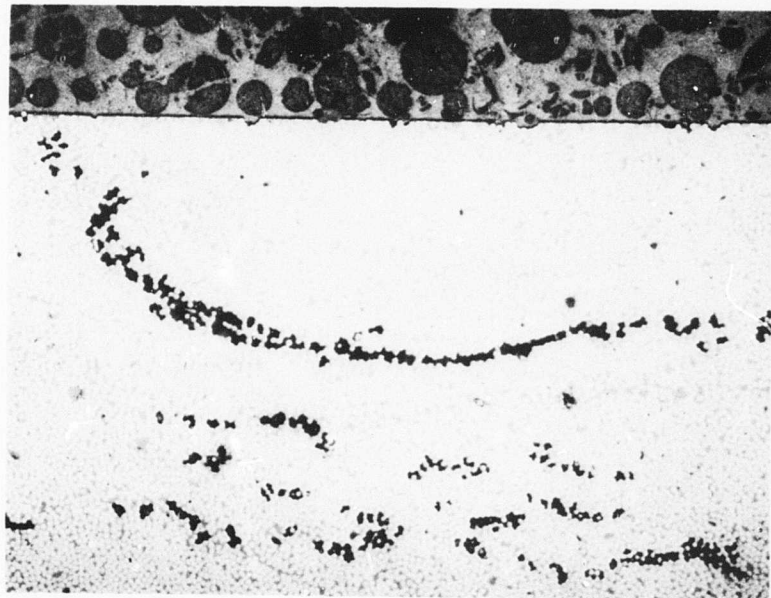


Figure 13. Cross Section of Composite Showing Voids,  
No. 232 (100X).

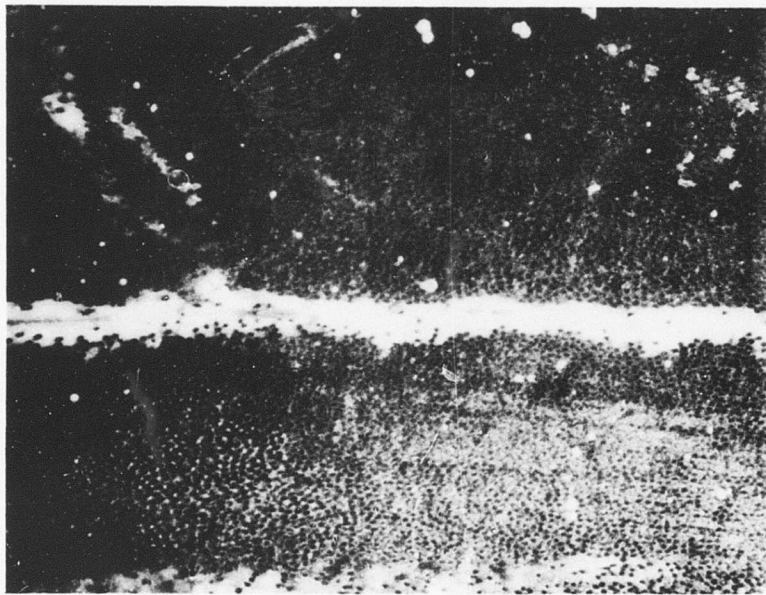


Figure 14. High Interlaminar Whisker Concentration,  
No. 234 (100X, dark field).

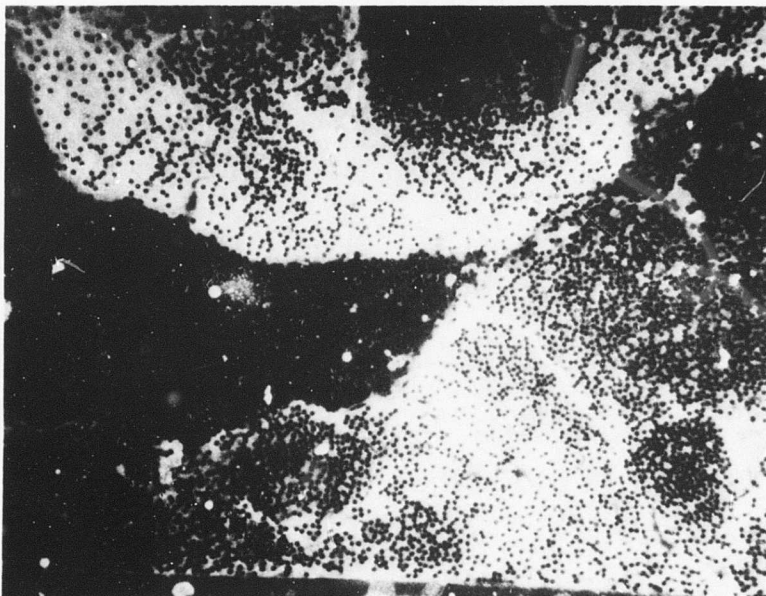


Figure 15. Maldistributions of Graphite Fiber, No. 167  
(100X, dark field).

layer to layer and the resultant differences in local resin flow under compaction. The interstitial region between graphite fibrils is shown in high magnification in Figure 16 for un-whiskerized fiber and in Figure 17 for a region of about 3% whiskerizing. Regions of graphite fibril contact can be found, but they tend to be less frequent in the whiskerized composites, presumably because of the tendency of the whiskers to keep fibrils apart under compaction. The appearance of the whiskers as regards size and configuration is typical, the more highly whiskerized specimens having more and, to a degree, longer whiskers. Undoubtedly, submicron whiskers that cannot be resolved are also present.

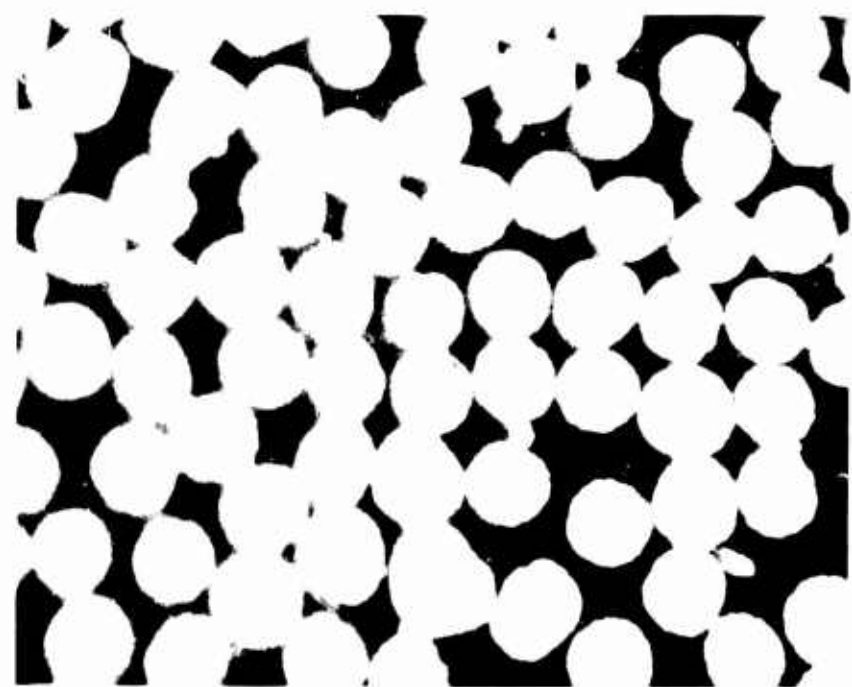


Figure 16. Un-Whiskerized Composite, No. 227 (1500X).

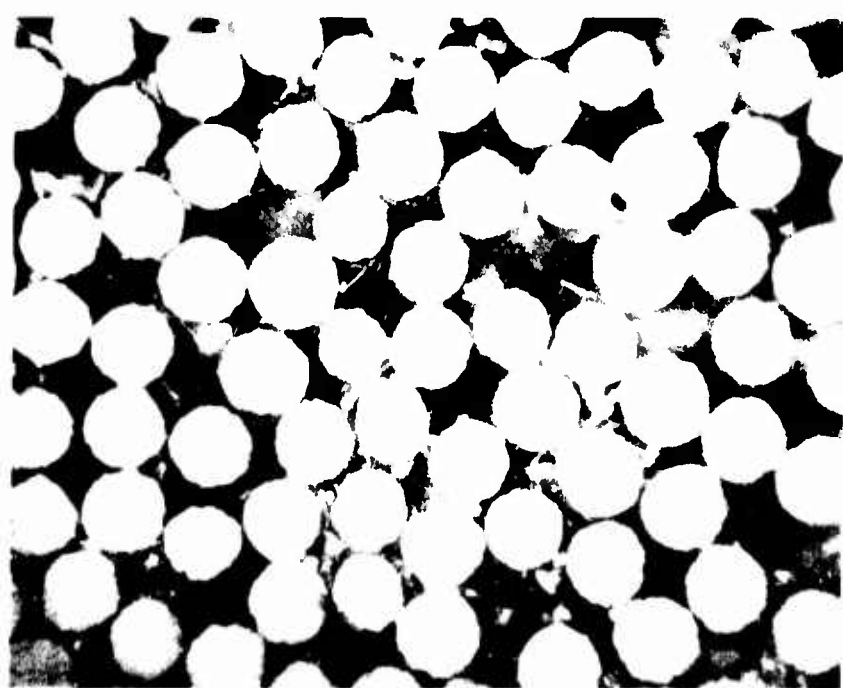


Figure 17. Whiskerized Composite, No. 152 (1500X).

## RESULTS OF FILAMENT-WOUND STRUCTURE PROPERTIES EVALUATIONS

### NOL RINGS

The results of the testing of the NOL rings cut from the filament-wound cylinders are given in Table XIV. The procedure consisted of testing all of the four rings for ring flexure modulus (nondestructive), testing two rings to failure in split-disc tensile, and cutting the other two rings into segments for shear testing and flexure strength. The appearance of failures in these NOL rings is shown in Figure 18.

The composition of the rings was determined by analysis after testing. Digestion by nitric acid yielded fiber weight content, and ignition in air yielded whiskerizing level.

The whiskerizing process was carried out at the standard conditions generally used to yield 3% whiskers by weight on the fiber. The analysis of the samples of composite yielded a value for the treatment level of 3.3% with a standard deviation of 0.3%. Thus the actual degree of whiskerizing was very close to the nominal for which process conditions were selected. The total fiber content of the composites as analyzed is given in Table I.

### TORSION TUBES

The torsion tubes were tested for torsion modulus by loading and unloading stepwise while recording load and strain gage output. The shear strength was then determined by loading at constant rate to failure. The results of these tests together with the physical characteristics of the specimens are given in Table XV.

The whiskerizing process was carried out at the standard conditions used to yield 3% whiskers on the fiber, identical on the continuous fiber to that used in the NOL ring winding phase and on the batch layups to that used in the optimized laminates for tensile fatigue testing. Fiber and void content were analyzed by the same technique as used with the NOL rings.

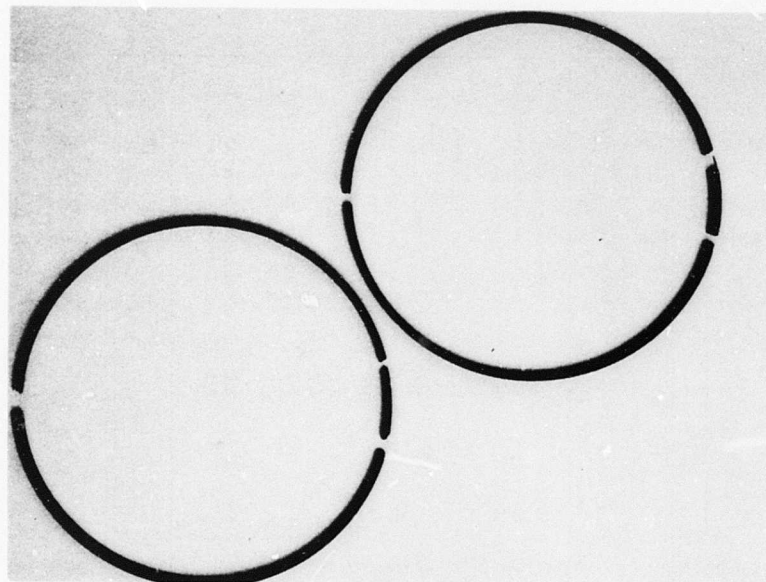
In certain of the tests, shear of the fiber glass torsion grip from the tube was the mechanism of failure, as noted in the data. In these cases, new grips were applied until specimen gage failure was obtained.

The visual appearance of the fractures obtained in typical torsion tube specimens is shown in Figure 19. The extent of fracture is far beyond that obtained at maximum load in order to allow maximum visualization of the fracture.

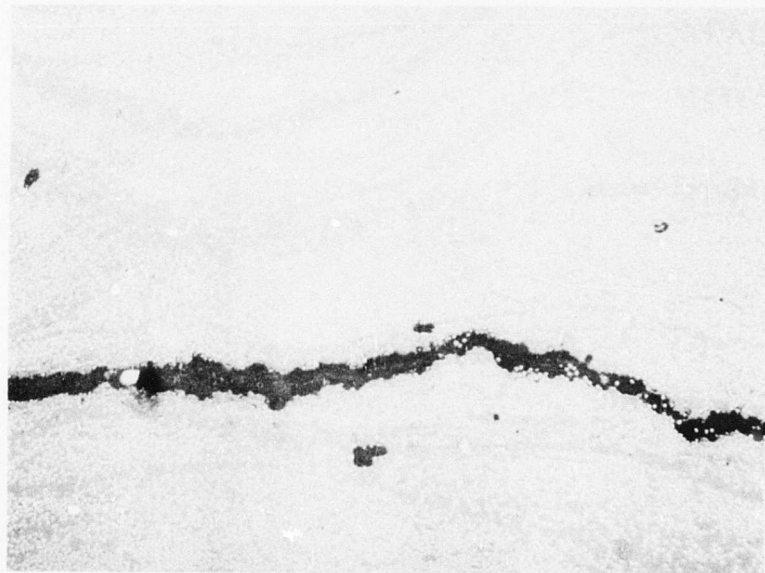
TABLE XIV. NOL RING TEST RESULTS

Winding Number	Fiber Treatment	Split-Disc (a)		Ring Flexure		Segment Flexure	
		Strength (10 <sup>3</sup> psi)	Modulus (10 <sup>6</sup> psi)	Modulus (b) (10 <sup>6</sup> psi)	Modulus (b) (10 <sup>6</sup> psi)	Strength (a) (10 <sup>3</sup> psi)	Shear Strength (c) (10 <sup>3</sup> psi)
160709	treated	59.0	23.6	16.0	90.0	3.88 ± 0.13	
160710	"	75.4	28.0	17.1	97.0	3.77 ± 0.03	
160711	"	50.7	22.7	15.0	79.9	4.37 ± 0.22	
160712	"	78.2	25.0	19.9	98.6	4.73 ± 0.21	
160713	"	55.7	24.2	19.0	102.2	6.57 ± 0.88	
160714	"	65.7	25.0	19.1	97.3	5.14 ± 0.42	
160715	"	70.8	30.6	19.7	96.5	6.38 ± 0.78	
160716	"	78.1	27.3	17.1	95.4	7.22 ± 0.78	
160717	"	103.3	31.0	18.6	108.4	6.86 ± 0.50	
160718	"	109.4	32.2	19.7	119.0	7.05 ± 0.43	
160720	3% whiskerized	45.5	23.5	15.1	58.2	7.75 ± 0.31	
160721	"	29.0	19.9	20.2	42.7	8.35 ± 0.41	
160722	"	31.8	25.0	20.1	62.8	> 5.20 (d)	
160723	"	19.8	15.1	10.2	38.7	4.89 ± 0.57	
160724	"	60.0	25.8	20.7	81.3	> 4.18 (d)	
106726	"	61.7	24.8	17.2	85.0	8.10 ± 0.62	
160727	"	75.4	31.0	18.1	97.6	8.90 ± 0.31	
160728	"	78.7	29.7	18.8	95.1	7.58 ± 0.73	
						8.63 ± 0.48	

(a) Average of 2 tests.  
 (b) Average of 4 tests.  
 (c) Average of 6 tests.  
 (d) Tensile failures.



a. Split-Disc Tensile.



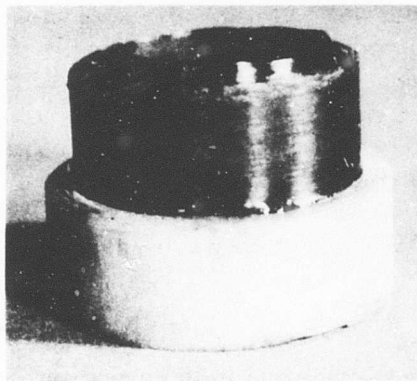
b. Interlaminar Shear Segment, 80X.

Figure 18. Typical Fracture of Graphite Fiber NOL Rings.

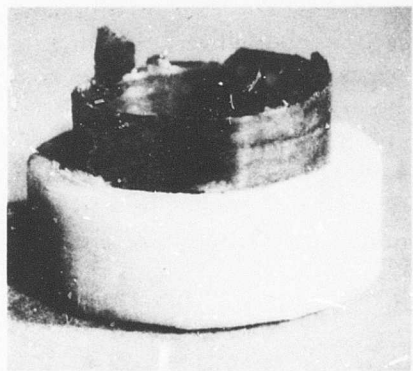
TABLE XV. RESULTS OF TUBE TORSION TESTING

Construction	Specimen No.	Thickness (in.)	Density (g. cc.)	Fiber Content w/o v/o	Apparent Void Content (v/o)		Shear Strength (10 <sup>3</sup> psi)	Shear Modulus (10 <sup>6</sup> psi)	Strain Gage Deflectionmeter	Fiber
					54	1.0				
Hoop-Wound (90°)	160730	0.123	1.57	64	54	1.0	6.3	0.68	0.70	treated high modulus
	160735	0.061	1.49	65	56	2.1	10.4	0.92	1.14	treated intermediate modulus
	160739	0.094	1.55	56	45	0.1	8.1	0.68	0.72	3% whiskerized high modulus
Orthotropic (90°-0°-90°)	160731	0.059	1.57	62	50	0.3	3.1	-	1.25	untreated high modulus - 0°
	160732	0.045	1.52	56	45	0.2	7.1	-	0.87	fibers, treated - 90° fibers
	160741	0.070	1.53	52	40	1.9	8.8	0.80	0.82	treated high modulus
	160743	0.109	1.42	41	30	1.3	8.9	0.91	0.93	3% whiskerized high modulus
Orthotropic (45°, 135°, 45°, 135°)	160733	0.051	1.43	39	28	1.0	16.2*	2.9	2.8	treated high modulus
	160734	0.055	1.46	52	40	2.6	27.3*	4.0	4.2	treated high modulus
	160740	0.063	1.46	50	38	2.1	25.1*	4.1	4.2	3% whiskerized high modulus
	160742	0.104	1.35	43	30	7.3	15.2	2.4	2.7	3% whiskerized high modulus
Isotropic (30°, 150°, 90°)	160736	0.063	1.55	56	45	0.1	12.6	2.6	2.7	treated high modulus
	160744	0.070	1.53	56	44	1.6	11.8	2.6	2.5	3% whiskerized high modulus

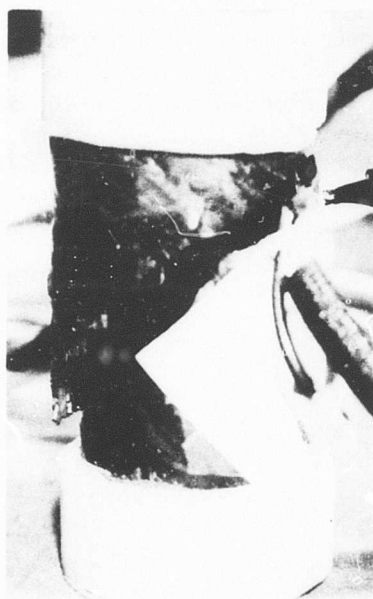
\* Glass fiber grip sheared in first test cycle; new grip bonded and retested to gage failure.



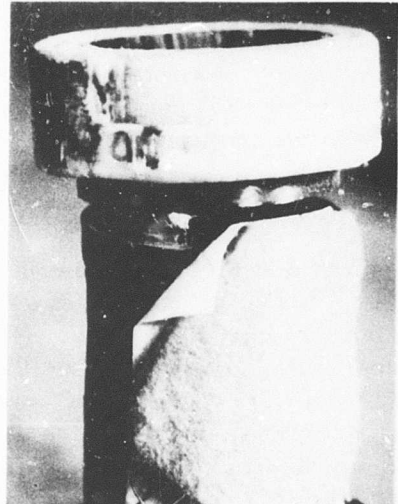
Unidirectional ( $90^\circ$ )



Orthotropic ( $90^\circ-0^\circ/0^\circ-90^\circ$ )



Orthotropic ( $45^\circ-135^\circ/45^\circ-135^\circ$ )



Isotropic ( $30^\circ-150^\circ-90^\circ$ )

Figure 19. Typical Modes of Failure of Torsion Tubes.

## DISCUSSION OF RESULTS

The whiskerized fiber used in most of these studies was high-modulus PAN-precursor-type fiber, which was obtained from the manufacturer in an untreated condition prior to whiskerizing. In the honeycomb sandwich beam test series, the un-whiskerized comparison composites were all fabricated from manufacturer surface-treated fiber. In the shear strength test series, the un-whiskerized comparison composites consisted of both untreated and manufacturer surface-treated fiber. The discussion presented here delineates the major effects found due to whiskerizing and compares and contrasts them where possible with the effect of simple surface treatment.

### TENSILE AND COMPRESSIVE STRENGTH

The strength data obtained by tensile and compressive testing in the honeycomb sandwich beam configuration are plotted versus percentage of whiskerizing in Figures 20 through 23. Whiskerizing is the major correlating parameter since fiber content and void content were held to within narrow limits. The data from the fatigue static tensile testing are superimposed in Figure 20 for comparison.

Figures 20 and 21 show a decrease in tensile strength with increasing percentage of whiskerizing in the  $0^\circ$  and  $0^\circ$ - $90^\circ$  composites, presumably due to fiber degradation accumulation in the whiskerizing process. There is no such clear-cut effect to be seen on compressive strength, partially as a result of the difficulty found in obtaining a complete set of compression failures. It was not possible to test any of the un-whiskerized  $0^\circ$ - $90^\circ$  composites to compression failure because of the persistent shear failure in the composite-to-adhesive bond. This tendency was also found to a lesser extent in the whiskerized composites, but several compressive failures were obtained with them.

The effect of whiskerizing on both the tensile and compressive strength of the  $45^\circ$ - $135^\circ$ / $45^\circ$ - $135^\circ$  composites was a pronounced increase. The exception to this was the very highly whiskerized (14.9%) specimen which also had a very high void content (7.4%), so it cannot be compared. The strengths at the 2.0-2.2% whiskerizing level were equivalent to those obtained with the manufacturer surface-treated fiber, indicating that this is the percentage of whiskerizing equivalent to that treatment in bonding capability. Since the breaks obtained in this test configuration involved shear and no appreciable fiber breakage, any fiber strength effect would not show up.

The use of narrow, straight-sided specimens to measure the strength of  $45^\circ$  or other off-axis cross-ply laminates is subject to criticism because of the discontinuous nature of some or all of the fibers in the gage section. This can lead to strength values that are markedly lower than those measured with "wide" specimens having

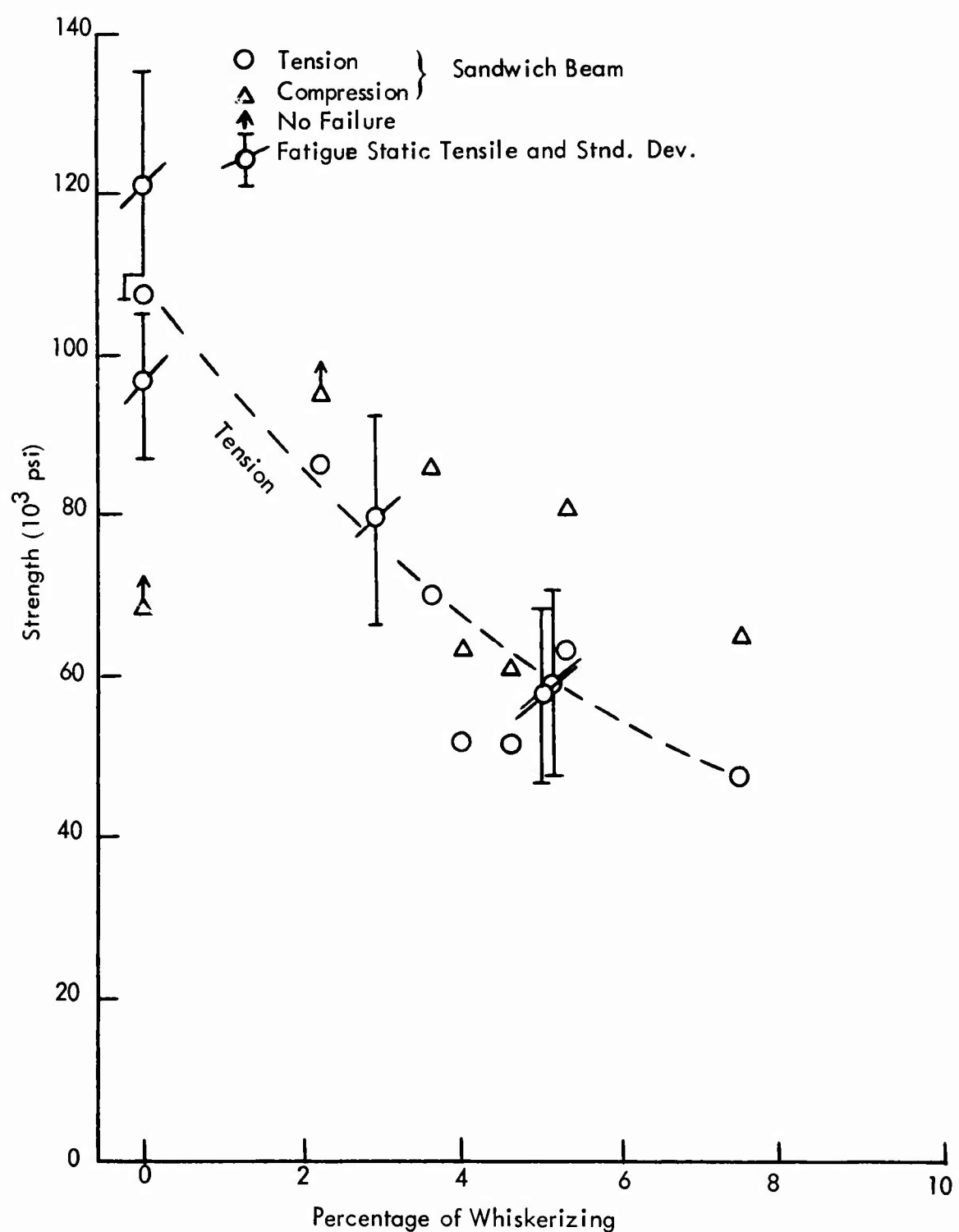


Figure 20. Strength of  $0^\circ$  Composites.

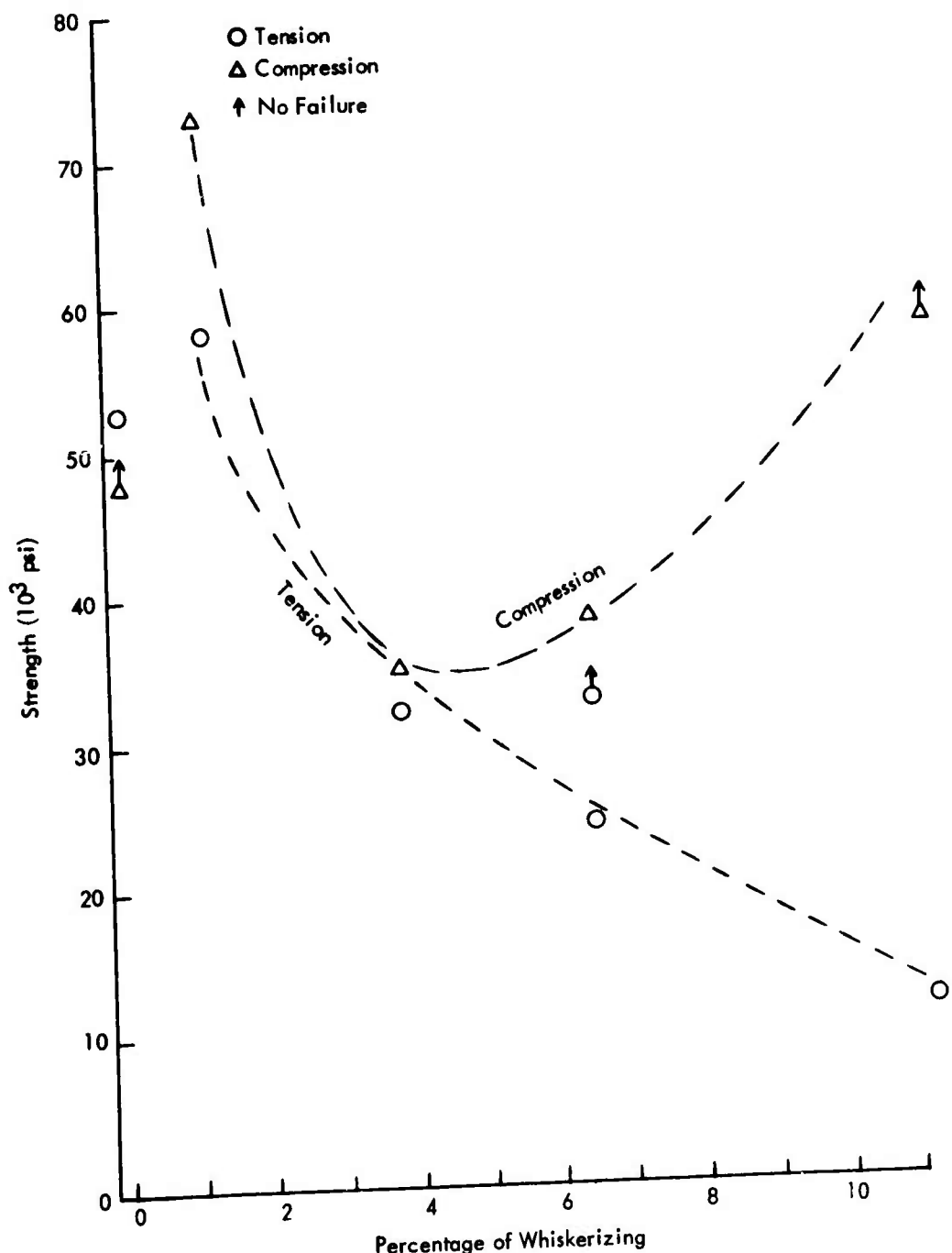


Figure 21. Strength of  $0^\circ$ - $90^\circ$ / $90^\circ$ - $0^\circ$  Composites.

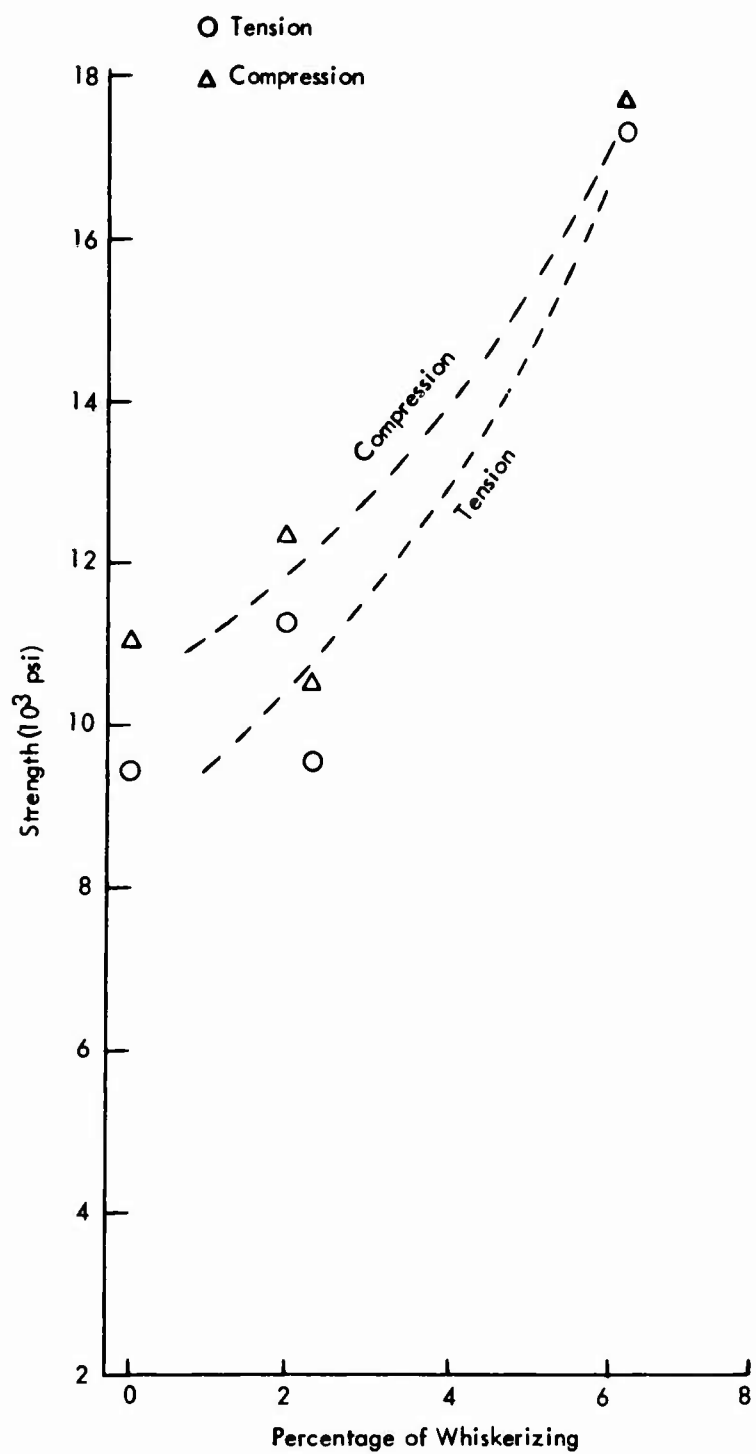


Figure 22. Strength of  $45^\circ$ - $135^\circ$ / $45^\circ$ - $135^\circ$  Composites.

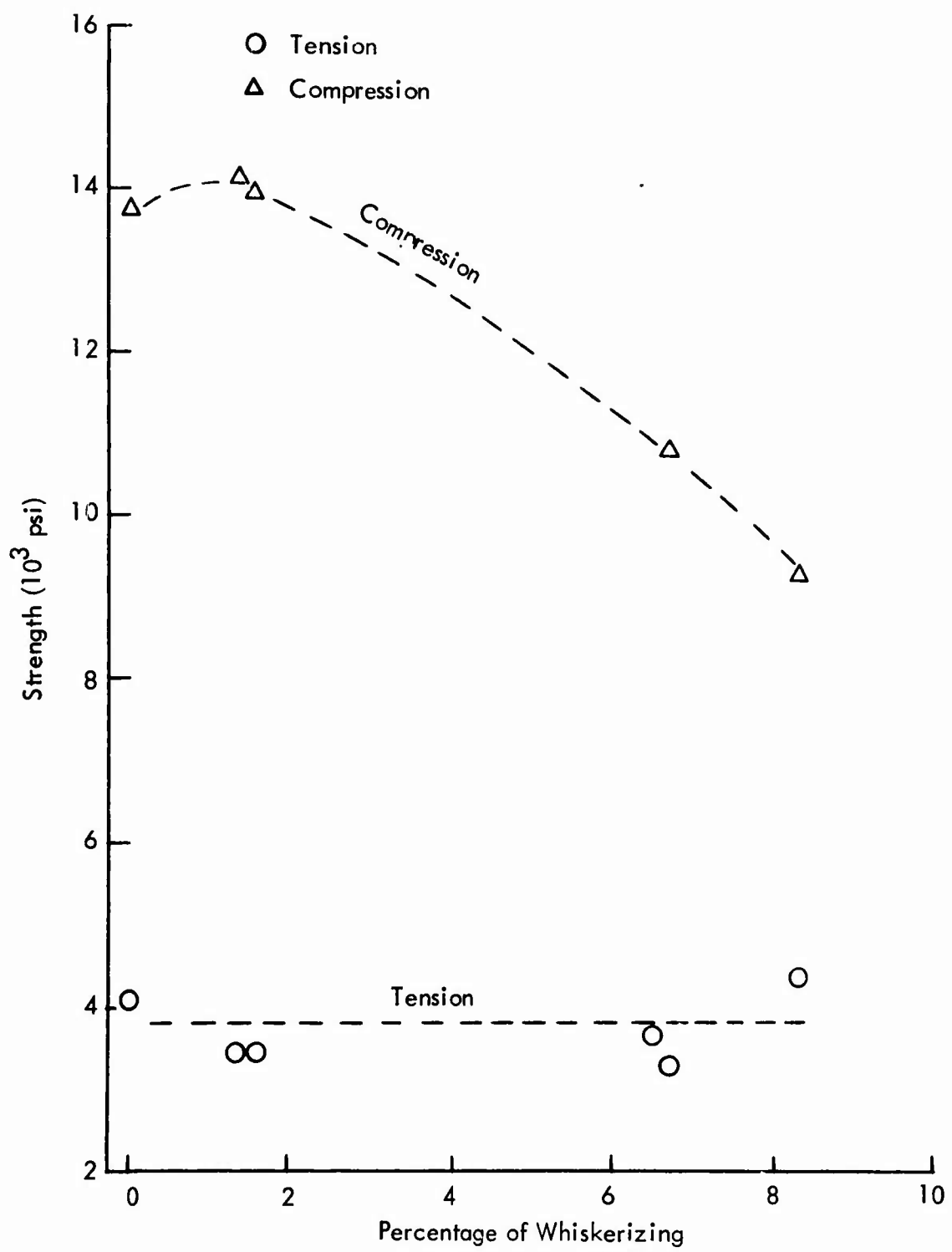


Figure 23. Strength of  $90^\circ$  Composites.

their edges cut along the angles of the fibers so that minimum width is in the middle of the gage section and all fibers are continuous into the tab ends, as has been found by other workers in tensile coupon testing with boron laminates (29, 30). In this work, the  $\pm 45^\circ$  tensile coupons were cut to a minimum gage width of 3-3/8 inches with  $45^\circ$  cuts meeting in a fillet radius. The strength measured was over twice that of the straight-sided tensile coupon of normal dimensions, leading to a value that was 80% of the strength of the  $0^\circ$ - $90^\circ$  crossply laminates in the "wide" specimen configuration versus 36% in the normal specimen. Since the  $\pm 45^\circ$  sandwich beam laminates measured from about 20% to about 67% of the  $0^\circ$ - $90^\circ$  values of tension or compression, depending directly on the degree of whiskerizing, the inference is that significantly higher values could have been measured with a suitably designed, nonstandard face place configuration similar to the "wide" tensile coupon in the gage section.

The  $90^\circ$  composites of whiskerized fiber showed tensile strengths approximately equivalent to the manufacturer surface-treated fiber at all levels of whiskerizing tested. The effect on compressive strength was one of decreasing strength with increasing whiskerizing, as seen in Figure 23. The values in the 1-2% whiskerizing range are equivalent to those obtained with the surface-treated fiber.

#### TENSILE AND COMPRESSIVE MODULUS

The modulus data from the sandwich beam tensile and compressive testing and fatigue static tensile testing were analyzed statistically, and there was no significant difference in modulus between the tensile and the compressive modes for any of the layup configurations. The data are plotted in Figure 24 as functions of percentage of whiskerizing. No effect on modulus due to whiskerizing can be seen, with the possible exception of the  $\pm 45^\circ$ , where there is an apparent increase in modulus due to whiskerizing in the 2% to 6% range.

The average modulus of  $33.7 \times 10^6$  psi for the  $0^\circ$  composites was obtained with average total fiber content in these composites of 54.3 v/o. This corresponds to a fiber modulus of  $62 \times 10^6$  psi. The  $0^\circ$ - $90^\circ$ / $90^\circ$ - $0^\circ$  composites had an average modulus of  $18.5 \times 10^6$  psi at an average fiber content of 55.6 v/o. Allowing for the  $1.64 \times 10^6$  psi modulus obtained in the  $90^\circ$  composites for half of the content of the  $0^\circ$ - $90^\circ$ / $90^\circ$ - $0^\circ$  composites, this computes to a  $0^\circ$  fiber modulus of  $64 \times 10^6$  psi in the  $0^\circ$ - $90^\circ$ / $90^\circ$ - $0^\circ$  composites, a reasonably close correspondence with the  $0^\circ$  composite results.

#### ULTIMATE ELONGATION

The ultimate elongation data from the honeycomb sandwich beam tensile and compressive tests versus percent whiskerizing are plotted in Figures 25 through 27. These values are similar for the  $0^\circ$  and  $0^\circ$ - $90^\circ$ / $90^\circ$ - $0^\circ$  layup configurations

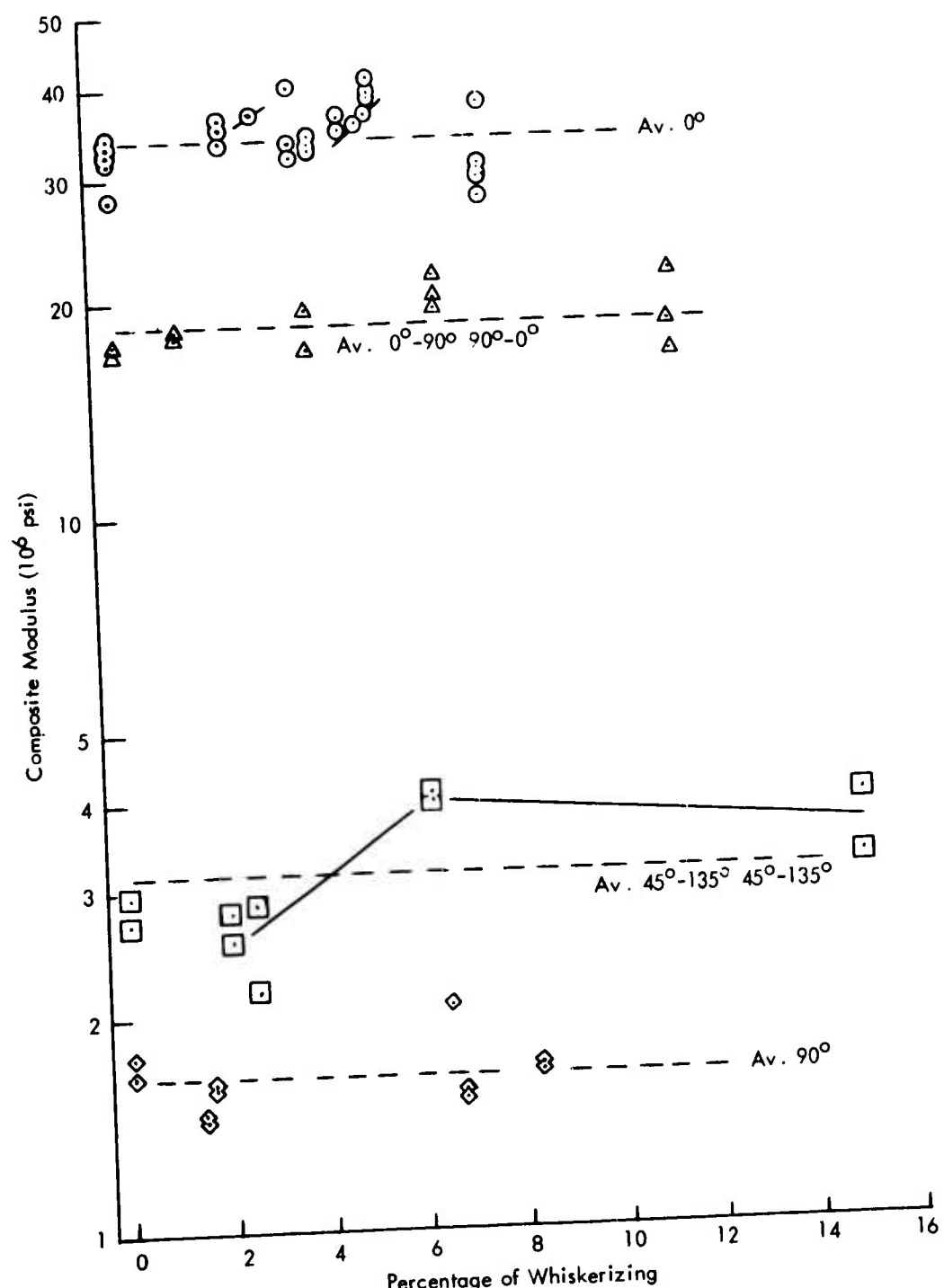


Figure 24. Tensile and Compressive Moduli.

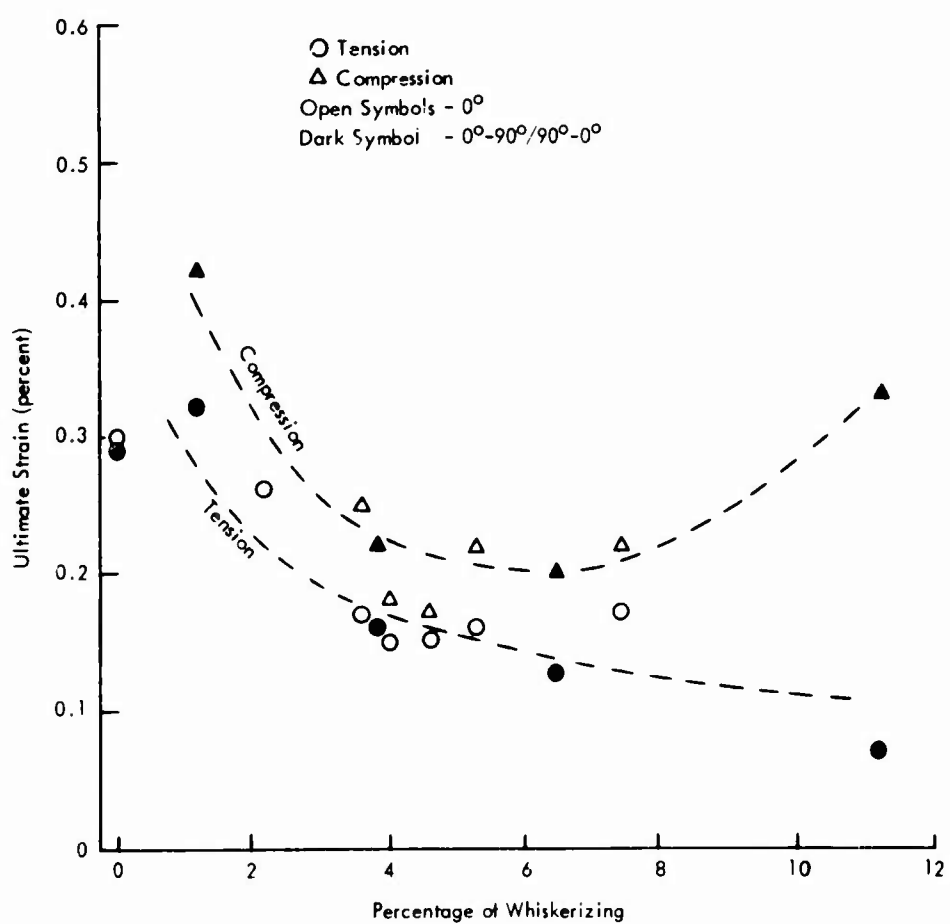


Figure 25. Effect of Whiskerizing on Ultimate Strain of  $0^\circ$  and  $0^\circ$ - $90^\circ$ / $90^\circ$ - $0^\circ$  Composites.

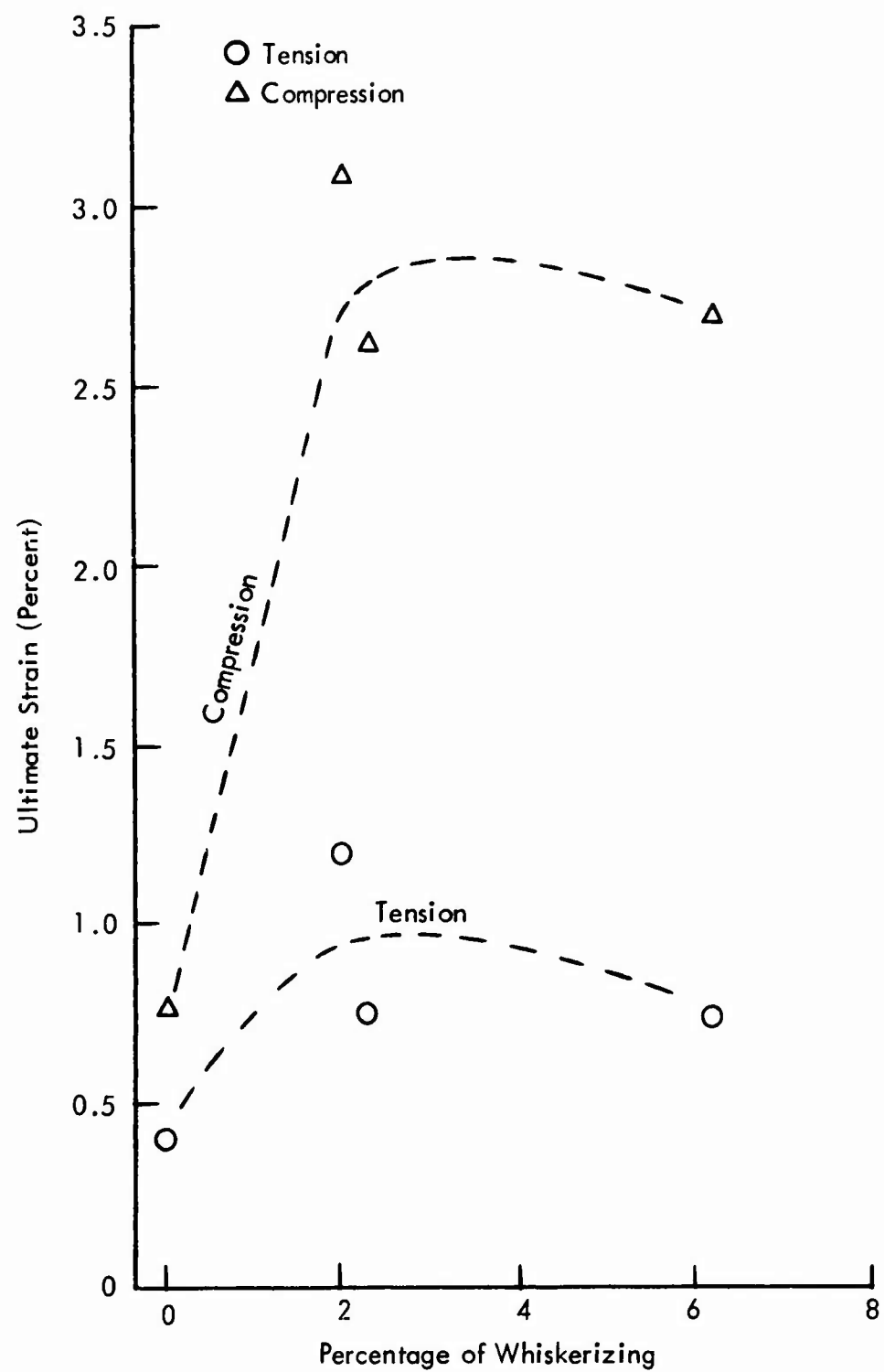


Figure 26. Effect of Whiskerizing in Ultimate Strain of  $45^\circ$ - $135^\circ$ / $45^\circ$ - $135^\circ$  Composites.

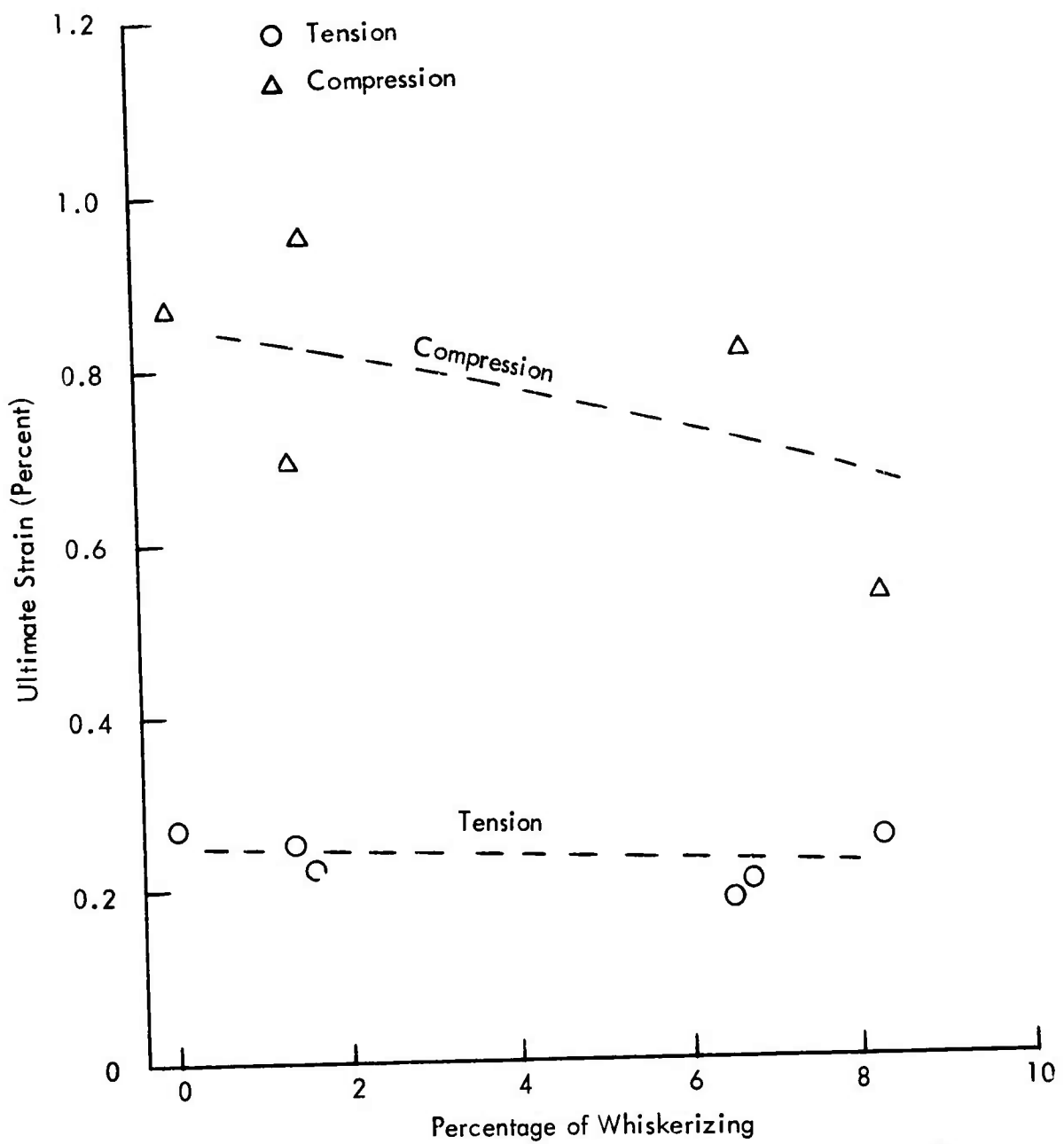


Figure 27. Effect of Whiskerizing on Ultimate Strain, 90°.

(see Figure 25), apparently because the effect of the  $0^\circ$  fibers predominates. There is a continual decrease in ultimate strain with degree of whiskerizing, which reflects the similar effect found with tensile strength, apparently due to graphite fiber degradation. The exception to this is the compression elongation at the very high 11.2% whiskerizing, which shows an increase over the intermediate whiskerizing levels, as did its compressive strength.

The results obtained in the  $\pm 45^\circ$  layups of whiskerized fiber showed remarkable elongations, as seen in Figure 26. In most instances, they exceed by two- to fourfold the elongations of the treated, un-whiskerized fiber composite. This is obviously due directly or indirectly to the presence of the whiskers, and this is therefore an unexpected finding. It amounts to a large increase in toughness of this type of layup, in the sense that the area under the stress-strain curve is increased severalfold by whiskerizing. For comparison stress-strain curves, see Figure 28. The ultimate elongations measured on the  $\pm 45^\circ$  laminates are probably subject to the same effect in straight-sided specimens due to fiber discontinuity, as was discussed earlier in the Tensile and Compressive Strength section. In this respect, the values presented here are presented as comparative rather than absolute or maximum values obtainable by modified techniques.

The ultimate elongations of the  $90^\circ$  composites, as seen in Figure 27, seem to be indistinguishable between the whiskerized and the surface-treated fiber. The compressive ultimate strains are two- to threefold those of the tensile mode.

#### POISSON'S RATIO

The Poisson's ratio data from the sandwich beam tensile and compression testing have been analyzed statistically for correlation with percentage of whiskerizing and tensile or compression mode. No correlation with percentage of whiskerizing is justified, but there were somewhat significant differences due to tensile or compression mode. This can be seen graphically in Figure 29 for the  $0^\circ$  and  $\pm 45^\circ$  composites. The data cross-analyzed for composite layup configuration and testing mode are as follows:

<u>Layup Configuration</u>	<u>Poisson's Ratio</u>	
	<u>Tension</u>	<u>Compression</u>
$0^\circ$	$0.57 \pm 0.04$	$0.67 \pm 0.06$
$0^\circ-90^\circ/90^\circ-0^\circ$	$0.036 \pm 0.008$	$0.022 \pm 0.014$
$45^\circ-135^\circ/45^\circ-135^\circ$	$0.83 \pm 0.18$	$0.94 \pm 0.13$
$90^\circ$	$0.007 \pm 0.002$	$0.008 \pm 0.002$

The values for all the configurations do not differ significantly beyond the one-sigma

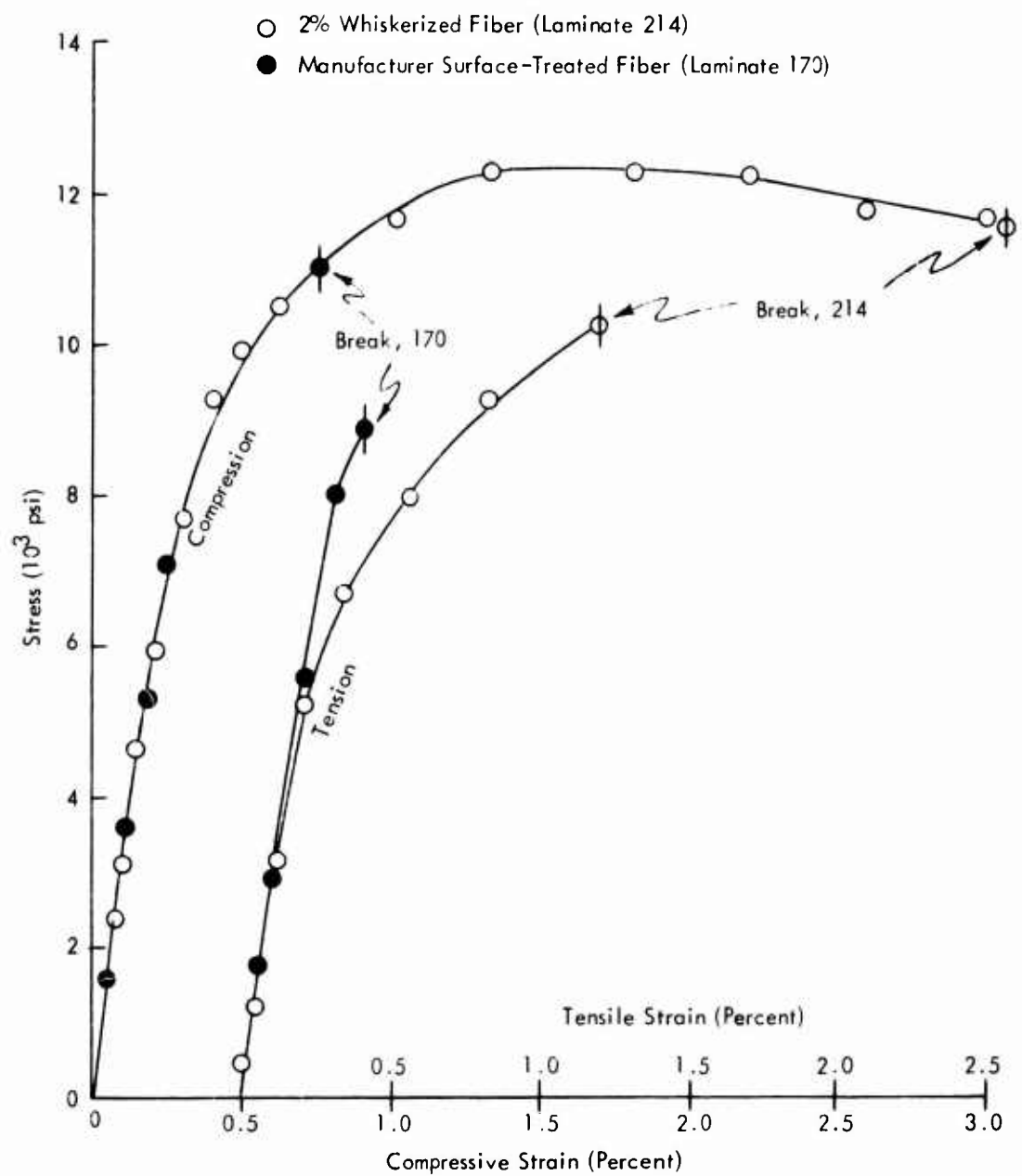


Figure 28. Stress-Strain Curves of  $45^\circ$ - $135^\circ$ / $45^\circ$ - $135^\circ$  Composites.

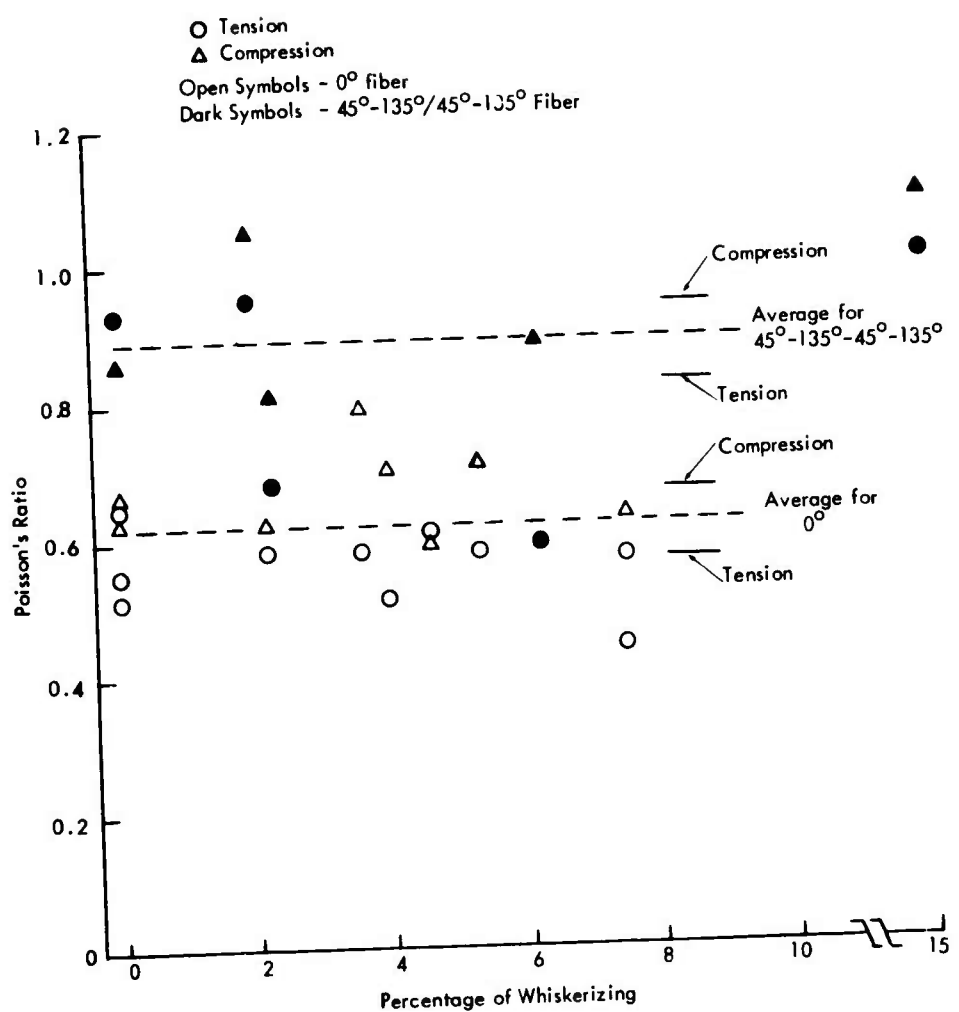


Figure 29. Poisson's Ratio vs. Percentage of Whiskerizing.

level due to tension or compression mode. The  $0^\circ$  configuration differs at the one-sigma (70% confidence) level. These are not high levels statistically. On the other hand, the differences due to layup configuration were highly significant, as would be expected.

### PLATE SHEAR MODULUS

The use of plate twisting to determine laminate shear modulus is justified so long as the laminate is unidirectional or symmetrically bidirectional, as has been discussed in detail by Whitney and coworkers(24,25). In this program, only unidirectional laminates have been tested by the plate twisting method. With this technique the diagonal corners are loaded, and the specimen assumes a "saddle" configuration in which the diagonal sections are parabolas. Another test has been used with the laminates in which the twisting modulus of shear is obtained - the rod torsion test. Similar tests have been used by several workers(25,26).

The laminate shear modulus data presented in this section were obtained not only from the diagonal loading of square plates but also from the twisting of rod specimens. The values from these two types of tests show a general consistency, with greater apparent scatter in the torsion rod data than in the plate data. The results are plotted in Figure 30 as functions of the degree of whiskerizing. In both sets of data, an increase in shear modulus with increase in percentage of whiskerizing was found. Also, the surface-treated fiber yielded composites of higher shear modulus (torsion) than the untreated fiber. The mechanistic explanation for the increase in shear modulus with whiskerizing is relatively straightforward; i.e., the whisker content of the matrix region increases the effective shear modulus of the matrix. It is difficult to rationalize the higher shear modulus due to surface treatment which apparently affects only the strength of the fiber-matrix bond. Because of the small dimensions of the rod torsion specimens and the high power to which diameter is carried in the shear modulus calculation, no conclusive difference can be justified between treated and untreated. However, the differences due to whiskerizing in the plate shear tests are quite significant.

### BEAM AND ROD SHEAR STRENGTH

The shear strength data as obtained from horizontal beam, torsion rod, and I-beam data are plotted in Figure 31 in correlation with percentage of whiskerizing. Several effects are apparent:

- a. Whiskerizing progressively increases shear strength at least in the region of 0-5% whiskerizing.
- b. Void contents of 1% and higher cause significantly lower shear strength than essentially void-free composites.

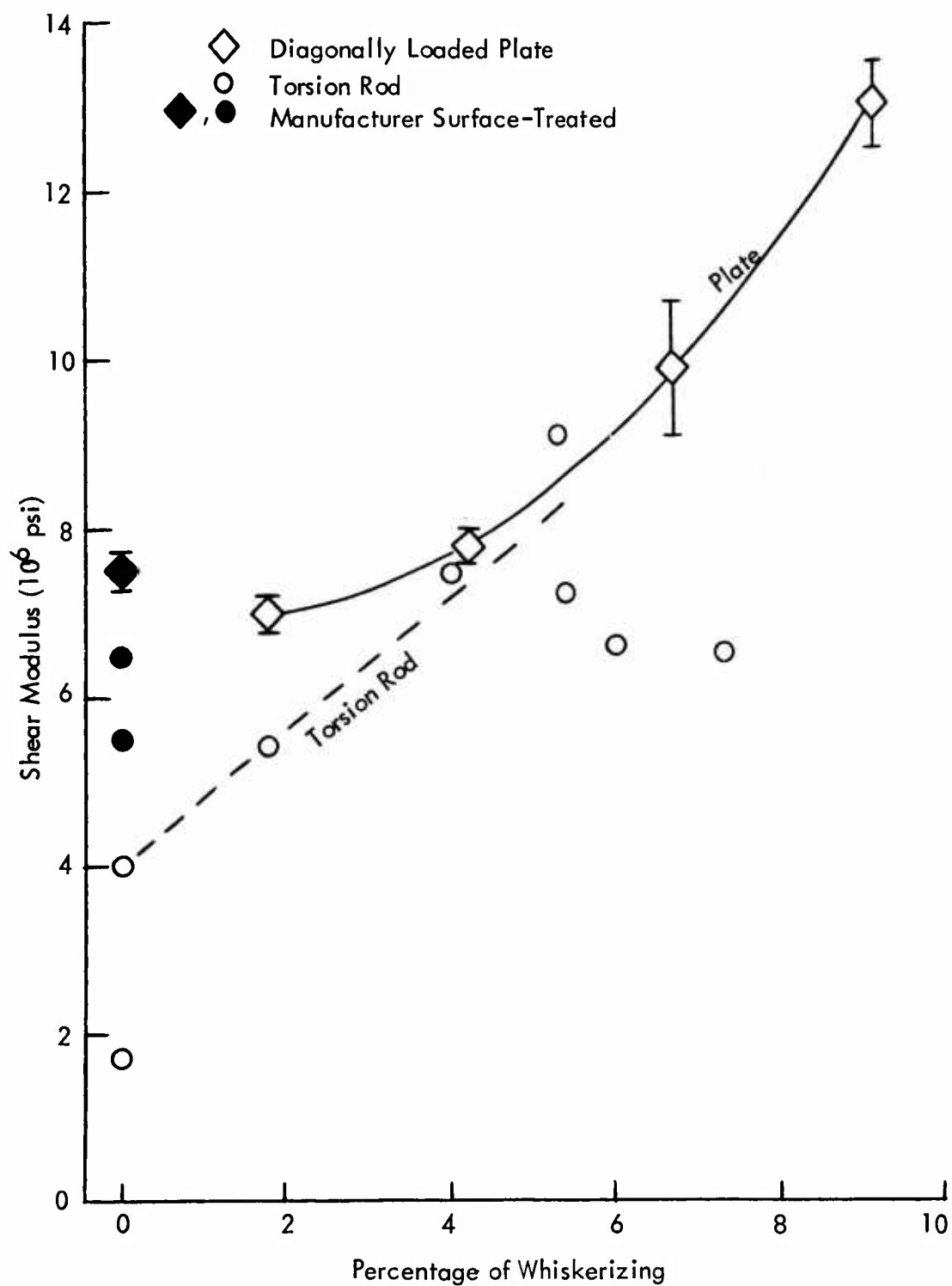


Figure 30. Effect of Whiskerizing on Shear Modulus.

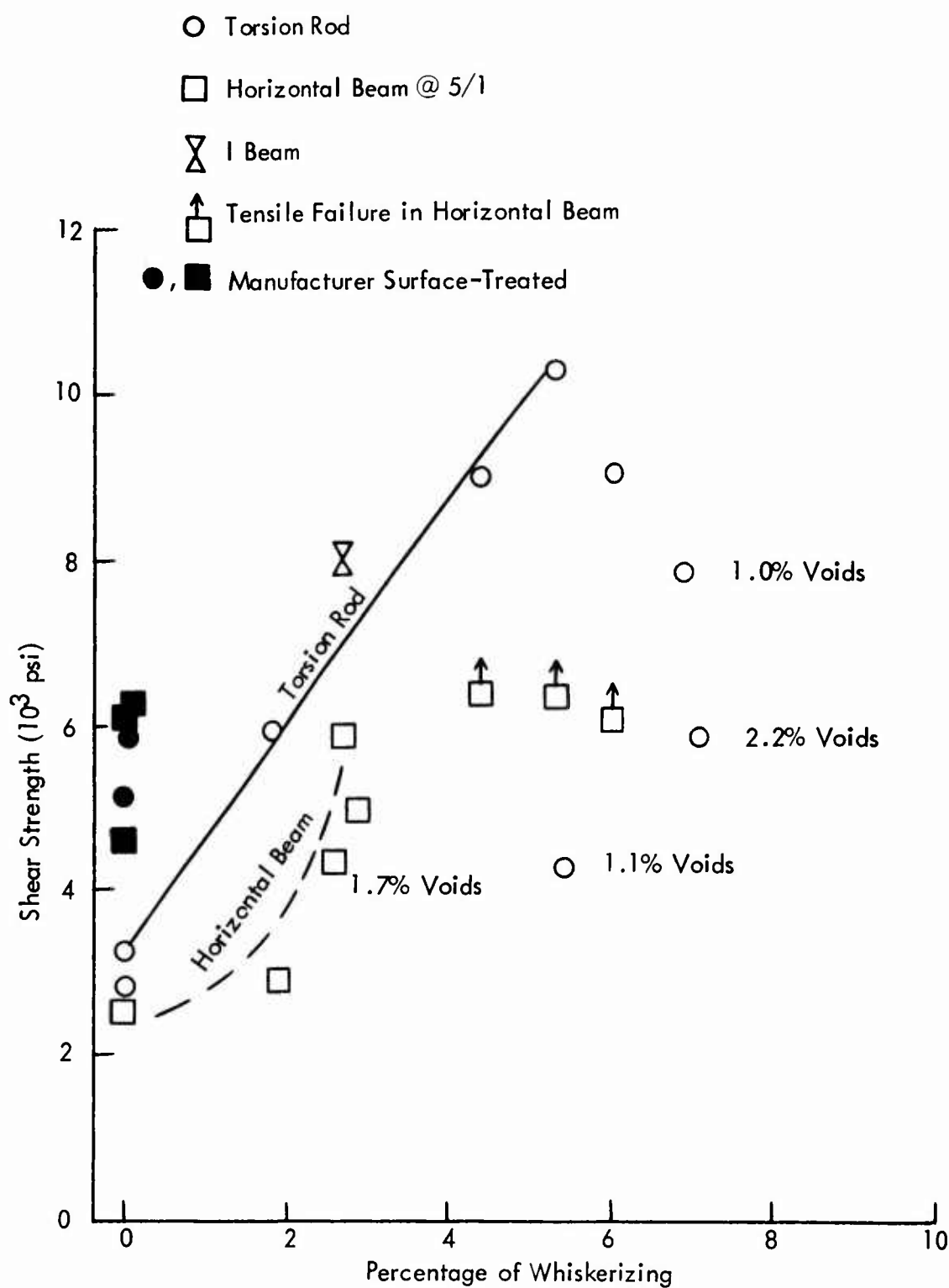


Figure 31. Effect of Whiskerizing on Shear Strength.

- c. Manufacturer surface-treated fiber yields composites of about twice the shear strength of untreated fiber.
- d. A 1.5-3% whiskerizing treatment is required to give shear strength equal to that of the surface-treated fiber, depending on which type of test is used for comparison.

The tests on un-whiskerized fiber composites yielded another pair of interesting correlations, which are shown in Figure 32. The untreated fiber showed decreasing shear strength with high fiber contents, an effect similar to that seen by many observers on other composite systems, such as glass fiber in epoxy. The surface-treated fiber, however, showed a strongly opposite effect, and this was unexpected. The apparent rationalization of these differing effects is that the untreated fiber is sufficiently unbonded to the matrix to act as voids, whereas the treated fiber is well bonded and acts to reinforce the matrix in the shear mode, if only by forcing a progressively more tortuous shear path as fiber content increases. Unfortunately, a completely consistent set of whiskerized shear data for such a correlation cannot be taken from the results for comparison. This would require a constant percentage of whiskerizing, low void content, and significantly varying fiber content. However, the somewhat inconsistent sets of points at 2.6-2.9% whiskerizing (Nos. 152, 162, and 167) have indications of showing increased shear strength with total fiber content. Since it was not an objective of this program to study a wide range of graphite contents, these data were accumulated in a manner that tends to defeat this sort of correlation.

In summation, it was conclusively demonstrated that whiskerizing increases shear strength of the high-modulus PAN-precursor graphite fiber, and treatment at a level of 3% or higher whiskerizing yields results superior to those obtained from a good non-whiskerizing surface treatment. The very significant effect of void content in reducing shear strength is probably due to the concentration of voids in the inter-laminar regions, as was found in the microstructure studies.

It is apparent that the positive correlations found between percentage of whiskerizing and shear strength and modulus are directly related to those found with  $\pm 45^\circ$  strength, modulus, and ultimate elongation. The  $\pm 45^\circ$  composites failed with a shear failure without exception. This was both interlaminar and interfiber, as seen by inspection after testing. It is therefore logical that the whiskerizing effects should be positively correlated in both situations. This points out that the foremost advantage to whiskerizing is reinforcement in the shear mode, and not simply an increase in bonding between the fiber and matrix.

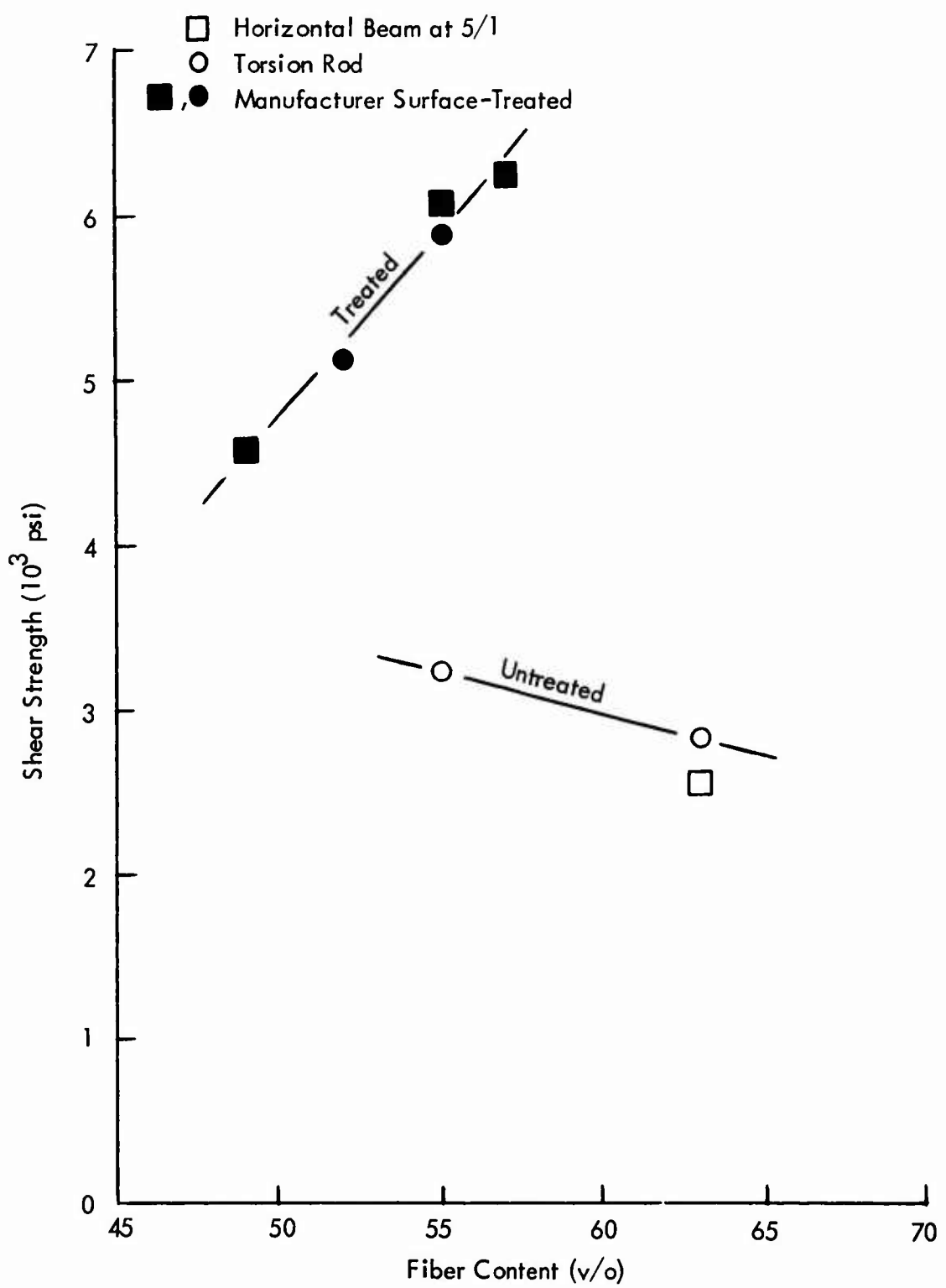


Figure 32. Effect of Fiber Content on Shear Strength.

## TENSILE FATIGUE

The results of the fatigue testing and static tensile testing are summarized in Figures 33, 34, 35, and 36, corresponding to the 5% whiskerized, 3% whiskerized, manufacturer surface-treated and untreated fiber laminates. The effect of the whiskerizing appears to be twofold:

- a. The strength level is reduced with increasing percentage of whiskerizing.
- b. The S-N curves are markedly flatter for the whiskerized than for the un-whiskerized laminates.

In effect, this means that the strength decrease due to whiskerizing is significantly less under cyclic conditions than at static, and at the 3% whiskerizing level the fatigue strength is essentially identical to that of the composites of the virgin fiber from which the whiskerized fiber was produced.

Examination of the static tensile testing data of Table IX in Section IV shows that even the static strength decrease due to whiskerizing may not be as great as is inferred from the sandwich beam tensile data and the treated, un-whiskerized vs whiskerized data of Table IX, because the untreated fiber used in the whiskerizing appears to be considerably lower in as-received strength than that of the treated fiber, although both are of the same type. The difference is 96,500 psi for the untreated vs 121,300 psi for the treated lot in the 52 v/o composite form. Based on 96,500 psi strength, the whiskerizing reduced static strength by 18% and 39% at the 3% and 5% whiskerizing levels, respectively.

The untreated fiber used in the whiskerizing work was obtained from the manufacturer as a several-pound batch before the initiation of this program, whereas the treated fiber consisted of a fractional-pound gratis sample. The difference in strength seen therefore may not be due to the treatment used by the manufacturer, but either to the selectivity exercised in selecting samples, to random chance variation in batch properties, or to process improvement between the times of manufacture of the two batches. In any event, the strength effects seen in this study should probably be interpreted as percentages of virgin strength of the fiber rather than strictly on the basis of absolute numbers.

The apparent fatigue limits found in this program ( $10^7$  cycles runout) are compared in several ways in Table XVI, among themselves and with composite fatigue data found in the literature, and interpreted in a standardized way. The parameters compared are stress at runout as psi, as percentage of static strength, and as strength-to-density ratio. This shows that the whiskerized fiber gives the highest retention of static strength to runout of any of the composites. On this basis, all the graphite

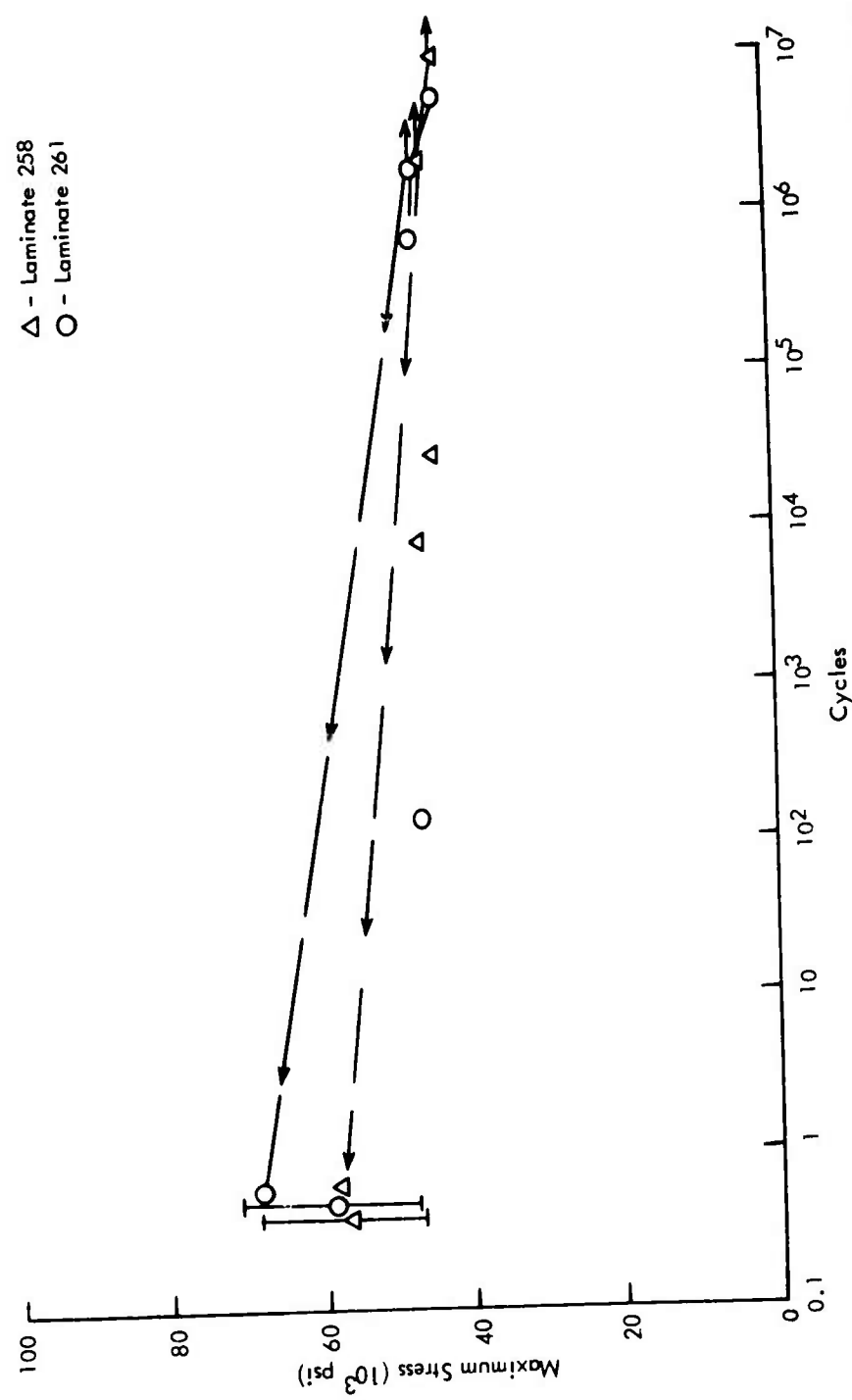


Figure 33. S-N Diagram for 0° Composites of 5% Whiskerized Graphite Fiber (Laminates 258, 261).

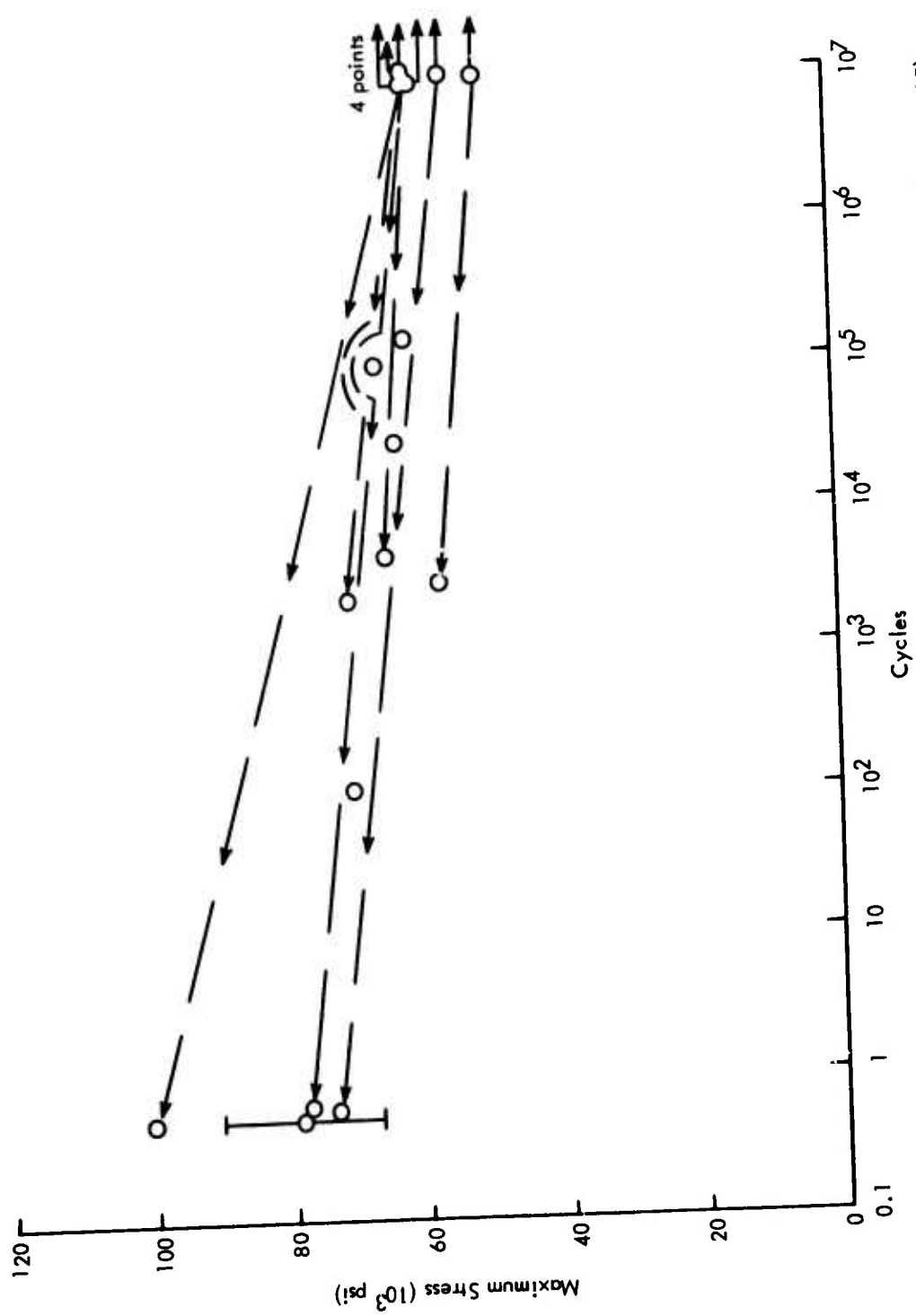


Figure 34. S-N Diagram for 0° Composite of 3% Whiskerized Graphite Fiber (Laminate 265).

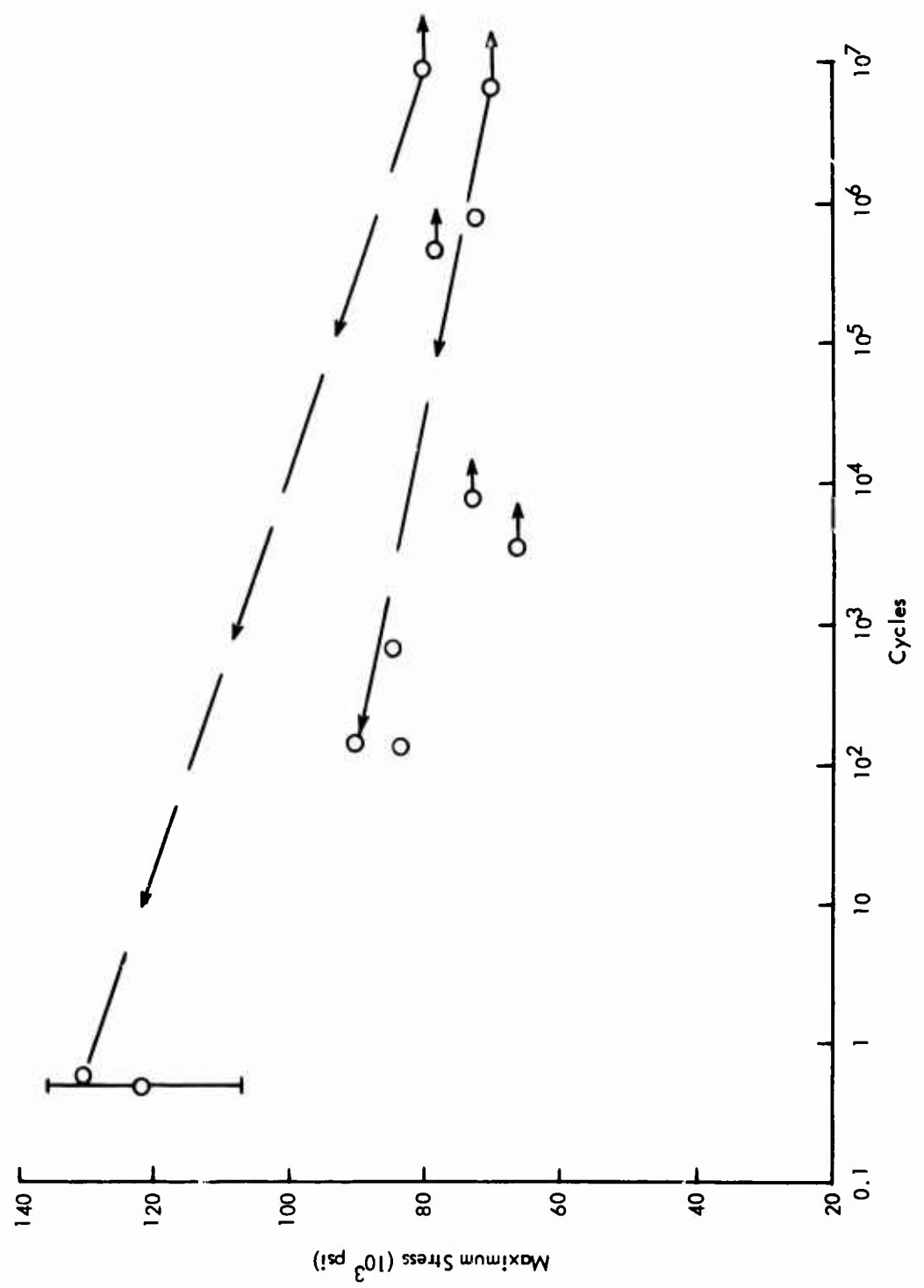


Figure 35. S-N Diagram for 0° Composite of Surface-Treated Graphite Fiber (Laminite 237).

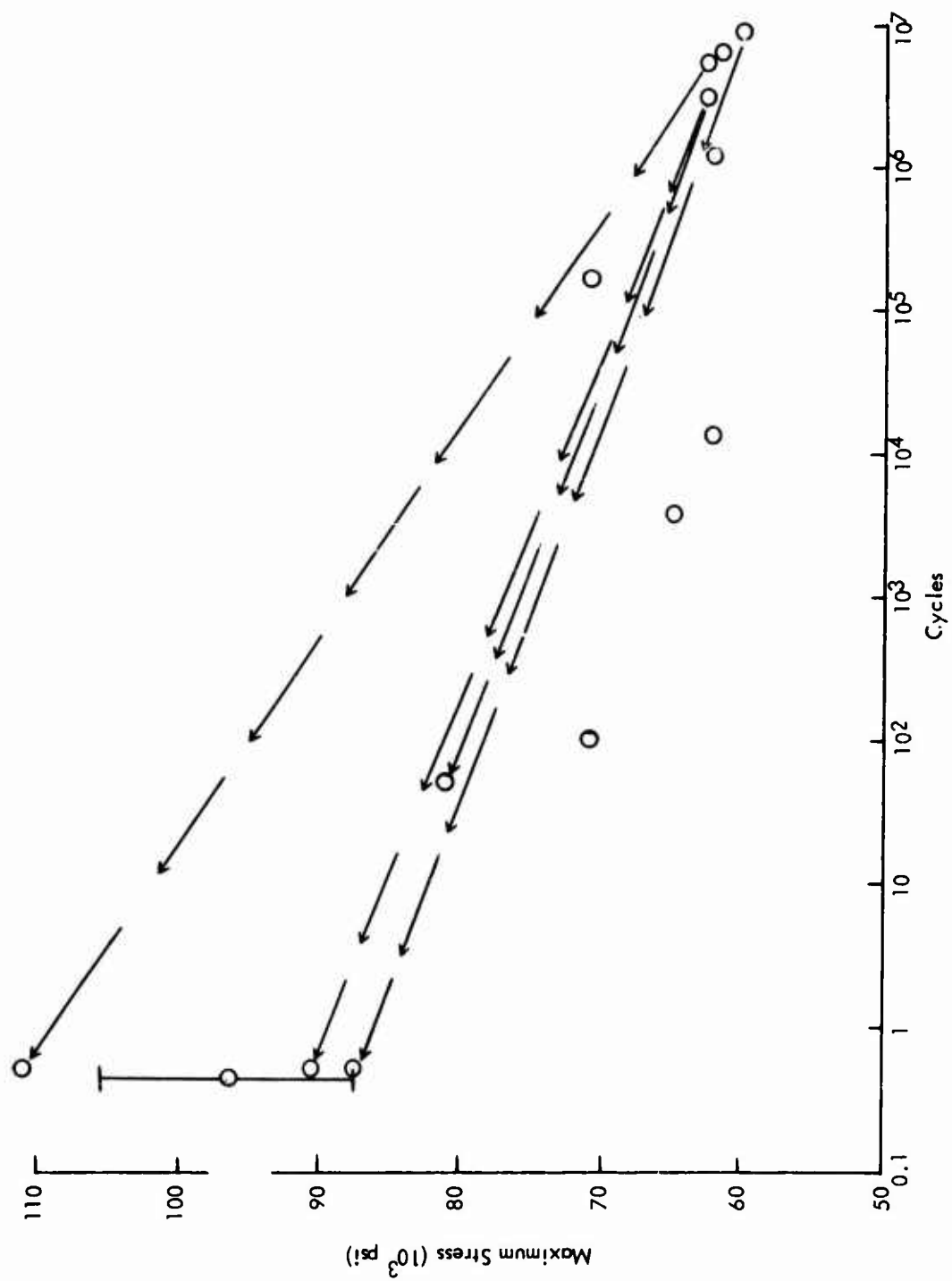


Figure 36. S-N Diagram for 0° Composite of Virgin Graphite Fiber (Laminate 238).

TABLE XVI. COMPARISON OF FATIGUE LIMITS(a) OF COMPOSITES

Material	Reference	Fatigue Limit Properties			Test Conditions
		% of Static Strength	Strength (10 <sup>3</sup> psi)	Strength/Density (10 <sup>6</sup> inches)	
Untreated PAN-precursor, high-modulus graphite	-	65	62.5	1.07	R = 0-0.05
Treated PAN-precursor, high-modulus graphite	-	66	80.0	1.38	R = 0-0.05
3% whiskerized PAN-precursor, high-modulus graphite	-	76	60.0	1.01	R = 0-0.05
5% whiskerized PAN-precursor, high-modulus graphite	-	78	45.0	0.75	R = 0-0.05
Boron - epoxy	(10)	49	67.5	0.91	R = 0-0.05
Glass - epoxy	(10)	?	?	0.63	R = 0.1
Boron - epoxy	(11)	?	?	1.0(b)	R = 0.05
S glass - epoxy	(11)	?	51.0	0.7(b)	R = 0.01-0.05
Biaxial E glass - epoxy	(12)	42	23.0	0.3(b)	R = 0.1
Biaxial Be - epoxy	(12)	45	20.0	0.4(b)	R = 0.1
25 million modulus, rayon-precursor graphite	(13)	67	60.0	1.2(b)	bending (c)
40 v/o PAN-precursor, high-modulus graphite in polyester	(14)	48	50	0.90	R = 0.2(d)

(a) 10<sup>7</sup> cycles.  
 (b) Assumed specimen density.  
 (c) 10<sup>6</sup> cycles only reported.  
 (d) 2 x 10<sup>7</sup> cycles reported.

composites are superior to the boron, glass, or beryllium composites. The only parameter in which boron composite is superior to the 3% whiskerized high modulus graphite composite is in absolute strength.

The retesting of the runout specimens in fatigue at higher stress levels generally yielded failure points that were indistinguishable from those brought directly to failure at that stress level without runout at a lower stress. The static testing of runouts for residual strength yielded values that were for the most part slightly higher than the average of the static strengths of random, uncycled specimens. It is believed that this is due to the combined effect of selectivity of the fatigue testing in eliminating those lower than average in strength before runout together with very little accumulated damage to specimens during cycling.

#### FILAMENT WINDING OF NOL RINGS

The filament-winding characteristics of the treated, un-whiskerized fiber and the 3% whiskerized fiber were found to be quite similar, and the filament-winding process was dominated by the very large tow bundle and its peculiar packing difficulties. Slightly higher winding tension was required with the 3% whiskerized fiber (3000 grams versus 2500), presumably due to the resistance to compaction provided by the interstitial whisker growths. The difference, however, was much less than expected. The maximum tension that could be applied without fiber tow failure was less with the whiskerized fiber. Tensions up to 6600 grams could be used on the un-whiskerized fiber, whereas substantial fraying would take place beyond about 3500 grams with the whiskerized. The higher possible tensions did not result in higher fiber contents in the composite. The only pertinent literature that could be found on this point was a paper by Desai and Kalnin(9), in which a maximum fiber content of 42 v/o was obtained with treated high-modulus fiber at a tension that was not specifically stated but was in the range of 3-10 pounds. It was stated that the winding tension was as close as practicable to the breaking strength of the yarn. At 5-1/2 to 7 pounds tension, we achieved 50 v/o composites, presumably because we formed 1-inch-wide rings rather than winding into a 1/4-inch mandrel slot.

#### NOL RING PROPERTIES

##### a. Shear Strength

Average shear strengths up to 7,750 psi were obtained with treated, un-whiskerized fiber and up to 8,900 psi with 3% whiskerized fiber. The average of windings 160716-160718 was 7,200 psi and of windings 160724-160728 was 8,300 psi. This compares to about 6,000 psi for the treated, un-whiskerized laminates and an estimated 7,800 psi for 3.3% whiskerized laminates. These results in filament winding are therefore at least as good as those obtained by laminating. The shear strength of treated high-modulus fiber NOL rings found in the work of Desai and

Kalnin<sup>(9)</sup> was 8,100 psi in ERLA 2256 - ZZL 082C resin, which checks reasonably well with the results in this program, considering the difference in resin.

The only major trend in shear strengths that could be found in the data was the adverse effect of void content. This is shown in Figure 37. The trend for the treated, un-whiskerized fiber is quite pronounced, but the whiskerized data cover too small a range of void contents to draw a significant correlation.

#### b. Modulus

The modulus of the NOL rings was taken in two ways: (1) by split-disc tensile testing\* and by ring flexure using load and crosshead travel. The results by these two methods were strikingly different. The ring flexure moduli were about 70% of the split-disc moduli. These latter values were 90 - 100% of rule-of-mixtures using 60 million psi as the fiber modulus. The reason for the difference is not known, but the ring flexure test is believed to be a very poor one because of the marked nonlinearity of the load-deflection curves and the "hysteresis" looping of these curves upon cycling. The modulus results using strain-gage-equipped rings on split disc fixture check well with the laminate moduli measured on tensile and compressive unidirectional sandwich beam plates and in static tensile testing during the fatigue testing phase.

#### c. Strength

Composite strength was measured two ways in this effort: split-disc tensile and segment flexure. The flexure strengths were consistently higher than the split-disc tensile. The treated, un-whiskerized rings averaged 27% higher by flexure, and the whiskerized averaged 40% higher by flexure. This is believed to be due to the very pronounced bending stresses superimposed on the tensile stress in the split-disc test. The peculiar fracture often found at two locations about 11° away from the split-disc separation (see Figure 18) is evidence of this. The strain gage mounting on NOL rings was used to study this effect. It was found that the maximum strain on the inner ring surface was at the disc split, whereas this was the location of the minimum outer surface strain. Moving away from the split, the inner surface strain rapidly decreased and the outer surface strain rapidly increased to relatively constant values in the range from 22° to 90° (158° to 90°). In this region of rapidly changing local strains, the averaged local strain peaked at about 11° from the split. This infers an inconstant average section stress in the ring which depends on distance from the split. Such a condition cannot be supported in static equilibrium unless friction effects are also operating. Since the rings were lubricated, it is

---

\*Using strain gages, detailed in Section VIII.

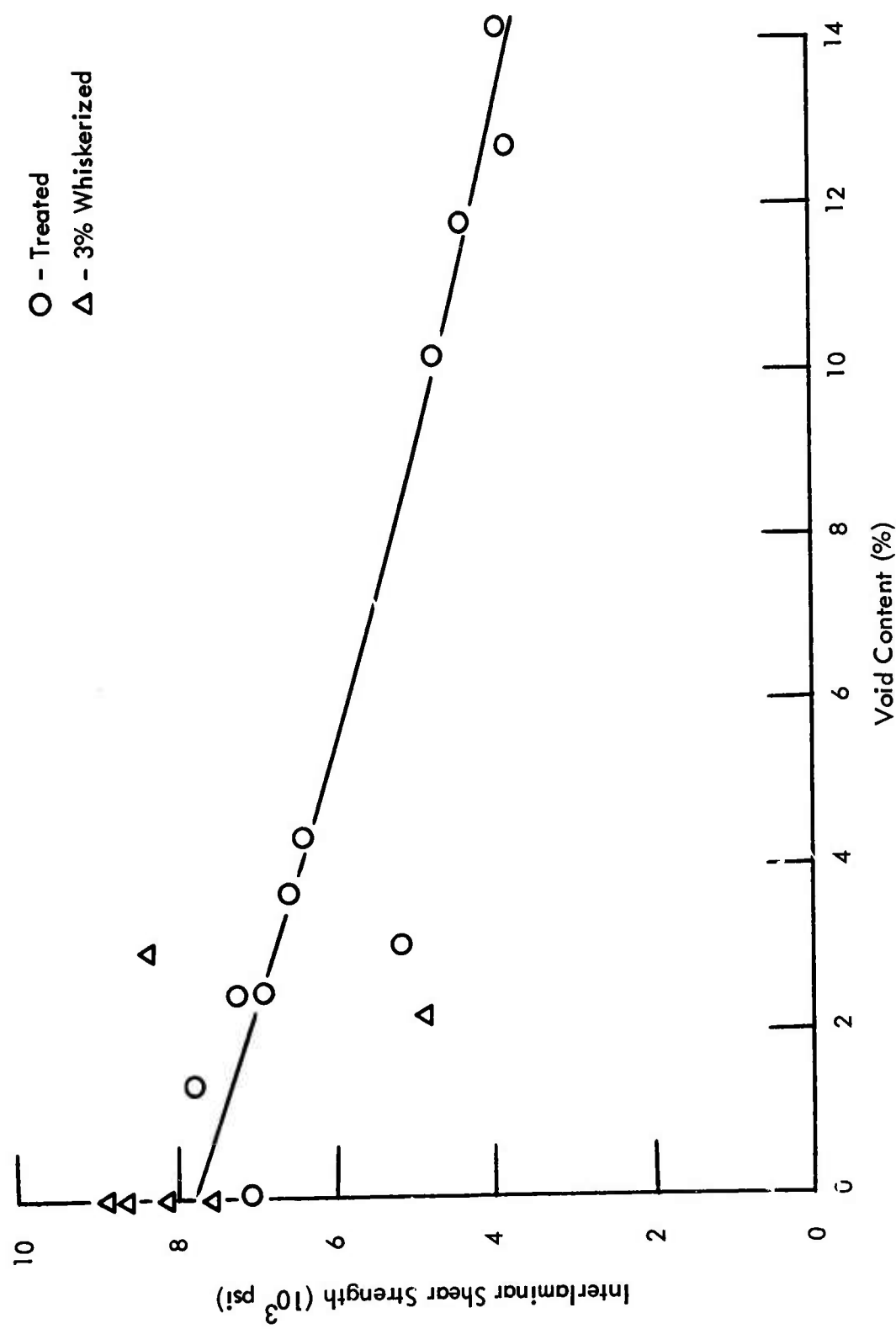


Figure 27. Effect of Void Content on Shear Strength of NOL Rings.

hard to believe that this can be so.

The rings in split-disc testing therefore failed in one or the other of two configurations: directly at the split ( $0^\circ$ ) or at  $11^\circ$  on either side of the split. Both types of failure can be attributed directly to the bending stresses superimposed on the tensile stress due to the peculiarity of the split-disc separation.

The comparison of strengths measured in this NOL ring phase and in the earlier laminate phases is shown in Table XVII.

TABLE XVII. COMPARISON OF STRENGTHS OF COMPOSITES BY SEVERAL TESTS			
Specimen Construction	Treatment	Test	Strength ( $10^3$ psi)
laminates	treated	sandwich beam	107.4
	3% whiskerized*	" "	75.0*
	treated	static tensile, tab end	121.3
	3% whiskerized	as above	79.2
	treated**	split disc	106.4
	3% whiskerized***	" "	77.1
	treated**	flexure	113.7
	3% whiskerized***	"	96.4
* Interpolated			
** Average of 160717 and 160718			
*** Average of 160727 and 160728			

In this regard, a strength reduction due to whiskerizing can be found, and the results in filament winding appear to be at least as high as those found in laminates.

### TORSION TUBES

The winding tensions and in-line, hot-resin impregnation technique developed in NOL ring winding were found to be suitable for forming tubes for torsion testing when the outer layer, at least, was hoop-wound ( $90^\circ$ ), as in the  $90^\circ$  unidirectional,  $90^\circ-0^\circ/0^\circ-90^\circ$  orthotropic, and  $\pm 30^\circ-90^\circ$  isotropic configurations. The degrees of compaction, fiber contents, and void contents were all similar to those obtained in NOL rings. On the other hand, the completely laid up orthotropic tubes ( $45^\circ-135^\circ/45^\circ-135^\circ$ ) compacted solely by polyethylene shrink tubing were of lower

degrees of compaction, as shown by lower densities and fiber contents; the best such tubes were above 38 v/o fiber as compared to 45-54 v/o for the tubes with hoop-wound compaction.

The use of thin-walled hollow cylinders in torsion to measure in-plane shear modulus requires that the composite be either unidirectional or symmetrically bidirectional(25). This requirement is satisfied in the composite tubes used in this program. In the testing of these tubes in torsion, it is important that they be unrestrained axially, since the coupling effects do cause varying degrees of axial strain during torsion(27). The testing fixture loading clamp was designed to be free to displace axially in response to the induced axial strain in the tubes.

The shear strengths and moduli measured on the tubes vary markedly from configuration to configuration. The test measures the in-plane (xy) shear properties as opposed to interlaminar shear, as measured by short beams. In a fully uniform, unidirectional composite the difference is trivial; but in complex laminar configurations, the difference is profound. The highest shear strengths and moduli by far were found in the  $\pm 45^\circ$  orthotropic tubes, with the isotropic tubes being somewhat less, but greater in both regards than the unidirectional or  $0^\circ-90^\circ$  orthotropic tubes. The comparison of the values measured on this program with some found with other fibers as reported in the literature is given in Table XVIII.

The comparison shows that the unidirectional ( $90^\circ$  or  $0^\circ$ ) tubes give torsional shear strengths that are generally consistent with interlaminar shear strengths for laminates of the same fibers. Thus the treated intermediate-modulus PAN-precursor graphite fiber and whiskerized high-modulus PAN-precursor graphite fiber gave higher shear strengths than the treated high-modulus PAN-precursor graphite fiber, which in turn were higher by significant amounts than those of the rayon-precursor graphite fiber composites and somewhat lower than the best glass fiber composites. The shear modulus of  $0.68 \times 10^6$  psi measured for both the treated and the whiskerized  $90^\circ$  high-modulus PAN-precursor graphite fiber tubes is similar to the values measured on the plate shear tests earlier in this program, giving allowance for the fact that the plates were slightly higher in fiber content:

Fiber Treatment	Fiber Content (v/o)	Test	G ( $10^6$ psi)
Manufacturer treated	57	Plate	0.75
" "	54	$90^\circ$ tube	0.68
4% Whiskerized	52	Plate	0.78
3% Whiskerized	45	$90^\circ$ tube	0.68

The effect of increased fiber content increasing the shear modulus has been demonstrated, as for example in work by Noyes and Jones(18) and Adams et al(26) with glass fiber. If the fiber content effect is normalized in these results, the presence

TABLE XVII. COMPARISON OF COMPOSITE TORSION TUBE DATA

Tube Configuration	Literature Citation	Fiber	Fiber Content (v/o)	Strength (10 <sup>3</sup> psi)	Modulus (10 <sup>6</sup> psi)
Unidirectional (90°)	-	high-modulus PAN-precursor graphite	51	6.3	0.68
"	"	intermediate-modulus PAN-precursor graphite	56	10.4	0.92
"	"	whiskerized high-modulus PAN-precursor graphite	44	8.1	0.68
"	"	40 million modulus, rayon-precursor graphite	57	3.2	0.65
"	"	25 " " "	53	2.9	0.57
"	"	50 " " "	50	2.7	0.63
"	(16)	glass	72	12.7	1.09
"	(17)	"	67	11.0	0.74
"	"	"	50	9.0	0.6
"	(17)	"	52	3.5	0.55
"	"	"			
"	(18)	"			
"	"	"			
Orthotropic (0°-90°)	-	high-modulus PAN-precursor graphite	43	7.1	0.87
"	"	whiskerized high-modulus PAN-precursor graphite	40	8.8	0.80
"	"	boron and glass	48	-	0.90
"	"	glass	41	-	0.56
Orthotropic (±45°)	-	high-modulus PAN-precursor graphite	38	27.3	4.0
"	"	" " "	28	16.2	2.9
"	"	whiskerized high-modulus PAN-precursor graphite	36	25.1	4.1
"	"	whiskerized high-modulus PAN-precursor graphite	29	15.2	2.4
"	"	50 million modulus, rayon-precursor graphite	50	27.1	5.3
"	"	glass	70	23.5	1.6

TABLE XVIII - Continued

Tube Configuration	Literature Citation	Fiber	Fiber Content (v/o)	Strength ( $10^3$ psi)	Modulus ( $10^6$ psi)
Isotropic ( $\pm 30^\circ$ , 90°)	-	high-modulus PAN-precursor graphite	44	12.6	2.6
"	-	whiskerized high-modulus PAN-precursor	43	11.8	2.6
"	"	graphite	47	-	4.4
"	"	boron and glass	40	-	1.1
		glass			

of whiskerizing appears to increase tube shear modulus, as was found earlier with plates.

The  $0^\circ$ - $90^\circ$  orthotropic tubes give slightly higher shear moduli and shear strengths than the  $90^\circ$  unidirectional. These may not be significant differences. If the torsion is dominated by an interlaminar shear mechanism in this configuration, this could explain the apparent similarity. Since the principal tensile and compressive stresses in torsion act at  $45^\circ$  and  $135^\circ$  to the longitudinal fibers, the composite tube may in fact be stressed in a manner similar to tensile stress of a  $\pm 45^\circ$  laminate in the  $0^\circ$  direction, which appeared to be shear dominated in the failure mechanism.

The  $\pm 45^\circ$  orthotropic tubes, on the other hand, show the highest strengths and moduli. This no doubt reflects the fact that the fibers are placed directly in line with the principal tensile and compressive stresses in torsion. Therefore, the torsion strengths and moduli should be strong functions of fiber content and fiber strength and modulus, which is apparent from Table XVIII.

The  $\pm 30^\circ$ ,  $90^\circ$  isotropic composites act intermediate in effect to the  $\pm 45^\circ$  and  $0^\circ$ - $90^\circ$  orthotropic tubes in the sense of magnitude of strength and modulus values. This probably reflects the fact that the  $\pm 30^\circ$  fibers are only  $15^\circ$  off the axes of the principal tensile and compressive stresses and therefore resolve significant portions of their properties in these axes. The isotropic tube properties are therefore complexly dominated, and the configuration is more naturally suited for a combination of stress states than it is for pure torsion.

It is interesting to note that the configurations having fibers in the  $\pm 30^\circ$  or  $\pm 45^\circ$  directions are not prone to failure by interlaminar shear mechanisms, as seen in the high torsion strength of the 50 million psi modulus rayon-precursor graphite fiber orthotropic shown in Table XVIII despite the very poor shear strength of 2700 psi in the  $0^\circ$  unidirectional configuration for this fiber. This illustrates the importance of proper design of the composite configuration for the intended application.

## CONCLUSIONS AND RECOMMENDATIONS

### LAMINATES

The application of the whiskerizing treatment to high-modulus PAN-precursor graphite fiber was demonstrated to cause a progressive increase in composite inter-laminar shear resistance, as determined by short-beam shear and torsion-rod testing, and in shear modulus, as determined by diagonal-loaded plates. These positive effects on shear properties are believed to be directly responsible for the increases in tensile and compressive strength, modulus, and ultimate elongation of the  $\pm 45^\circ$  composites that accompanied increases in whiskerizing degree. The strengths and elongations were exceptional in that they significantly exceeded the properties of the un-whiskerized but surface-treated composites. This was especially true of ultimate elongation. Elongations in excess of 1% in tension and in excess of 3% in compression were found in the optimal  $\pm 45^\circ$  composites. The un-whiskerized, surface-treated control composite yielded good strength but only about one-third the ultimate elongation in this configuration. This is indicative of reinforcement in the shear mode due to whiskers, and not merely an increase in bond strength as was obtained by the simple surface treatment.

The effect of whiskerizing on the intrinsic graphite fiber tensile strength is one of progressive degradation. This was demonstrated in the tensile testing of the  $0^\circ$  and  $0^\circ-90^\circ/90^\circ-0^\circ$  composites. A  $0^\circ$  composite strength of 75,000 psi at 3% whiskerizing was found, which corresponds to a fiber stress of 136,000 psi. The modulus of these  $0^\circ$  composites was found to be independent of the degree of whiskerizing, within the range studied, and averaged  $33.7 \times 10^6$  psi in tension and compression. This corresponds to a fiber modulus of  $62 \times 10^6$  psi.

The shear strength of the composites of manufacturer surface-treated fiber was about 6,000 psi at 55 v/o fiber by both the short-beam and the torsion-rod tests. Two percent whiskerizing yielded this amount of shear strength in the torsion-rods, whereas by the short-beam tests 3% whiskerizing was the equivalent of the surface treatment.

In fatigue testing whiskerizing was found to increase the percentage of static strength of uniaxial laminates retained at runout. This resulted in the highest such values of any composite system found in the literature for this type of fatigue test. The strength degradation due to whiskerizing the fiber was therefore less under the cyclic loading than at static conditions. The strength and strength-to-density ratio at runout for the surface-treated fiber were highest of all. The 3% whiskerized fiber composite exceeded the comparison boron composite at runout on a strength-to-density basis.

Residual strength of cycled specimens was indistinguishable from the undamaged composite static strength for all the graphite fiber composites tested.

#### FILAMENT-WOUND NOL RINGS AND TUBES

Fiber contents up to 50 v/o can be obtained with either surfaced-treated fiber or 3% whiskerized high-modulus PAN-precursor graphite fiber. Higher fiber contents do not result from increased tension. The optimum winding tension is about 2500 grams per tow for treated fiber and 3000 grams for 3% whiskerized fiber.

The interlaminar shear strengths from NOL ring segments are at least as good as from molded laminates, and 3% whiskerized fiber gives slightly higher shear strengths than surface-treated fiber. The use of split-disc tensile testing on NOL rings was found to be a poor method for deriving fundamental properties because of the complex stress state. Whole ring flexure did not yield modulus values consistent with other methods. The NOL ring segment flexure strengths were consistently higher than split-disc tensile strengths.

The hoop-wound (90°) torsion tubes reflected the interlaminar shear strengths found in laminates and NOL ring sections, despite the fact that the tube torsion is in-plane shear rather than interlaminar. This is probably due to the unidirectional symmetry. The two types of orthotropic cross-ply tubes, 90°-0°/0°-90° and 45°-135°/45°-135°, differed markedly in shear properties. The latter were much stronger and of higher modulus in torsion. This is a reflection of the fact that the principal tensile and compressive forces lie on the 45° and 135° helices in pure torsion. No significant difference in properties due to whiskerizing versus treated fiber in these latter orthotropic tubes was found. This same conclusion can be made about the isotropic tubes ( $\pm 30^\circ$ , 90°). Thus the principal shear advantage to whiskerizing appears when the failure mechanism is highly dependent on the matrix-fiber bond rather than on the properties of the fiber itself, as in interlaminar shear testing and unidirectional tubes in torsion.

It is recommended that a pre-reg system involving a thinning and flattening of the large tow bundle into a tape be evolved to overcome the unfavorable filament winding characteristics of the 10,000-fiber tow bundle. Tow bundles of smaller fiber quantity (e.g., 5000 fibers) would probably be more suitable for direct filament winding than the current material.

### LITERATURE CITED

1. Nabarro, F.R.N., and Jackson, P.J., "Growth of Crystal Whiskers", Growth and Perfection of Crystals, Proceedings of the International Conference on Crystal Growth, Cooperstown, N. Y., John Wiley and Sons, Inc., August 27-29, 1958.
2. Ellis, W.C., Gibbons, D.F., and Treuting, R.G., "Growth of Metal Whiskers from the Solid", ibid.
3. Shyne, J.J., et al., "Development of Processes for the Production of High-Quality, Long-Length SiC Whiskers", AFML-TR-67-402, Jan. 1968.
4. Prosen, S.P., and Simon, R.A., "Carbon Fibre Composites for Hydro and Aerospace", The Plastics Institute, London, Filament Winding Conference, Oct. 17-18, 1967, paper 18.
5. Prosen, S.P., and Simon, R.A., "Shear Strength Improved 300 Percent in Graphite-fiber Composites", Reinforced Plastics and Composites World, Sept. - Oct. 1967, p. 20.
6. Simon, R.A., and Prosen, S.P., "Graphite Fiber Composites; Shear Strength and Other Properties", Proceedings of the 23rd Annual Conf. of the SPI Reinforced Plastics/Composites Div., Feb. 6-9, 1968, Washington, D. C., Section 16-B.
7. Shaver, R.G., "Silicon Carbide - Whiskerized Carbon Fiber", AIChE Materials Conference, Mar. 31 - Apr. 4, 1968, Philadelphia, paper 24e.
8. Shaver, R.G., "Laminates and Filament-Wound Structures of Whiskerized High-Modulus Carbon Fiber", Proceedings of the 24th Annual Conf. of the SPI Reinforced Plastics/Composites Div., Feb. 4-7, 1969, Washington, D. C., Section 15-B.
9. Desai, R.R., and Kalnin, I.L., "The Effect of Process Variables on the Performance of Carbon or Fiberglass Reinforced NOL Rings", 24th Annual Conf., SPI Reinforced Plastics/Composites Division.
10. Rogers, C. W., et al., "Application of Advanced Fibrous-Reinforced Composite Materials to Airframe Structures", AFML-TR-66-313, Vol. II.

11. Pinckey, R.L., and Hoffstedt, D.J., "The Design and Construction of Filament-Reinforced Composite Rotor Blades", The Boeing Co., Vertol Div. 10th National SAMPE Symposium, San Diego, Nov. 1966.
12. Mahieu, W., and Schwartz, H.S., "Time Dependent Mechanical Behavior of Beryllium Wire Reinforced Plastic Composites", 12th National SAMPE Symposium, Anaheim, Nov. 1967.
13. Hanley, H.B., and Cross, S.L., "Studies Related to the Acoustic Fatigue Resistance of Advanced Composites", 12th National SAMPE Symposium, Anaheim, Nov. 1967.
14. New Products Data Sheet, Morganite Research and Development Limited.
15. "Integrated Research on Carbon Composite Materials", AFML-TR-66-310, Part II, Dec. 1967.
16. Bell, J.E., "Graphite-Epoxy Composite Material Properties", 15th National SAMPE Symposium, Los Angeles, April 1969.
17. Card, M.F., "Experiments to Determine Elastic Moduli for Filament-Wound Cylinders", NASA-TN D-3110, Nov. 1965.
18. Noyes, J.V., and Jones, B.H., "Crazing and Yielding of Reinforced Composites", AFML-TR-68-51, March 1968.
19. Herring, H.W., et al., "Mechanical Behavior of Boron-Epoxy and Glass-Epoxy Filament-Wound Cylinders Under Various Loads", NASA TN D-5050, March 1969.
20. Kuhbander, Ronald J., "Determining Fiber Content of Graphite Yarn-Plastic Composites", AFML-TR-67-243, August 1967.
21. "High-Modulus, High-Strength Reinforcement for Structural Composites", ML-TBR-64-88, Part II, Texaco Experiment Inc., Dec. 1964, p. 139.
22. Fried, N., "Survey of Methods of Test for Parallel Filament Reinforced Plastics", ASTM Special Technical Publication No. 327, 1962, p. 24.
23. McGowan, H.C., and Milewski, J.V., "Single Filament-vs-Impregnated Yarn Tensile Testing of Graphite Fibers", 24th Annual Conf. of the SPI Reinforced Plastics/Composites Div., paper 2A, Feb. 1969.

24. Hennessey, J.M., and Whitney, J.M., "Experimental Methods for Determining Shear Modulus of Fiber Reinforced Composite Materials", AFML-TR-65-42, Sept. 1965.
25. Whitney, J.M., "Shear Modulus Determination in Laminated Composite Materials", AFML-TR-67-22, March 1967.
26. Adams, D.F., et al., "Mechanical Behavior of Fiber-Reinforced Composite Materials", AFML-TR-67-96, May 1967.
27. Whitney, M.M., and Halpin, J.C., "Use of Laminated Anisotropic Tubes for Determining the Mechanical Properties of Fiber Reinforced Composite Materials", AFML-TR-68-48, Oct. 1968.
28. Hoggatt, J.T., et al., "Development of Processing Techniques for Carbon Composites in Missile Interstage Application", AFML-TR-68-155, June 1968.
29. Dickerson, E.O., and DiMartino, B., "Off-Axis Strength and Testing of Filamentary Materials for Aircraft Application", 10th National SAMPE Symp., Advanced Fibrous Reinforced Composites, Nov. 9-11, 1966, pp. H-23 to H-50.
30. Lenoe, E.M., "Evaluation of Test Techniques for Advanced Composite Materials", AFML-TR-68-166, Part I, June 1968.

## APPENDIX EXPERIMENTAL TECHNIQUES

### LAMINATE FABRICATION

#### a. Sandwich Beam Face Plates, Shear Modulus Plates, and Tensile Fatigue Laminates

The layup technique for composite fabrication was the lamination of batch-whiskerized layers of single-tow thickness. Because the graphite fiber tows are 10,000 fibril bundles of 6-micron-diameter fibrils, the amount of material in a single-tow thickness is considerable. For example, if the material in a single tow were composited into a square cross-sectional bar of 60 v/o fiber content, the composite thickness would be 35 mils. Because the tows have no twist, they slump somewhat during layup for the whiskerizing process, and it was found that a uniformly coherent and naturally spaced layup contained approximately 14 grams of fiber per 3-inch by 13-inch lamina. This made a composite lamina 20 mils thick at 55 v/o. It was found that laminas containing less than 14 grams of fiber could not be handled as a coherent whole after whiskerizing; they had large gaps between tows that were difficult to control and tended to come apart into several small tapes.

To accomplish composite fabrication, laminas close to each other in percentage of whiskerizing were selected to be laminated into individual specimens at various levels of whiskerizing. The laminas were individually impregnated, processed through B-staging, and thereafter laid up. The beam-face plate panels were of two- or four-layer thickness. The 0° orientation plates were two-layered. The 0°-90°, ±45°, and 90° plates, as well as the shear modulus plates, were four-layered. The process used in this compositing was:

- (1) Strip from carbon cloth interleaves.
- (2) Remove two centerline tows for sample and trim to 13 inches, if necessary.
- (3) Weigh and calculate necessary resin.
- (4) Impregnate at a ratio of fiber/resin of 60/40 by weight using 0.2 gram of resin per milliliter of solution in acetone.
- (5) Evaporate at ambient conditions in a hood for 2 hours.
- (6) Vacuum-treat for 1-1/2 hours.
- (7) Retreat in vacuum until constant weight is obtained.

- (8) B-stage at 90°C for 3/4 hour.
- (9) Cut into appropriately shaped pieces for layup configuration.
- (10) Lay up in mold.
- (11) Press to precalculated panel thickness at mold temperature of 100°C.
- (12) Cure in mold at 125°C for 1 hour.
- (13) Postcure in mold at 177°C for 2 hours.

Commercial mold release agent for epoxy resin was used throughout this program, and no problem with adherence to mold parts was encountered. The appearance of some of these laminates before and after processing into honeycomb beams is shown in Figure 38.

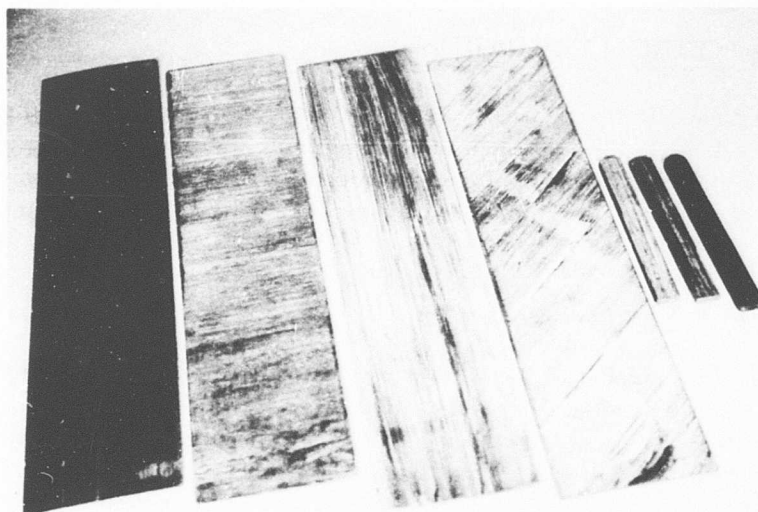
b. Shear Beam Preparation

Sections of B-staged laminas were cut 4.5 inches by 0.5 inch in order to lay up in matched metal dies for shear beams. Stops on the dies permitted a thickness of 0.25 inch. The weight of B-staged laminas necessary to yield the desired volume % of fiber was calculated, and the appropriate weight was placed into the mold. A typical shear beam consisted of 8 to 11 laminas 4.5 inches by 0.5 inch.

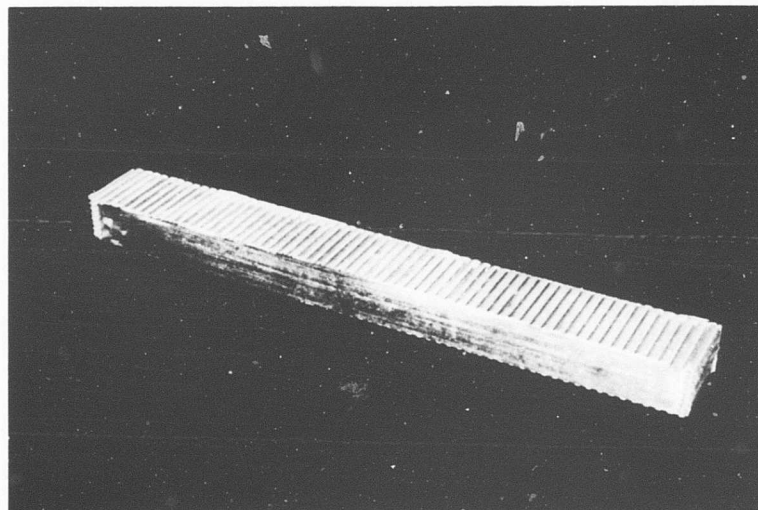
After the cure cycle, the flash was removed, the sample was weighed, and the fiber weight % was determined by material balance procedures. Density was determined by weight in air and in water. The known fiber weight and composite density permitted calculation of fiber volume and void volume by the method cited in a subsequent section.

c. Torsion Sample Preparation

The weight of B-staged lamina necessary to yield a desired volume % of fiber in torsion samples was calculated prior to cutting and weighing samples 4 inches long. Two mold diameters were used: 0.109 inch and 0.171 inch. Because of the relatively small diameters, the samples consisted of only a few tows of impregnated, B-staged fiber. When they were placed into the mold, the piston was introduced and pressed to stops in order to yield a cylinder 4 inches long after cure. The analytical technique was the same as for shear beams. The compaction pressure is applied perpendicular to the fiber axes.



a. As-Fabricated Composites: Beam Membranes  
( $0^\circ$ ,  $90^\circ$ ,  $0^\circ$ - $90^\circ$ ,  $\pm 45^\circ$ ) and Shear Beam  
Blanks (Left to Right).



b. Aluminum-Core Honeycomb Sandwich Beam,  $0^\circ$  Fibers.

Figure 38. Graphite-Epoxy Composite Specimens.

## INITIAL COMPOSITION EVALUATION

The laminate composite specimens, whether panels, beams, plates, or rods, were evaluated as-fabricated for fiber content, void content, and other composition parameters by the following techniques in order to assess, before destruction, their suitability. Where possible, the analogous procedure was used with filament-wound structures.

### a. Percentage of Whiskerizing

The degree of whiskerizing of the fiber as-received was determined by ignition analysis of a sample stripped from the axial centerline of the unimpregnated laminas. Two side-by-side full-length tows were selected. The analysis consisted of ignition in air under quantitative conditions at 800° - 900°C for about two hours. The quantitative removal of the graphite from the silicon carbide whiskers was apparent as an abrupt disappearance of the black graphite and a white or light green residue. Percentage of whiskerizing was expressed as weight of the residue divided by the total weight of graphite plus whiskers.

### b. Fiber Content, Weight %

To obtain fiber content, a careful material balance on the fiber in each layup was made. The as-fabricated specimen was carefully trimmed to remove all resin flash but to retain essentially all fiber. The fiber weight % was then determined as the weight of dry fiber in the layup divided by the weight of panel trimmed to this extent.

### c. Composite Density

Composite density of all specimens, whether laminate or filament-wound, was determined by the same techniques. The specimen was trimmed if necessary to form smooth edges with regular corners. The panel was then weighed dry and submerged in water in the apparatus shown in Figure 39. The composite density was calculated as:

$$\text{Composite density (g/cc)} = \frac{\text{dry weight (g)}}{\text{dry weight (g)} - \text{submergent weight (g)}} \quad (1)$$

The average of three values of each weighing was used.

### d. Fiber Content, Volume %

The volumetric fiber content was calculated from the preceding measurements. The calculation assumes the addition of partial volumes of the pure constituents. The

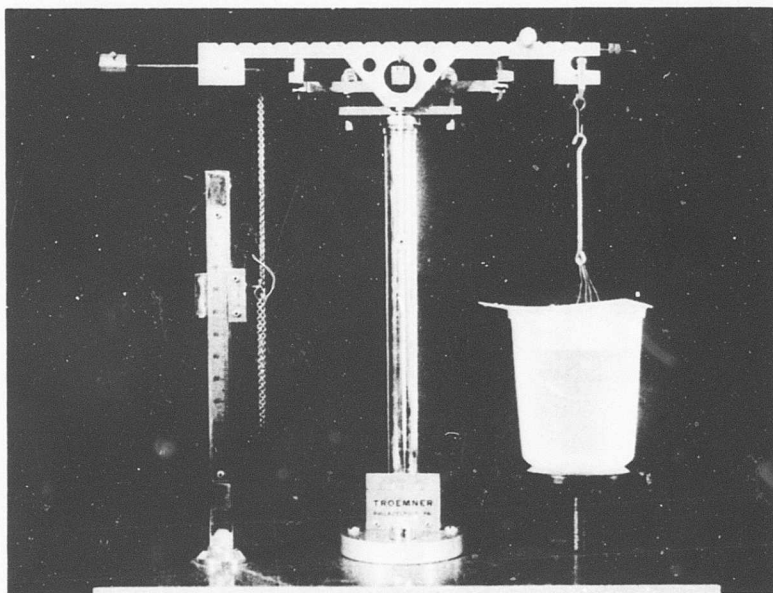


Figure 39. Composite Specimen Density Measurement Apparatus.

calculation was:

$$\text{Fiber content, v/o} = \frac{(\text{fiber content, weight \%}) \times \text{panel density}}{\text{fiber density}} \quad (2)$$

Fiber density was a calculated value based on the manufacturer reported values of density of high-modulus PAN-precursor graphite fiber (1.99 g/cc) and beta silicon carbide whiskers (3.21 g/cc). The calculation assumed additive partial volumes of the two materials:

$$\text{Fiber density, (g/cc)} = \frac{100}{\frac{(\% \text{ whiskerizing})}{3.21} + \frac{(100-\% \text{ whiskerizing})}{1.99}} \quad (3)$$

#### e. Void Content

The void content was a calculated, not directly measured, value. It assumed that the total panel volume consisted of the volume of fiber plus volume of resin plus volume of void. To perform this calculation, the density of void-free pure resin in the typical state of cure must be known. The value measured at GTC with the cure cycle used was 1.23 g/cc. The void content calculation was:

$$\begin{aligned} \text{Void v/o} = 100 + & \left[ \text{fiber v/o} \times \left( \frac{\text{fiber density} - \text{resin density}}{\text{resin density}} \right) \right] \\ & - \left[ \frac{100 \times \text{composite density}}{\text{resin density}} \right] \end{aligned} \quad (4)$$

Since this calculation involves the subtraction of nearly equal values, slightly positive or negative void contents can be calculated on essentially void-free specimens. Based on the experience using this method, together with visual observation of cross sections, it is believed that these values are generally good within  $\pm 1\%$  of the total panel volume.

### COMPOSITE ANALYSIS

All types of specimens were subjected to composite analysis as follows. The analytical procedure used for fiber content determination of these graphite yarn composites is essentially the same as the Kuhbader method.<sup>(20)</sup> The principle of the procedure is to oxidize and/or decompose the resin matrix with 70% nitric acid and leave the unaffected whiskerized or treated graphite in extraction thimbles.

The composite specimen samples were placed into extraction thimbles of known weights and were weighed. The thimbles had fritted glass bottoms of fine porosity to assure retention of fibers and whiskers when they were placed in beakers of 70%

nitric acid. The beakers and acid were heated to 70°C with an oil bath. Most of the fibers were separated after remaining in the acid overnight. Thimbles were removed and placed into beakers of fresh acid. Two hours later the samples were placed in other beakers of fresh acid to ensure removal of all resin. One hour later the thimbles of resin-free fiber were washed with water and dried 1-1/2 hours at 110°C. The thimbles and fiber were again weighed analytically to determine resin loss. Calculation of fiber content is then:

% whiskerized graphite by weight =

$$100 \times \frac{(\text{weight of thimble} + \text{whiskerized fiber}) - (\text{weight of thimble})}{(\text{weight of thimble} + \text{composite}) - (\text{weight of thimble})} \quad (5)$$

The percentage of whiskers in the whiskerized graphite remaining from the acid analysis was determined by removing fibers from the thimbles, placing them into combustion boats, weighing analytically, and placing the boats into a muffle furnace at 800°C for two hours. The boats were cooled to room temperature and weighed analytically. Whiskers remaining after ignition of graphite were removed and boat weight was determined. Calculation of whisker content is then:

% whiskerizing =

$$100 \times \frac{(\text{weight of boat and whiskers after ignition}) - (\text{boat weight})}{(\text{weight of boat and whiskerized graphite before ignition}) - (\text{boat weight})} \quad (6)$$

An additional check on the percentage of whiskerizing was made by ignition of composite samples (resin, fiber and all) in combustion boats. The procedure and calculations were analogous to those shown above. The further calculation needed to determine percentage of whiskers in whiskerized graphite was:

$$\% \text{ whiskerizing} = 100 \times \frac{\text{w/o whiskers in composite}}{\text{w/o whiskerized fiber in composite (from acid analysis)}} \quad (7)$$

### HONEYCOMB SANDWICH CONSTRUCTION

Two designs of honeycomb sandwich structures were used to evaluate the graphite fiber-epoxy lamina. The first design, shown at the top of Figure 40, was as long as the fabricated composite panel (13 inches) and consisted of aluminum honeycomb sandwiched between and bonded to a stainless-steel panel and the composite panel to be evaluated. The second design, shown at the bottom of Figure 40, was lengthened to 23.5 inches to increase the moment arm in the structure during testing. This decreased the shear stress in the bonded interface at any given tensile or compressive load on the composite panel face. This design consisted of the same sandwich structure as in design No. 1 except that steel extenders and shear doublers

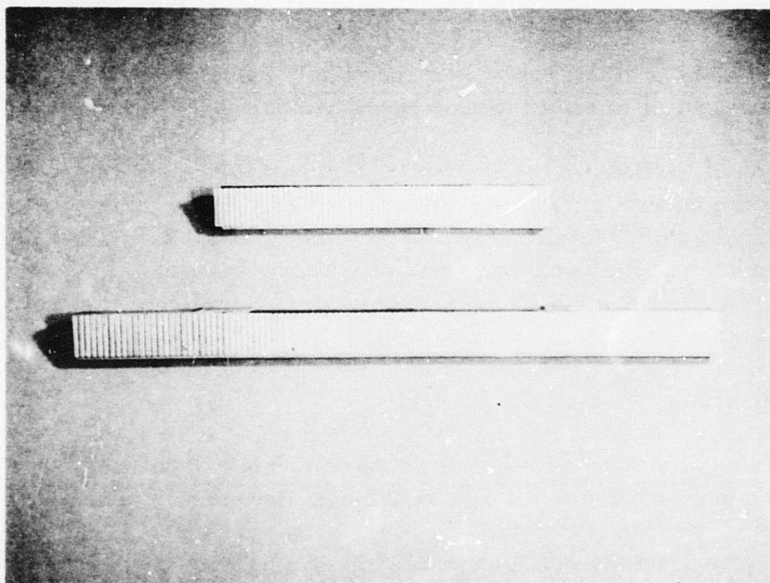


**Figure 40. Honeycomb Sandwich Beams, 13-Inch and 24-Inch Lengths.**

were utilized on both ends of the 13-inch-long composite panel. Both designs employ transverse and axial strain gages mounted in the center of the 2.4-inch-gage section of the composite face panel.

a. Materials

In both designs, the blank face panel of the sandwich structure was 1/8-inch-thick by 1-inch-wide type 304 stainless steel.

The composite face panels were fabricated by cutting the molded 3-inch by 13-inch panels into three 1-inch-wide by 13-inch-long pieces. The exact thickness and width of each piece were recorded before assembly.

The honeycomb used in both designs was type 5052 aluminum, 0.006 inch thick with 1/8-inch cell size, and had a density of 23 lbs/ft<sup>3</sup>. The honeycomb cores in the sandwich structures were 1.5 inches thick and 1 inch wide by either 13 or 23.5 inches long. The ribbon direction of the core was always along the longitudinal axis of the structure.

The extenders on design No. 2 were of 1-inch-wide mild steel. The thicknesses were selected to match that of the composite panel on the structure. The shear doublers were also of 1-inch-wide mild steel, 1/8 inch thick, and 3 inches long.

The adhesive used to bond the steel and composite face panels to the honeycomb was Epon 828 epoxy resin catalyzed with 11 parts of diethylenetriamine per hundred of resin. A small amount of amorphous silica gel was added to impart thixotropic flow properties to the uncured resin. This resin system is a room-temperature-setting type.

b. Assembly Procedure

The following procedure was followed in the assembly of the honeycomb structures:

- (1) The stainless-steel blank face panel and mild steel extenders and doublers were degreased with acetone.
- (2) The surfaces of the steel pieces requiring bonding were sandblasted to roughen the surface and then were cleaned and degreased again.
- (3) The honeycomb core was degreased with acetone.
- (4) The surface of the composite face panel to be bonded was slightly roughened with No. 320 grit sandpaper and then wiped with a cloth, damp with acetone, until no discoloration of a clean cloth occurred.

- (5) A heavy layer of adhesive resin was applied to the treated surfaces of both the stainless-steel and composite panels, and the panels were then placed in position on the honeycomb core and held firmly with C-clamps.
- (6) When fabricating a long No. 2 design structure, the steel extenders and shear doublers were applied in the same manner and held in place with additional C-clamps. The shear doublers were positioned so that they overlapped 1-1/2 inches on both the composite face panel and the steel extender.
- (7) The strain gages were applied to the surface of the composite face panel by preparing the surface as indicated above and bonding them with Duco cement. One gage was oriented in the transverse direction on one side of the centerline of the composite face panel, and the other gage was oriented in the longitudinal direction on the opposite side of the center line. The type of strain gage used required no clamping.
- (8) The bonded assembly was allowed to cure at room temperature for 24 hours.
- (9) After removal of the C-clamps, lead wires were soldered to the strain gages, and the structure was ready for testing.

#### SANDWICH BEAM TESTING

The sandwich beams were instrumented with two bonded strain gages in the gage section: one longitudinal and one transverse. The gage section was 2.4 inches in length, which was determined by the distance between the two 1/2-inch-round loading points fixed by a pivot to the cross-head of the Tinius Olsen tester. The reaction supports were also 1/2 inch round with separations of either 22 inches or 12 inches, depending on whether a 24-inch or a 13-inch beam was being tested. The beams were separated from the loading and reaction points by 1-inch-long by 1/8-inch-thick pads of aluminum alloy to distribute stress. The orientation of the composite face plate with respect to the supports determined whether it was tested in tension or compression.

The testing procedure consisted of loading stepwise in six increments to about one-half percent elongation and then unloading stepwise. The longitudinal and transverse strains were recorded at each point. Then the beam was loaded continuously to failure while continuously following the strain by keeping the strain bridge in balance. The strain was recorded at occasional intervals. The loading rate was 0.025 inch per minute for the 13-inch beams and 0.050 inch per minute for the 24-inch beams.

Analysis of face plate stress was carried out according to the following equation, which represents a moment balance within the gage section between the composite face plate and the supports:

$$\sigma = \frac{PA}{2W t_B (t_C + t_p + t_B)} \quad (8)$$

where  $\sigma$  = face plate stress

$P$  = total load

$A$  = moment arm =  $1/2$  (span minus gage section length)

$W$  = composite width

$t_B$  = composite thickness

$t_C$  = honeycomb plus adhesive thickness

$t_p$  = steel backing plate thickness

The thickness of the honeycomb plus adhesive thickness was determined in practice by measuring the total beam thickness in the gage section and subtracting the thicknesses of the face and backing plates.

Calculation of Young's modulus and Poisson's ratio was accomplished by plotting the stepwise load-strain data and drawing best-fit lines through them. Poisson's ratio was determined as the ratio of the slopes of the two lines in terms of strain per pound of load. The Young's modulus was calculated by dividing the stress per unit load factor,  $\sigma/P$ , calculated from the previous equation by the slope of the strain-load curve. Ultimate elongation was read from the strain gage bridge, which was continuously balanced during the loading until break.

#### SHEAR MODULUS PLATE TESTING

The shear modulus plate laminates, nominally 80 mils thick, were trimmed to 4-inch length and width. The diagonal-loading fixture had diagonal separation of 5 inches, which is equivalent to 3.535-inch corner separations. The testing fixture had three fixed corner points and a single movable point through which the load was transmitted from the cross-head of the Tinius Olsen tester. The deflection of that corner was recorded by a deflectometer directly below the loading nose. Tests were conducted at room temperature and 0.5 inch/minute crosshead rate. The plates were loaded on

each of the four corners twice, the plates being inverted for the second series, making a total of 8 measurements for each plate. The corners were deflected a total of 0.2 inch. The slopes of the load-elongation curves were used to calculate shear modulus as follows:

$$G = \frac{3(P/Y)L^2}{t^3} \quad (9)$$

where  $G$  = shear modulus

$P/Y$  = slope of load/deflection curve

$L$  = distance between adjacent supports

$t$  = plate thickness

The values of shear modulus so measured were corrected for the amount of plate extending beyond the support points by means of a correction factor which was determined from the slope of the curve of calculated modulus versus plate overhang measured on a 1/8-inch-thick aluminum alloy plate. This correction factor is in agreement with earlier experience of Texaco Experiment Inc. with boron composite(21).

#### SHORT-BEAM SHEAR TESTING

Short-beam shear testing was carried out on an adjustable span fixture with 1/4-inch-diameter supports and loading nose. The shear testing procedure consisted of testing at span-to-depth ratios decreasing from 5:1 until tensile failure was eliminated. In highly shear-resistant samples this could not be obtained at the lowest ratio, 2.1:1. In order to detect a shear failure, it was found advantageous to (1) limit beam overhang to about 1 mm and (2) follow the loading rate to discern the momentary tailoff in load that accompanies shear. The limited overhang permitted the shear to penetrate the end of the beam, where it could be seen. A very large overhang would not shear at the beam ends, causing the specimen to appear undamaged after load was removed, or on occasion to assume a "chair" configuration.

All shear testing with horizontal short beams was carried out at a loading rate of 0.1 inch per minute at room temperature. The calculation of shear stress was as follows:

$$\sigma_s = \frac{0.75 P}{bd} \quad (10)$$

where  $\sigma_s$  = shear stress

P = load at failure

b = specimen width

d = specimen depth

The I-beam configuration testing was carried out at 5:1 span-to-depth and otherwise identical conditions to the above except the web thickness was used in the above equation for b, specimen width.

### TORSION ROD TESTING

The machined or molded torsion rods were tested in a torsion fixture consisting of an adjustable reaction mounting containing a fixed Jacob's chuck and a bearing-mounted shaft with loading pulley and Jacob's chuck mounted on it. The specimens were mounted in the chucks with 3/4-inch-long, closely fitted brass collets on each end, which were grasped by the chucks. The loading was accomplished through a wire attached to the pulley. Load and pulley deflection were recorded. For purposes of computing shear modulus, the gage length was taken to be the distance between the middles of the two collets. All tests were at room temperature at 1/2 radian per minute. The testing fixture and some machined specimens are shown in Figure 41.

The calculation of shear strength and shear modulus was as follows:

$$S_s = \frac{8 PD}{\pi d^3} \quad (11)$$

and  $G = \frac{8}{\pi} \frac{(P/Y)}{d^4} \frac{D^2 L}{D^2 L}$

where  $S_s$  = shear strength, psi

$G$  = shear modulus, psi

P = load, lb

$(P/Y)$  = load/pulley perimeter deflection, lb/in.

D = pulley effective diameter, in.

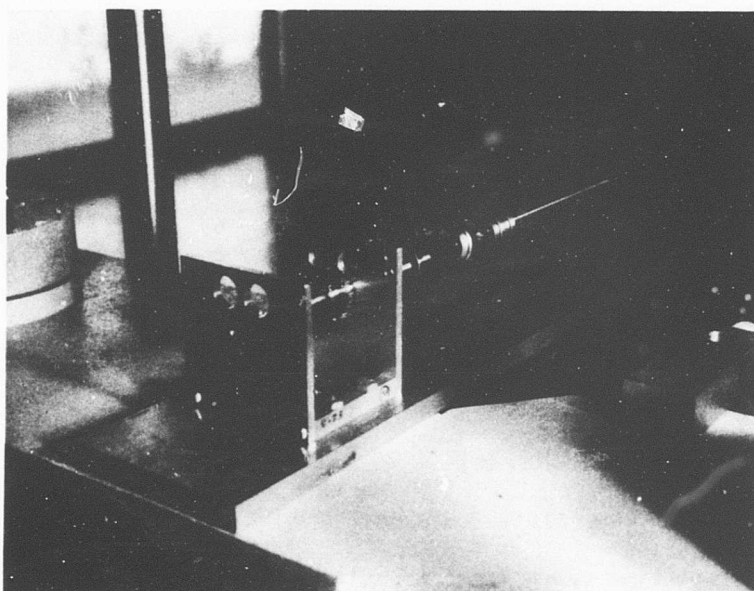
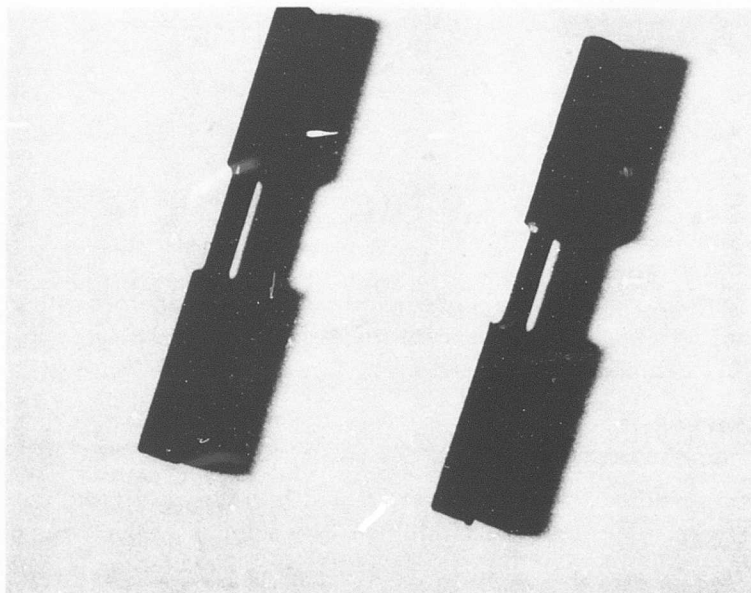


Figure 41. Torsion Rod Fixture and Machined Specimens.

$d$  = specimen diameter, in.

$L$  = gage length, in.

### FATIGUE SPECIMEN PREPARATION AND TESTING

Tensile and fatigue specimens were prepared to conform to the specimens used in the work reported in AFML-TR-66-313, Volume II<sup>(10)</sup>, with boron filament. The specimen configuration limits were detailed in Figure 139, page 261, of that report. The overall length was 9 inches; tabs of Scotchply were 1-1/2 inches long, leaving a 6-inch gage section. Width varied from 1/4 to 1 inch; a nominal 1/4-inch width was used during this program to keep loads within the 800-pound capacity of the fatigue tester.

Nine-inch-long sections were cut from the laminates; the 1-1/2-inch end regions were lightly abraded with emery paper and wiped with acetone, and the Scotchply was applied. Curing of tabs was carried out in accordance with the manufacturer's recommendation.

The 1/4-inch-wide specimens were then sliced with a thin diamond cutting wheel from the prepared laminate. Care was taken to slice parallel to the edge of the laminate to keep fiber orientation as near to 0° as possible.

The specimens were measured for width and thickness at the top, middle, and bottom of the gage section. The minimum area was used for computation of stress. The specimens were clamped top and bottom in the test fixture, and the crank was set for the approximate load desired. At all times, a stress ratio,  $R$ , of minimum to maximum not exceeding 0.05 or not less than 0 was used to conform to the procedure in AFML-TR-66-313, Volume II. Final fine adjustment of the load was accomplished by preloading the specimen with a wrench on the adjustment screw, keeping the load such that the condition of  $0.05 > R > 0$  was adhered to.

Shutdown automatically occurred at any failure release of load.

Retest of runout specimens at higher stress levels involved resetting the crank throw and preloading to obtain the new stress and retain  $0.05 > R > 0$ .

### STATIC TENSILE TEST PROCEDURE

Static tensile testing was carried out in the Tinius Olsen apparatus at 0.1 inch per minute crosshead rate with wedging grips. A 1-inch gage extensometer was used to measure modulus. Testing consisted of at least five specimens with breaks in the 6-inch gage section.

## NOL RING FABRICATION AND TEST SPECIMEN PREPARATION

The equipment consisted of a let-off spool with an adjustable friction brake, an impregnation bath, a traversing head, and a heated mandrel. In the preliminary impregnations by solvent-diluted resin, a heated drying tunnel was inserted between the bath and the traverse head. Subsequently this was removed and a heated resin bath was substituted for the simple solvent-resin bath. Tension was set on the friction drag prior to a run. On those runs in which fiber breakage occurred, the tension was reset to eliminate breakage, and the tension was measured after the run. The winding was finished off with a layer of Teflon film tape.

The mandrel was not deliberately heated until winding number 160716; at this point, heat was applied to allow maximum resin squeeze-out. Mandrel temperatures in the range of 90° to 110°C were experienced in this manner, whereas mandrel temperatures ranged only up to about 40°C when heated only by resin carry-over.

Curing and postcuring were carried out on the mandrel at the following schedule:

1 hour at 130°C  
1-1/4 hours at 177°C

Analysis of composite composition was carried out according to the techniques in sections 2 and 3.

The cylinders resulting from the filament-winding operation were turned down to exactly 1/8-inch thickness on a lathe with a carbide-tipped tool. The rings were then cut off with a thin steel tool.

Rings for split-disc testing were prepared by mounting a strain gage on the outer surface in tangential orientation to be positioned at 45° from the split.

Segments for shear and flexure testing were cut off with a water-cooled diamond wheel.

## NOL RING TESTING

### a. Shear Strength Test Procedure

Segments 0.625 inch long were tested according to ASTM D-2344. This is a 3-point flexure test at an apparent span-to-depth ratio of 5:1.

### b. Split-Disc Test Procedure

The rings were tested according to ASTM D-2290 with regard to strength. In

addition, the modulus was obtained by means of a strain gage mounted on the outer surface at 45° from the split. This location has been found to be stable and relatively free of bending effects. The split disc fixture is shown in Figure 42.

c. Ring Flexure Test Procedure

This test was performed according to a method described by Fried<sup>(22)</sup>, in which the ring is deflected along a diameter in compression. The ring deflects by bending into an ovoid, and modulus is calculated from the load-deflection curve. In this work, the rings were loaded to 10 pounds cyclically to obtain a load-deflection curve that was as reproducible as possible.

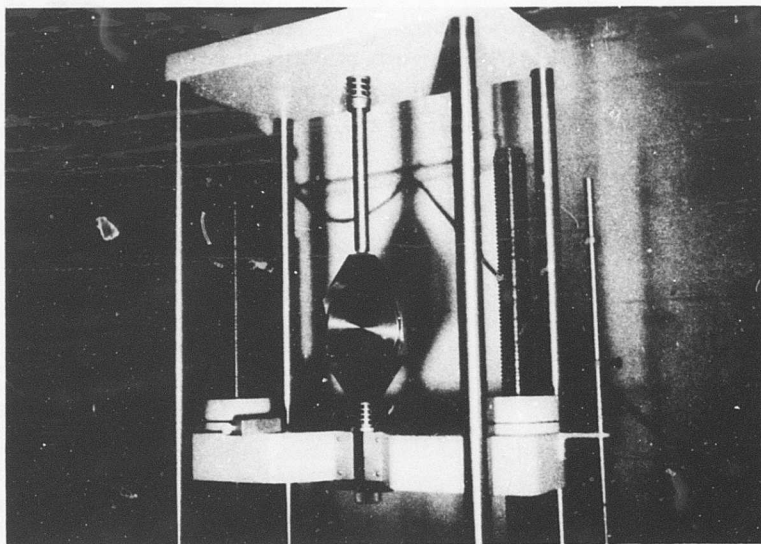
d. Segment Flexure Test Procedure

Segments 2.2 inches in length were subjected to 3-point flexure on a 2-inch span in a manner similar to ASTM D-790. This is a 16:1 span-to-depth ratio. Modulus was not calculated because of the extreme nonlinearity and looping of the load-deflection curves. The segments were loaded with the outer surface of the original ring in tension. The loading nose was 1/4-inch-diameter steel, and the supports were 45° angle steel knife edges, with the edges rounded off to a radius of approximately 0.01 inch.

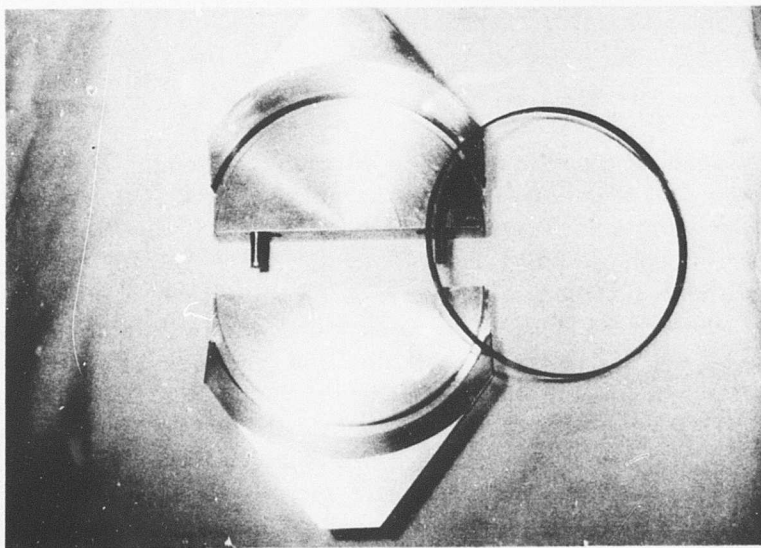
e. Wet Strand Fiber Strength Test

The as-received spool of graphite tow was evaluated for strength by an impregnated strand technique. This technique is similar to that used by GTC to evaluate rayon-precursor graphite yarns<sup>(23)</sup>. A length of the whole 10,000-fiber tow was impregnated by passing through a warmed bath of Epon 828/TETA (90/10). The impregnated tow was hung with a weight to straighten, excess resin was wiped off, and the tow was allowed to cure for 24 hours. The cured strand was cut into 5-inch lengths which were potted into 1/2-inch-diameter steel rod tabs having longitudinal V-slots (90° angle) milled to allow the strand to lie at the center line. The tabs were then placed in slots in a graphite block to cause perfect alignment. The block was heated to 130°C. The 5-inch strand lengths were placed in the tab V-slots with 1-1/2 inches in each tab end. Epoxy adhesive was allowed to flow around the strand ends, embedding them and forming a fillet into the gage section. A 2-inch gage section resulted. Resin cure was effected within a minute. The appearance of the finished specimens is shown in Figure 43.

The cured, potted strands were then tensile tested on the Tinius Olsen test at 0.1 inch per minute using the alignment grips that had been employed for fatigue tensile testing (see Figure 8). An average of 5 gage section breaks were used to compute strength. The cross-sectional area used to calculate strength was obtained from the



a. Tester With Grip Installed.



b. Detail of Grip.

Figure 42. Tinius Olsen Testing Machine With Split-Disc Grip.

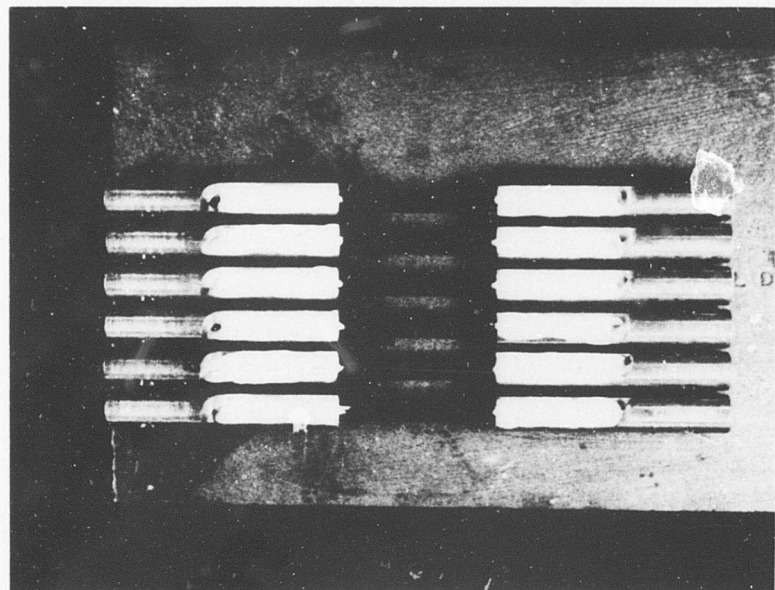


Figure 43. Wet Strand Fiber Strength Specimens.

dry fiber denier and the fiber density. This value is  $7.67 \text{ inches by } 10^{-4} \text{ square inches}$  for normal high-modulus PAN-precursor graphite 10,000-fiber tow. The strengths obtained in this test have been found to be within the range specified by the manufacturer for fiber strength (200 - 300 ksi).

### TORSION TUBE FABRICATION

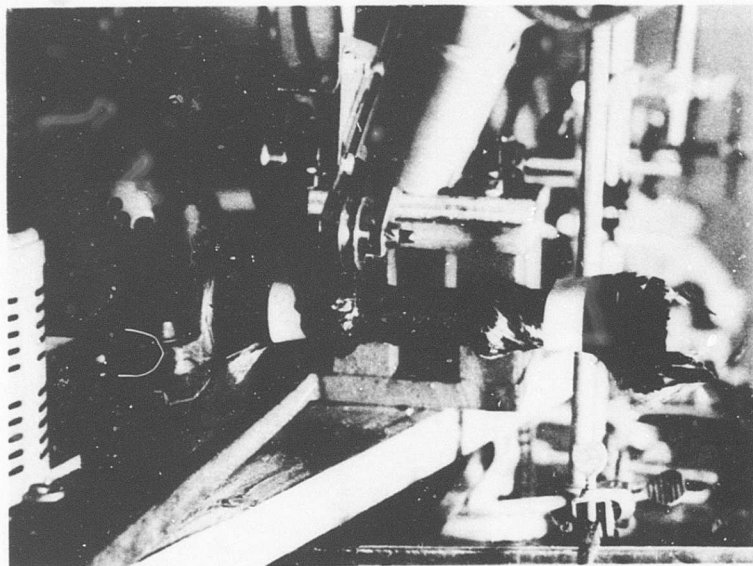
The torsion tubes used in this program to study in-plane shear properties were fabricated by a combination of filament-winding and layup techniques on 1-inch-diameter mandrels to form specimens of nominal dimensions of 1-inch ID, 0.05-inch to 0.10-inch wall thickness, and 2-inch gage section. Overall length was approximately 3 inches. Filament winding, using the tension and impregnation techniques developed in the NOL ring winding phase, was used for all hoop winding ( $90^\circ$ ) plies in these tubes. Winding tension was 3000 grams per tow. Resin\* impregnation was carried out by immersion in a hot resin bath. The axial fibers ( $0^\circ$ ) in the  $0^\circ$ - $90^\circ$  orthotropic and longitudinal configurations were applied to the surface of the mandrel under axial tension in impregnated state and taped down outside the nominal tube length. This can be seen in Figure 44, wherein the finishing hoop winding to a  $90^\circ$ - $0^\circ$ / $0^\circ$ - $90^\circ$  configuration is being applied over the longitudinal fibers. Other fiber configuration plies, namely  $\pm 45^\circ$  or  $\pm 30^\circ$  to the axis, were applied as impregnated, oriented laminas. These were cut to precise angle and size from unidirectional layups and were wrapped around the mandrel by hand, using a backing Mylar film which was subsequently removed before applying the next layer. Thus the layups for the  $\pm 45^\circ$  layers were parallelograms of unidirectional, prepregged fiber with  $45^\circ$  and  $135^\circ$  corners, and the layups for  $\pm 30^\circ$  layers were parallelograms with  $60^\circ$  and  $120^\circ$  corners. The layup procedure involved the hoop-wound layer as finishing layer wherever possible to achieve maximum compaction. This was possible on the  $90^\circ$ - $0^\circ$ / $0^\circ$ - $90^\circ$  orthotropic and the  $30^\circ$ - $150^\circ$ - $90^\circ$  isotropic configurations.

The  $45^\circ$ - $135^\circ$ / $45^\circ$ - $135^\circ$  tubes were hand laid up and compacted solely by the use of shrinkable polyethylene tubing as a finishing layer. All composites, whether hoop-wound or not, were finished with the shrink tubing. The appearance of the  $\pm 45^\circ$  tube surface resulting from the shrink tubing compaction is shown in Figure 45. The  $135^\circ$  orientation of the outer layer of fibers is evident, and the slight seam impression resulting from the inner surface of the shrink tubing can be seen running lengthwise near the center.

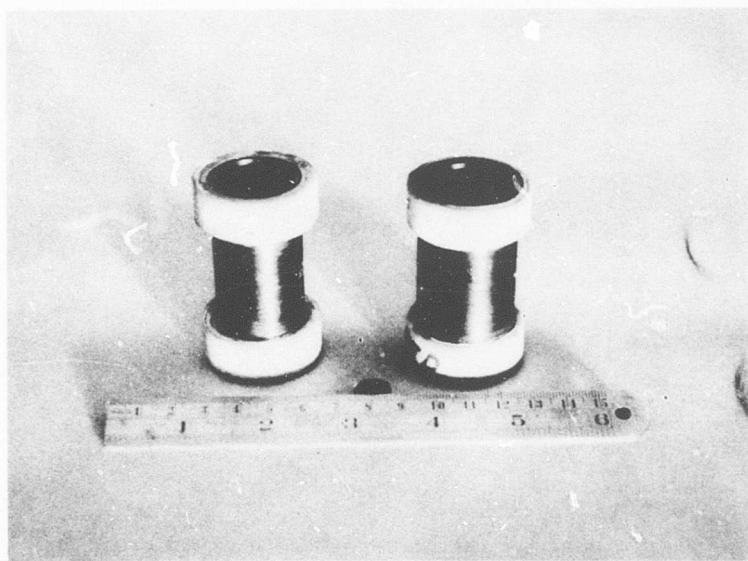
The cure cycle used with the torsion tubes was the same as in all previous phases of this program. After cure, the shrink tubing was removed by slitting with a knife.

---

\* Epon 828/1031/NMA/BDMA



a.  $0^{\circ}$ - $90^{\circ}$  Torque Tube Being Filament-Wound.



b. Finished Tubes With Scotchply Grips Applied.

Figure 44. Torque Tube Winding.

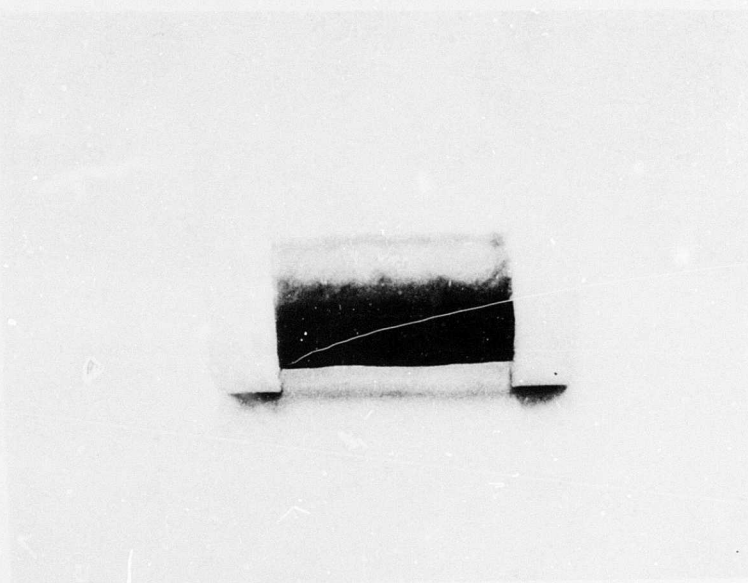


Figure 45.  $\pm 45^\circ$  Torsion Tube Specimen.

Glass fiber prepreg tape was then applied by wrapping under tension to both ends of the tubes and these were cured in place at 167°C for 1 hour, which also constituted the postcure cycle for the tubes. The tube test specimen configuration was then finished by machining the glass composite ends to the grip diameter, 1.50 inches, centered on the tube axis.

Each torsion tube was instrumented with  $\pm 45^\circ$  strain gage rosettes applied to the gage section with adhesive. This gage configuration gives temperature compensation, insensitivity to axial loads, and a bridge constant of two when used as adjacent arms in the Wheatstone bridge.

### TORSION TUBE TESTING

The tubes were tested in the fixture shown in Figure 46. This fixture clamps the tube in two end grips, one of which is fixed and the other is rotated by a pulley load by a steel cable connected to the Tinius Olsen test machine. The tube is free to deflect axially but not in flexure. A 1/2-inch steel rod through the center of the tube specimen transmits the bend loads to the bearings at both ends of the specimens.

The loading rate to failure was 0.25 radian per minute. Modulus curves using the strain gages were generated by loading sequentially in 6 steps up and 5 steps down to a maximum torque of 230 lb-in, recording the strain at each point. The strain during this part of the testing sequence was read from the  $\pm 45^\circ$  gages used as adjacent active arms in the instrumentation bridge. The torsional strain was further monitored by measuring the rotation of the loading pulley at the movable end of the test fixture. Thus the torsional modulus was calculated two ways: with the strain per unit torsional load from the strain gages, and with the angular rotation per unit length per unit torsional load from the deflectometer reading. After generation of the modulus curve, the specimen was loaded from zero to failure at the nominal rate.

The calculations of shear strength and modulus were as follows:

$$S_s = \frac{8 P D d_o}{\pi(d_o^4 - d_i^4)} \quad (12)$$

$$\text{strain gage } G_{xy} = \frac{8 D d_o}{\pi(d_o^4 - d_i^4) (\epsilon/P)}$$

$$\text{extensometer } G_{xy} = \frac{8 D^2 L (P/Y)}{\pi(d_o^4 - d_i^4)}$$

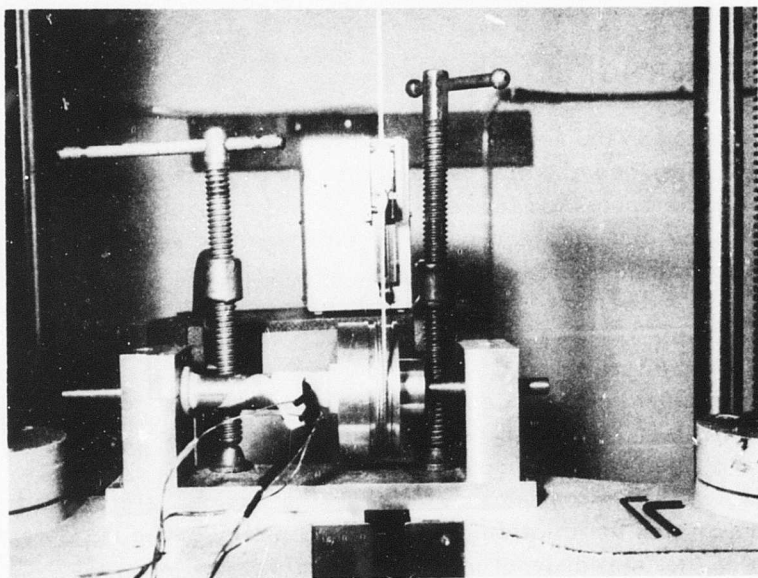


Figure 46. Torsion Tube Test Fixture and Specimen With  
Strain Gage Rosette and Deflectometer  
Attached.

where  $S_s$  = shear strength, psi

$G_{xy}$  = in-plane shear modulus, psi

$P$  = load transmitted to test machine, lb

$D$  = diameter of torsion-loading pulley, in.

$d_o$  = specimen outside diameter, in.

$d_i$  = specimen inside diameter, in.

$(\epsilon/P)$  = strain per unit load,  $\text{lb}^{-1}$ , determined from plot of strain gage and load data

$(P/Y)$  = load per unit deflection of pulley circumference, lb/in., determined from slope of load-extensometer curve

$l$  = gage length, in.

## UNCLASSIFIED

Security Classification

## DOCUMENT CONTROL DATA - R &amp; D

(Security classification of title, body of abstract and indexing annotation must be entered when the overall report is classified)

1. ORIGINATING ACTIVITY (Corporate author) General Technologies Corporation 1821 Michael Faraday Drive Reston, Virginia	2a. REPORT SECURITY CLASSIFICATION UNCLASSIFIED
2b. GROUP	

3. REPORT TITLE

## GRAPHITE FIBER-RESIN COMPOSITE STRUCTURE STUDY

4. DESCRIPTIVE NOTES (Type of report and inclusive dates)  
Final Technical Report, May 1968 - April 1969

5. AUTHOR(S) (First name, middle initial, last name)

Robert G. Shaver

6. REPORT DATE October 1969	7a. TOTAL NO. OF PAGES 120	7b. NO. OF REFS 30
8a. CONTRACT OR GRANT NO. DAAJ02-68-C-0062	9a. ORIGINATOR'S REPORT NUMBER(S) USAAVLABS Technical Report 69-67	
b. PROJECT NO. Task 1F162204A17001	9b. OTHER REPORT NO(S) (Any other numbers that may be assigned this report) GTC 160.7	
c.		
d.		
10. DISTRIBUTION STATEMENT This document is subject to special export controls, and each transmittal to foreign governments or foreign nationals may be made only with prior approval of US Army Aviation Materiel Laboratories, Fort Eustis, Virginia 23604.		
11. SUPPLEMENTARY NOTES	12. SPONSORING MILITARY ACTIVITY U. S. Army Aviation Materiel Laboratories Fort Eustis, Virginia	

13. ABSTRACT *W.W.* This program has been concerned with the development of techniques to fabricate filament-wound tube structures of whiskerized graphite fiber in epoxy resin. The first efforts on the program were devoted to the selection of an optimized whiskerizing level on high-modulus PAN-precursor graphite fiber through evaluation of flat laminates in tensile, compressive, shear, and fatigue testing. An optimum level of 3% whiskerizing was selected based on a balance of interlaminar shear strength and retained fiber strength. Continuous whiskerized fiber impregnation and filament-winding techniques were developed by fabricating NOL rings. The techniques were then applied to fabrication of torsion tubes in several fiber configurations: unidirectional, orthotropic, and isotropic. Fiber content of 50 v/o was achieved by filament winding of the 3% whiskerized high-modulus PAN-precursor graphite fiber. This is similar to the fiber content that can be achieved with the un-whiskerized form of the same fiber. The 3% whiskerizing level provided shear strengths in the various specimen configurations equal or superior to the fiber manufacturer's surface treatment. Whiskerizing was further found to increase shear modulus in unidirectional composites, which is a result of the interstitial reinforcement provided by the whiskers. All specimen configurations in which shear between the fiber and matrix determined the composite properties were considerably improved by the presence of whiskerizing.

DD FORM 1 NOV 68 1473

REPLACES DD FORM 1473, 1 JAN 64, WHICH IS  
OBSOLETE FOR ARMY USE.

UNCLASSIFIED

Security Classification

**UNCLASSIFIED**

Security Classification

14 KEY WORDS	LINK A		LINK B		LINK C	
	ROLE	WT	ROLE	WT	ROLE	WT
Graphite Fiber Composites Whiskers Filament Winding Laminates Fatigue Properties Shear Properties						

**UNCLASSIFIED**

Security Classification

100-6-1